BINDING SERVICES
Tel +44 (0)29 2087 4949
Fax +44 (0)29 20371921
e-mail bindery@cardiff.ac.uk

Observational Manifestations of Gravitational Waves in Ground Based Interferometers and the Cosmic Microwave Background Radiation

by

Deepak Baskaran

School of Physics & Astronomy, Cardiff University,
Cardiff, CF24 3YB, U.K.

A thesis submitted to the
University of Wales
for the degree of
Doctor of Philosophy

June 2006

Supervisor: Prof. L. P. Grishchuk

ProQuest LLC
789 East Eisenhower Parkway
P.O. Box 1346
Ann Arbor, MI 48106-1346

DECLARATION

This work has not previously been accepted in substance for any degree and is not concurrently submitted in candidature for any degree.

Signed ..... (candidate) Date 11/08/2006.

STATEMENT 1

This thesis is being submitted in partial fulfillment of the requirements for the degree of PhD.

Signed ..... (candidate) Date 11/08/2006.

STATEMENT 2

This thesis is the result of my own independent work/investigation, except where otherwise stated. Other sources are acknowledged by explicit references.

Signed ..... (candidate) Date 11/08/2006.

STATEMENT 3

I hereby give consent for my thesis, if accepted, to be available for photocopying and for inter-library loan, and for the title and summary to be made available to outside organisations.

Signed ..... (candidate) Date 11/08/2006.

Acknowledgements

Firstly I would like to deeply thank my family and Marina for their love and unconditional support. Without them this work would not have been possible!

I would like to thank my supervisor Prof. Leonid Petrovich Grishchuk for his constant guidance and fruitful discussions through the whole period of my study, as well as support with various logistical issues that kept creeping up over the years. I have learnt a great deal from him, 'both off and on the pitch'. It is an honour to be a student of Lyonya Petrovich! I would also like to express my gratitude to Dr. Alexander Polnarev, for his constant hospitality and very insightful scientific discussions. Work with Alex has been very stimulating and of great educational value.

Cardiff Relativity Group has been a fantastic place to work. I am thankful to all the guys in room N3.24 for keeping a working yet cheerful atmosphere. I would like to thank Prof. B.S. Sathyaprakash, Dr. J. Romano, Dr. S. Babak for insightful scientific discussions. Thanks are also due to the rest of the 'relativity gang' (in random order) - Anand, Dave, Thomas, Chris, Gerald, Jack, Gareth, Craig and Edmund for discussions on various topics, not restricted to just science. I am also grateful to the people at the general office, especially Louis Winter, for arranging all sorts of formalities, and making my life much more easier.

On the personal side I would like to thank all the people that have made my stay in Cardiff memorable. I would especially like to express my gratitude to Sathya & Uma, Bala & Radha, Stas & Isabelle for making me feel at home, especially during my first year, in Cardiff. I am also very thankful to Prof. Leonenko family and Prof. Wickramasinghe family for their warm hospitality and help. I am also extremely fortunate to have made close friends here - Erik, Timour, Anna, Jani and Vitaly. I am very thankful to my friends for making my life here interesting and joyful, as well as helping me whenever needed. I would also like to thank all my friends back in Moscow for all sorts of help over the years. In this respect, I am especially indebted to Sasha Belinski, for providing invaluable help in all sorts of matters from computers to airplane tickets.

Finally, I would like to thank once again Marina, who over the years has shared all my ups and downs, and whose love has been my driving force.

To Mom, Dad, Marina & Darshan.
You are my strength & inspiration!

Abstract

In this work we analyze two possible observational manifestations of gravitational waves. We consider the effects of gravitational waves on ground based laser interferometric detectors, and the imprints of relic gravitational waves on the Cosmic Microwave Background (CMB) radiation.

In order to study the effect of a gravitational wave on a laser interferometer it is crucial to understand the movement of free test particles. The detailed knowledge of this motion is important conceptually and practically, because the mirrors of laser interferometric detectors of gravitational waves are essentially free test masses. A gravitational wave bring about the relative motion of free test masses. In particular, analogous to movement of free charges in a field of an electromagnetic wave, a gravitational wave drives the masses in the plane of the wave-front and also, to a smaller extent, back and forth in the direction of the wave's propagation. To describe this motion, we introduce the notion of "electric" and "magnetic" components of the gravitational force. Using different methods, we demonstrate the presence and importance of the "magnetic" component of motion of free masses. We then explicitly derive the full response function of a 2-arm laser interferometer to a gravitational wave of arbitrary polarization. We give a convenient description of the response function in terms of the spin-weighted spherical harmonics. We show that the previously ignored "magnetic" component may provide a correction of up to 10%, or so, to the usual "electric" component of the response function.

Another promising venue for detecting gravitational waves are the anisotropies in temperature and polarization of the CMB radiation. A strong variable gravitational field of the very early Universe inevitably generates relic gravitational waves by amplifying their zero-point quantum oscillations. These relic gravitational waves leave their imprint on the anisotropies of the CMB. We explain and summarize the properties of relic gravitational waves that are needed to derive their effects on CMB temperature and polarization anisotropies. Analyzing the radiative transfer equations, we reduce them to a single integral equation of Voltairre type and solve it analytically as well as numerically. We formulate the possible correlation functions $C_\ell^{XX'}$ and derive their amplitudes, shapes and oscillatory features. We show that the TE correlation at lower ℓ's must be negative, if it is caused by gravitational waves, and positive if it is caused by density perturbations. This difference in TE correlation may be a signature more valuable observationally than the lack or presence of the BB correlation, since the TE signal is about 100 times stronger than the expected BB signal. We discuss the detection by WMAP of the TE anticorrelation at $\ell \approx 30$ and show that such an anticorrelation is possible only in the presence of a significant amount of relic gravitational waves (within the framework of all other common assumptions). We propose models containing considerable amounts of relic gravitational waves that are consistent with the measured TT, TE and EE correlations.

Contents

Chapter 1

A General Introduction

The existence of gravitational waves is an inevitable consequence of Einstein's theory of General Relativity. The field equations of general relativity permit wave-like solutions, known as gravitational waves, which travel at the speed of light and are, in some aspects, similar to electromagnetic waves that stem from Maxwell's equations [1, 2, 3, 4]. Strictly speaking gravitational waves must exist in any relativistic theory of gravity [5]. Thus, the existence of gravitational waves is firmly rooted in the principles of special relativity, which govern all the branches of modern theoretical physics. On the experimental side, the decay of orbital period in binary pulsar PSR1913+16 [6], although an indirect evidence for gravitational waves, leaves little doubt to their existence.

With the advent of twenty first century gravitational wave astronomy is approaching a crucial milestone, when finally, after almost a century, the experimental precision is approaching the level of theoretical predictions [7, 5]. We are currently in the process of opening up a new window into the Universe, the gravitational window, which will allow us to see further and deeper into the structure and evolution of the physical world. Together with other 'windows', like electromagnetic and/or neutrino astronomy, gravitational wave astronomy will prove an invaluable tool in validating or falsifying the most fundamental theories in physics. The weakness of gravity as a physical interaction forms the strength of gravitational wave astronomy as a scientific tool [7]. Gravitational waves are difficult to detect because they carry energy practically without scattering

or absorbtion. This difficulty turns into a unique opportunity to observe events which no other window can offer, like events at the beginning of the Universe, or events in the vicinity of merging black holes. Arguably, gravitational wave research currently represents one of the most rich and exciting directions in physics. A detailed introduction to gravitational wave research can be found in reviews [8, 9, 10, 11, 12, 13, 7, 5].

The magnitude and frequency range of expected sources of gravitational waves varies greatly, with $h \sim 10^{-5}$ and $\nu \sim 10^{-18} Hz$ for gravitational waves of cosmological origin, to $h \sim 10^{-21}$ and $\nu \sim 10^{3} Hz$ for coalescing compact binaries[1]. Although there is considerably effort on the theoretical and experimental side to detect gravitational waves in practically all frequency ranges, currently the two most promising 'observatories' are the ground based interferometers and the Cosmic Microwave Background (CMB) radiation.

The current ground based interferometers focus attention at detecting gravitational waves in the frequency ranges $10 - 10^{4} Hz$. These detectors aim to observe a variety of sources of gravitational waves like compact binaries, supernovae explosions, black hole ring down, and primordial gravitational wave background, to name a few.

On the other end of the gravitational wave astronomy frontier lies the observation of temperature and polarization anisotropies in the CMB radiation. The CMB allows us to probe the gravitational wave background on cosmological scales, $10^{-18} - 10^{-15} Hz$, corresponding to wavelengths comparable to the present day Hubble radius. If the currently observed large scale anisotropies in temperature and polarization of the CMB [14, 26, 15] are generated by cosmological perturbations of quantum-mechanical origin, then a significant fraction of these anisotropies must come from the relic gravitational wave background [16]. The existence of a relic gravitational wave background is firmly rooted in the validity of general relativity and quantum mechanics [17, 16]. Along with being a possible observatory for gravitational waves, in general, the CMB has

[1]Here h denotes the dimensionless characteristic gravitational wave amplitude, explained in Section 2.

proven to be one of the most powerful and precise tools in observational cosmology and holds a wealth of information on very fundamental questions about the nature of the physical universe. The CMB has the promise to address a host of questions like the age and geometry of the universe, its matter-energy content, the ionization history, primordial spectrum of density perturbations, among others. A general introduction to the physics of temperature anisotropies and polarization in the CMB can be found in reviews [18, 19, 20, 21, 22, 23].

It is worth noting that the experimental effort to observe gravitational waves is at a truly fantastic level. It involves ingenious techniques together with state of the art technologies to give us an ability to measure effects that at the first sight might seem impractical. For example, the current laser interferometric detectors of gravitational waves have a characteristic size $l \sim 1\ km$, the expected displacement of arms due to a gravitational wave with $h \sim 10^{-21}$ is $\delta l \sim lh \sim 10^{-16} cm$ (which corresponds to subnuclear distances). A general introduction into the operation of laser interferometric detectors can be found in [24]. In the case of CMB we are dealing with effects that are no less subtle. The mean temperature of the CMB is approximately $T \sim 2.7°K$, which is a very low temperature in itself. The angular variations in temperature are just a minute fraction to this already low temperature, $\delta T/T \sim 10^{-5}$, with linear polarization being a magnitude smaller $\sim 10^{-6}$. Thus in CMB we are interested in temperature and polarization fluctuations at a level of fractions of micro-Kelvins. Some of the subtleties involved in measurements of the CMB are discussed comprehensively in [25, 26, 27].

In this work we shall concentrate on two possible observational manifestations of gravitational waves, mentioned above. Firstly, we shall study the the movement of test particles in the field of a gravitational wave. Using this analysis, we shall consider the implication for ground based interferometers. We then shift our attention to the CMB radiation. More specifically, we shall focus on the signature of gravitational waves in the temperature and polarization anisotropies of the CMB.

The large-scale interferometers for the detection of gravitational waves are approaching their planned level of sensitivity [28]. In the coming years, we may be observing the rare, but most powerful, sources of gravitational waves (for reviews, see for example [8, 9, 11, 12, 13, 7]). These initial instruments are scheduled to be upgraded in a few years time. The upgraded (advanced) interferometers will be more sensitive than the initial ones. They will enable us to determine with high accuracy the physical parameters of various astrophysical sources. The knowledge of the detailed and accurate response function of the instrument to the incoming gravitational wave (g.w.) of arbitrary polarization becomes an important priority. A laser interferometer monitors distances between the central mirror(s) and the end-mirrors in the interferometer's arms. In the existing instruments, the length l of the interferometer's arm is significantly shorter than the wavelengths λ of the gravitational waves which the instrument is most sensitive to. The evaluation of the change δl of the distance between two mirrors is usually formulated as $\delta l/l \approx h$, where h is the characteristic amplitude of the incoming wave. This is a correct answer, but it is correct only in the lowest, zero-order, approximation in terms of the small parameter l/λ. The next approximation introduces a "magnetic" correction [29] to $\delta l/l$, which is of the order of $h(l/\lambda)$. This correction depends on the ratio l/λ whose numerical value is at the level of several percents for the instruments with $l = 4km$ and typical g.w. frequencies $\nu = c/\lambda \approx 10^3 Hz$. This contribution may be especially important for the advanced interferometers operating in the "narrow-band" mode aimed at detecting relatively high-frequency quasi-monochromatic g.w. signals.

Moving on to CMB radiation, the detection of primordial gravitational waves is rightly considered a highest priority task for the upcoming observational missions [27]. Relic gravitational waves are inevitably generated by strong variable gravitational field of the very early Universe. The generating mechanism is the superadiabatic (parametric) amplification of the waves' zero-point quantum oscillations [17]. In contrast to

other known massless particles, the coupling of gravitational waves to the 'external' gravitational field is such that they could be amplified or generated in a homogeneous isotropic Friedmann-Lemaître-Robertson-Walker (FLRW) universe. This conclusion, at the time of its formulation, was on a collision course with the dominating theoretical doctrine. At that time, it was believed that the gravitational waves could not be generated in a FLRW universe, and the possibility of their generation required the early Universe to be strongly anisotropic (see, for example, [30]).

The generating mechanism itself relies only on the validity of general relativity and quantum mechanics. But the amount and spectral content of relic gravitational waves depend on a specific evolution of the cosmological scale factor (classical 'pumping' gravitational field) $a(\eta)$. The theory was applied to a variety of $a(\eta)$, including those that are now called inflationary models (for a sample of possible spectra of relic gravitational waves, see Fig.4 in Ref. [31]). If a unique $a(\eta)$ were known in advance from some fundamental 'theory of everything', we would have derived the properties of the today's signal with no ambiguity. In the absence of such a theory, we have to use the available partial information in order to reduce the number of options. This allows us to evaluate the level of the expected signals in various frequency intervals. The prize is very high - the actual detection of a particular background of relic gravitational waves will provide us with the unique clue to the 'birth' of the Universe and its very early dynamical behaviour.

A crucial assumption that we make in this and previous studies is that the observed large-scale cosmic microwave background (CMB) anisotropies are caused by cosmological perturbations of quantum-mechanical origin. If this is true, then general relativity and quantum mechanics tell us that relic gravitational waves should be a significant, if not a dominant, contributor to the observed large-scale anisotropies. From the existing data on the amplitude and spectrum of the CMB fluctuations we infer the amplitude and spectral slope of the very long relic gravitational waves. We then derive detailed

predictions for indirect and direct observations of relic gravitational waves in various frequency bands.

At this point, it is important to clarify the difference between the concepts of relic gravitational waves and what is now called inflationary gravitational waves. The statements about inflationary gravitational waves ('tensor modes') are based on the inflation theory. This theory assumes that the evolution of the very early Universe was driven by a scalar field, coupled to gravity in a special manner. The theory does not deny the correctness of the previously performed calculations for relic gravitational waves. However, the inflationary theory proposes its own way of calculating the generation of density perturbations ('scalar modes'). The inflationary theory appeals exactly to the same mechanism of superadiabatic (parametric) amplification of quantum vacuum fluctuations, that is responsible for the generation of relic gravitational waves, but enforces very peculiar initial conditions in the 'scalar modes' calculations.

According to the inflationary initial conditions, the amplitudes of the 'gauge-invariant' metric perturbations ζ associated with the 'scalar modes' (or, in other words, the amplitudes of the curvature perturbations called ζ or $\mathcal{R}$) can be arbitrarily large from the very beginning of their evolution. Moreover, the theory demands that these amplitudes must be infinitely large in the limit of the deSitter expansion law $a(\eta) \propto |\eta|^{-1}$ which is responsible for the generation of a flat (Harrison-Zeldovich-Peebles, 'scale-invariant') primordial spectrum, with the spectral index n = 1. At the same time, the amplitudes of the generated gravitational waves are finite and small for all spectral indices, including n = 1. Since both, gravitational waves and density perturbations, produce CMB anisotropies and we see them small today, the inflationary theory substitutes (for 'consistency') its prediction of infinitely large amplitudes of density perturbations, in the limit n = 1, by the claim that it is the amount of primordial gravitational waves, expressed in terms of the 'tensor/scalar ratio r', that should be zero, $r = 0$. For a detailed critical analysis of the inflationary conclusions, see [16]; for arguments aimed

at defending those conclusions, see [32].

The science motivations and CMB data analysis pipelines, designed to evaluate the gravitational wave contribution, are usually based on inflationary formulas [33, 15, 34, 35]. In particular, according to the inflation theory, the primordial power spectrum of density perturbations has the form (it follows, for example, from Eqs. (2.12a) and (2.12b) in Ref.[35]):

$$P_S(k) = \frac{1}{4\pi^3 M_{Pl}^2}\frac{1}{r}H^2|_{(k=aH)}.$$

Despite the fact that this spectrum diverges at $r = 0$ ($n_s = 1$), the CMB data analysts persistently claim that the inflation theory is in spectacular agreement with observations and the CMB data are perfectly well consistent with $r = 0$ (the published confidence level contours always include $r = 0$ and are typically centered at that point).

Our analysis in this work, based on general relativity and quantum mechanics, is aimed at showing that there is evidence of signatures of relic gravitational waves in the already available CMB data. We also make predictions for some future experiments and observations.

The structure of the thesis is as follows. In Chapter 2 we give a brief general introduction to gravitational waves, and summarize their properties that would be required in further considerations. Here, we also summarize the properties of a random background of relic gravitational waves that are needed for CMB calculations. The emphasis is on the gravitational wave (g.w.) mode functions, power spectra, and statistical relations.

In Chapter 3 we shift our attention to the motion of free test particles and consequently to the response of a laser interferometer in the presence of a gravitational wave. We start from the motion of free charges in the field of an electromagnetic wave, section 3.1. Then, we turn our attention to the main subject of the chapter – motion of free masses in the field of a gravitational wave. In section 3.2 the positions and motion of free test masses is described in the local inertial reference frame associated

with one of the masses. This choice of coordinates is the closest thing to the global Lorentzian coordinates that are normally used in electrodynamics. The identification of the "electric" and "magnetic" components of motion, as well as comparison with electrodynamics, are especially transparent in this description. In section 3.3 we exploit the geodesic deviation equation for the derivation of equations of motion and identification of the components of the gravitational force. The usually written equation, with the curvature tensor in it, is only the zero-order approximation in terms of l/λ. This approximation is sufficient for the description of the "electric" part of the motion, but is insufficient for the description of the "magnetic" part. In the next approximation, which is a first order in terms of l/λ, the geodesic deviation equation includes the derivatives of the curvature tensor, and this approximation is fully sufficient for the description of the "magnetic" force and "magnetic" component of motion. From these considerations it follows that the component of motion which we call, with some reservations, "magnetic" is, in any case, the finite-wavelength correction to the usual infinite-wavelength approximation. In the end of this section we compare our interpretation with other analogies cited in the literature. In section 3.4 we switch from the positions and trajectories of individual particles to the distances between them. The calculation of distances is especially simple in the local inertial frame, since the metric tensor, in the required approximation, is simply the Minkowski tensor. However, the conclusions about distances, including their "magnetic" contributions, do not depend on the choice of coordinates. We show that the universal definitions of distance, based on the light travel time and the length of spatial geodesics, lead to the same result in the appropriate approximation. In section 3.5 we use the derived results for the construction of the response function of a 2-arm ground-based interferometer. It is assumed that a gravitational wave of arbitrary polarization is coming from arbitrary direction on the sky. We explicitly identify the "magnetic" contribution to the response function and demonstrate its importance. Then in section 3.6 we formulate the

response function in terms of the spin-weighted spherical harmonics. In section 3.7 we give numerical estimates of the "magnetic" contribution to the response function of the presently operating instruments, in the context of realistic astrophysical sources. We show that the lack of attention to the "magnetic" components can lead to a considerable systematic error in the estimation of parameters of the g.w. source. Some technical details are moved into the Appendices.

After considering the manifestations of gravitational waves in ground based interferometers we move on to consider the imprints of gravitational waves on the CMB radiation. We begin in Chapter 4 with a general characterization of the radiation field. In section 4.1 we explain the existence of four invariants I, V, E, B that fully characterize the radiation field. In section 4.2 we explain the Thomson scattering process, which is the main scattering mechanism for radiation prior to decoupling of CMB from matter. We then formulate the general equation of radiative transfer in the cosmological context of a slightly perturbed FLRW Universe.

In Chapter 5 we consider the radiation transfer equation in the presence of gravitational waves. We first formulate the linearized equations in the presence of a single Fourier mode of gravitational waves. We prove that there exists a choice of variables that reduces the problem of temperature and polarization anisotropies to only two functions of time $\alpha(\eta)$ and $\beta(\eta)$. Section 5.2 is devoted to further analysis of the radiative transfer equations. The main result of this section is the reduction of coupled integro-differential equations to a single integral equation of Voltairre type. Essentially, the entire problem of the CMB polarization is reduced to a single integral equation. This allows us to use simple analytical approximations and give transparent physical interpretation. In Section 5.3 we generalize the analysis to a superposition of random Fourier modes with arbitrary wavevectors. We derive (and partially rederive the previously known) expressions for multipole coefficients $a^X_{\ell m}$ of the radiation field. We show that the statistical properties of the multipole coefficients are fully determined by the

statistical properties of the underlying gravitational perturbations. This section contains the expressions for general correlation and cross-correlation functions $C_\ell^{XX'}$ for invariants of the radiation field. We work out astrophysical applications in Sec. 5.4 and Sec. 5.5 where we discuss the effects of recombination and reionization era, respectively. Although all our main conclusions are supported by exact numerical calculations, we show the origin of these conclusions and essentially derive them by developing and using semi-analytical approximations. The expected amplitudes, shapes, oscillatory features, etc. of all correlation functions as functions of ℓ are under analytical control. The central point of this analysis is the TE correlation function. We show that, at lower multipoles ℓ, the TE correlation function must be negative (anticorrelation), if it is induced by gravitational waves, and positive, if it is induced by density perturbations. We argue that this difference in sign of TE correlations can be a signature more valuable observationally than the presence or absence of the BB correlations. This is because the TE signal is about two orders of magnitude larger than the expected BB signal and is much easier to measure. We summarize the competing effects of density perturbations in Appendix F.

Theoretical findings are compared with observations in Sec. 5.6. In the context of relic gravitational waves it is especially important that the WMAP team [34] stresses (even if for a different reason) the actual detection of the TE anticorrelation near $\ell \approx 30$. We show that this is possible only in the presence of a significant amount of relic gravitational waves (within the framework of all other common assumptions). We analyze the CMB data and suggest models with significant amounts of gravitational waves that are consistent with the measured TT, TE and EE correlation functions. Our final conclusion is that there is evidence of the presence of relic gravitational waves in the already available CMB data, and further study of the TE correlation at lower ℓ's has the potential of a firm positive answer.

Chapter 2

Gravitational Waves

In this chapter we will give a brief introduction to gravitational waves as well as introduce the basic notations that will be used in following chapters.

2.1 Gravitational waves in Vacuum

In General Relativity the gravitational field is completely characterized by the metric tensor (metric) $g_{\mu\nu}$ [1, 2, 3]. Choosing a coordinate system x^α the invariant interval between two infinitely close events x^α and $x^\alpha + dx^\alpha$ in space-time is given by [1]

$$ds^2 = g_{\mu\nu}(x^\alpha)dx^\mu dx^\nu.$$

In a gravitational field, specified by a metric, a free test particle moves along geodesic lines which are specified by the geodesic equations. On the other hand the gravitational field itself (i.e. the metric) is produced by matter and is coupled to matter fields (to the components of the stress energy tensor) through the Einstein equations.

In the context of linearized general relativity in flat space time (vacuum), the gravitational field $h_{\mu\nu}(x^\alpha)$ represents a small perturbation (i.e. $|h_{\mu\nu}| \ll 1$) to a flat space time:

$$ds^2 = [\eta_{\mu\nu} + h_{\mu\nu}(x^\alpha)]\, dx^\mu dx^\nu, \tag{2.1}$$

[1]Here $x^0 = ct$ denotes the time coordinate, and x^i denote the three spatial coordinates. The Greek indices run from 0 to 3, while the Latin indices run from 1 to 3, and the usual Einstein summation rule is implied

where $\eta_{\mu\nu} = diag(-1, 1, 1, 1)$ is the Minkowski metric tensor for a flat space time.

The simplest plane wave solution to the linearized Einstein equations in vacuum (with an appropriate coordinate condition) for $h_{\mu\nu}$ is given by [2]

$$h_{\mu\nu}(x^\alpha) = Re\left[A_{\mu\nu}e^{in_\alpha x^\alpha}\right],$$

Where $A_{\mu\nu}$ (complex amplitude) and n_α (wavevector) are constants satisfying the constraints

$$n_\alpha n^\alpha = 0, \quad A_{\mu\alpha}n^\alpha = 0,$$

(note that the first of the above constraints implies that the gravitational wave propagates with the speed of light c.)

To the above four constraints on $A_{\mu\alpha}$, using the remaining freedom in choosing the coordinate system, it is possible to impose four additional independent constraints

$$A_{0\alpha} = 0, \quad A^\alpha_\alpha = 0.$$

Thus, out of the initial ten degrees of freedom for the quantity $A_{\mu\nu}$ (since $A_{\mu\nu}$ is symmetric 4×4 tensor), due to the constraints, we are left with only two independent degrees of freedom. These two degrees of freedom correspond to the two possible linearly independent polarization states of a gravitational wave. An arbitrary plane gravitational wave can be decomposed into two independent polarization states

$$A_{\mu\nu} = \sum_{s=1,2} \overset{s}{h}\overset{s}{p}_{\mu\nu},$$

where $\overset{s}{p}_{\mu\nu}$ are any two linearly independent polarization tensors (satisfying the same set of constraints as $A_{\mu\nu}$, hence $\overset{s}{p}_{0\mu} = 0$), and $\overset{s}{h}$ are their corresponding (complex) amplitudes.

The two independent linear polarization states of a plane wave can be described by two real polarization tensors

$$\overset{1}{p}_{ij}(\mathbf{n}) = l_i l_j - m_i m_j, \quad \overset{2}{p}_{ij}(\mathbf{n}) = l_i m_j + m_i l_j, \tag{2.2}$$

where spatial vectors $(\mathbf{l}, \mathbf{m}, \mathbf{n}/n)$ are unit and mutually orthogonal vectors. These polarization tensors (2.2) satisfy the conditions

$$\overset{s}{p}_{ij}\, \delta^{ij} = 0, \quad \overset{s}{p}_{ij}\, n^i = 0, \quad \overset{s'}{p}_{ij} \overset{s}{p}^{ij} = 2\delta_{s's}. \tag{2.3}$$

The eigenvectors of $\overset{1}{p}_{ij}$ are l_i and m_i, whereas the eigenvectors of $\overset{2}{p}_{ij}$ are $l_i + m_i$ and $l_i - m_i$. In both cases, the first eigenvector has the eigenvalue $+1$, whereas the second eigenvector has the eigenvalue -1.

Due to the linear nature of the problem, a general gravitational wave field can be thought of as a linear superposition of plane gravitational waves. Thus, an arbitrary gravitational wave field (i.e. an arbitrary solution to the vacuum Einstein equations with appropriate coordinate constraints) can be Fourier decomposed as:

$$h_{\mu\nu}\left(x^\alpha\right) = \frac{1}{(2\pi)^{3/2}} \int_{-\infty}^{+\infty} \frac{d^3\mathbf{n}}{\sqrt{2n}} \sum_{s=1,2} Re\left[\overset{s}{h}\left(\mathbf{n}\right) \overset{s}{p}_{\mu\nu}\left(\mathbf{n}\right) e^{in_\alpha x^\alpha}\right],$$

where $n = \sqrt{\delta_{ij} n^i n^j}$. After the Fourier decomposition each individual mode can be analyzed separately.

2.2 Gravitational waves in cosmology

We now shift our attention to gravitational waves in the cosmological context. Here we summarize some properties of cosmological perturbations of quantum-mechanical origin. We will need formulas from this section for our further calculations.

2.2.1 Basic definitions

In this work we shall restrict our analysis to homogeneous and isotropic cosmological models. As usual (for more details, see, for example, [36]), we write the perturbed gravitational field of a flat Friedmann-Lemaître-Robertson-Walker (FLRW) universe in the form

$$ds^2 = -c^2 dt^2 + a^2(t)(\delta_{ij} + h_{ij}) dx^i dx^j = a^2(\eta)\left[-d\eta^2 + (\delta_{ij} + h_{ij}) dx^i dx^j\right]. \tag{2.4}$$

The metric of the unperturbed background cosmological model is fully determined by a single function $a(\eta)$ (the scale factor). The scale factor $a(\eta)$ is governed by matter with the unperturbed values of energy density ϵ_0 and pressure p_0:

$$\begin{aligned} \frac{3}{a^4}\left(\frac{da}{d\eta}\right)^2 &= \kappa\epsilon_0 \\ -\frac{1}{a^2}\left[2\frac{d}{d\eta}\left(\frac{1}{a}\frac{da}{d\eta}\right)+\left(\frac{1}{a}\frac{da}{d\eta}\right)^2\right] &= \kappa p_0 \end{aligned}$$

where $\kappa = 8\pi G/c^4$. The Hubble parameter is $H = \frac{1}{a}\frac{da}{dt} = \frac{c}{a^2}\frac{da}{d\eta}$. Coupled with the effective equation of state $p_0 = p_0(\epsilon_0)$ (which in the simplest cases is of the form $p_0 = q\epsilon_0$ where $q = \text{const}$), the above equations allow us to calculate the scale factor. In the simplest cases the scale factor behaves as a simple power law function $a(\eta) = l_o|\eta|^n$. For example in an universe filled with cold matter ($p_0 = 0$), the scale factor behaves as $a(\eta) \propto \eta^2$. In a universe filled with radiation ($p_0 = \epsilon_0/3$) the scale factor behaves as $a(\eta) \propto \eta$. We shall discuss a more realistic model with both matter and radiation in the next sub section.

We shall denote the present moment of time by $\eta = \eta_R$ and define it by the observed quantities, for example, by today's value of the Hubble parameter $H_0 = H(\eta_R)$. In addition, we take the present day value of the scale factor to be $a(\eta_R) = 2l_H$, where $l_H = c/H_0$.

The functions $h_{ij}(\eta, \mathbf{x})$ describing the perturbations to the unperturbed FLRW Universe can be expanded over spatial Fourier harmonics $e^{\pm i\mathbf{n}\cdot\mathbf{x}}$, where $\mathbf{n}$ is a dimensionless time independent wave-vector. The wavenumber n is $n = (\delta_{ij}n^i n^j)^{1/2}$. The wavelength λ, measured in units of laboratory standards, is related to n by $\lambda = 2\pi a/n$. The waves whose wavelengths today are equal to today's Hubble radius carry the wavenumber $n_H = 4\pi$. Shorter waves have larger n's and longer waves have smaller n's.

The often used dimensional wavenumber k, defined by $k = 2\pi/\lambda(\eta_R)$ in terms of today's wavelength $\lambda(\eta_R)$, is related to n by a simple formula

$$k = \frac{n}{2l_H} \approx n\left(1.66 \times 10^{-4}\ h\right)\text{Mpc}^{-1}.$$

The expansion of the field $h_{ij}(\eta, \mathbf{x})$ over Fourier components $\mathbf{n}$ requires a specification of polarization tensors $\overset{s}{p}_{ij}(\mathbf{n})$ (s = 1, 2). They have different forms depending on whether the functions $h_{ij}(\eta, \mathbf{x})$ represent gravitational waves, rotational perturbations, or density perturbations.

As was mentioned in the previous section, in the case of gravitational waves, two independent linear polarization states can be described by two real polarization tensors (2.2). In terms of spherical coordinates (θ, ϕ), we choose for $(\mathbf{l}, \mathbf{m}, \mathbf{n}/n)$ the right-handed triplet:

$$\begin{aligned} \mathbf{l} &= (\cos\theta\cos\phi,\ \cos\theta\sin\phi,\ -\sin\theta), \\ \mathbf{m} &= (-\sin\phi,\ \cos\phi,\ 0), \\ \mathbf{n}/n &= (\sin\theta\cos\phi,\ \sin\theta\sin\phi,\ \cos\theta). \end{aligned} \tag{2.5}$$

With this convention, vector $\mathbf{n}$ points along the wavevector in the direction defined by (θ, ϕ) on the sky, vector $\mathbf{l}$ points along a meridian in the direction of increasing θ, while the vector $\mathbf{m}$ points along a parallel in the direction of increasing ϕ. With this specification, polarization tensors (2.2) will be called the '+' and '×' polarizations respectively. The eigenvectors of '+' polarization correspond to north-south and east-west directions, whereas the '×' polarization describes the directions rotated by 45°.

With a fixed $\mathbf{n}$, the choice of vectors $\mathbf{l}, \mathbf{m}$ given by Eq. (2.5) is not unique. The vectors can be subject to continuous and discrete transformations. The continuous transformation is performed by a rotation of the pair $\mathbf{l}, \mathbf{m}$ in the plane orthogonal to $\mathbf{n}$:

$$\mathbf{l}' = \mathbf{l}\cos\psi + \mathbf{m}\sin\psi, \quad \mathbf{m}' = -\mathbf{l}\sin\psi + \mathbf{m}\cos\psi, \tag{2.6}$$

where ψ is an arbitrary angle. The discrete transformation is described by the flips of the $\mathbf{l}, \mathbf{m}$ vectors:

$$\mathbf{l}' = -\mathbf{l}, \quad \mathbf{m}' = \mathbf{m} \qquad \text{or} \qquad \mathbf{l}' = \mathbf{l}, \quad \mathbf{m}' = -\mathbf{m}. \tag{2.7}$$

When (2.6) is applied, polarization tensors (2.2) transform as

$$\begin{aligned} \overset{1}{p'}_{ij}(\mathbf{n}) &= l'_i l'_j - m'_i m'_j = \overset{1}{p}_{ij}(\mathbf{n})\cos 2\psi + \overset{2}{p}_{ij}(\mathbf{n})\sin 2\psi, \\ \overset{2}{p'}_{ij}(\mathbf{n}) &= l'_i m'_j + m'_i l'_j = -\overset{1}{p}_{ij}(\mathbf{n})\sin 2\psi + \overset{2}{p}_{ij}(\mathbf{n})\cos 2\psi, \end{aligned} \tag{2.8}$$

and when (2.7) is applied they transform as

$$\overset{1}{p'}_{ij}(\mathbf{n}) = \overset{1}{p}_{ij}(\mathbf{n}), \qquad \overset{2}{p'}_{ij}(\mathbf{n}) = -\overset{2}{p}_{ij}(\mathbf{n}). \tag{2.9}$$

Later in this section and in Appendix C, we are discussing the conditions under which the averaged observational properties of a random field $h_{ij}(\mathbf{n}, \eta)$ are symmetric with respect to rotations around the axis $\mathbf{n}/n$ and with respect to mirror reflections of the axes. Formally, this is expressed as the requirement of symmetry of the g.w. field correlation functions with respect to transformations (2.6) and (2.7).

In this work we will also be dealing with density perturbations. In this case, the polarization tensors are [37]

$$\overset{1}{p}_{ij} = \sqrt{\frac{2}{3}}\delta_{ij}, \quad \overset{2}{p}_{ij} = -\sqrt{3}\frac{n_i n_j}{n^2} + \frac{1}{\sqrt{3}}\delta_{ij}. \tag{2.10}$$

These polarization tensors satisfy the last of the conditions (2.3).

In the rigorous quantum-mechanical version of the theory, the functions h_{ij} are quantum-mechanical operators. We write them in the form:

$$h_{ij}(\eta, \mathbf{x}) = \frac{C}{(2\pi)^{3/2}} \int_{-\infty}^{+\infty} \frac{d^3\mathbf{n}}{\sqrt{2n}} \sum_{s=1,2} \left[\overset{s}{p}_{ij}(\mathbf{n})\, \overset{s}{h}_n(\eta)\, e^{i\mathbf{n}\cdot\mathbf{x}}\, \overset{s}{c}_{\mathbf{n}} + \overset{s}{p}_{ij}^{\,*}(\mathbf{n}) \overset{s}{h}_n^{\,*}(\eta) e^{-i\mathbf{n}\cdot\mathbf{x}}\, \overset{s\dagger}{c}_{\mathbf{n}} \right], \tag{2.11}$$

where the annihilation and creation operators, $\overset{s}{c}_{\mathbf{n}}$ and $\overset{s\dagger}{c}_{\mathbf{n}}$, satisfy the relationships

$$[\overset{s'}{c}_{\mathbf{n}}, \ \overset{s\dagger}{c}_{\mathbf{n}'}] = \delta_{s's}\delta^{(3)}(\mathbf{n} - \mathbf{n}'), \quad \overset{s}{c}_{\mathbf{n}} |0\rangle = 0. \tag{2.12}$$

The initial vacuum state $|0\rangle$ of perturbations is defined at some moment of time η_0 in the remote past, long before the onset of the process of superadiabatic amplification. This quantum state is maintained (in the Heisenberg picture) until now. For gravitational waves, the normalization constant is $C = \sqrt{16\pi} l_{Pl}$.

The relationships (2.12) determine the expectation values and correlation functions of cosmological perturbations themselves, and also of the CMB's temperature and

polarization anisotropies caused by these cosmological perturbations. In particular, the variance of metric perturbations is given by

$$\langle 0|\, h_{ij}(\eta,\mathbf{x})h^{ij}(\eta,\mathbf{x})\,|0\rangle = \frac{\mathcal{C}^2}{2\pi^2}\int\limits_0^\infty n^2 \sum_{s=1,2} |\overset{s}{h}_n(\eta)|^2 \frac{dn}{n}. \tag{2.13}$$

The quantity

$$h^2(n,\eta) = \frac{\mathcal{C}^2}{2\pi^2} n^2 \sum_{s=1,2} |\overset{s}{h}_n(\eta)|^2 = \frac{1}{2}\sum_{s=1,2} |\overset{s}{h}(n,\eta)|^2, \tag{2.14}$$

is called the metric power spectrum. Note that we have introduced

$$\overset{s}{h}(n,\eta) = \frac{\mathcal{C}}{\pi} n\, \overset{s}{h}_n(\eta). \tag{2.15}$$

The quantity (2.14) gives the mean-square value of the gravitational field perturbations in a logarithmic interval of n. The spectrum of the root-mean-square (rms) amplitude $h(n,\eta)$ is determined by the square root of Eq. (2.14). Having evolved the classical mode functions $\overset{s}{h}_n(\eta)$ up to some arbitrary instant of time η (for instance, today $\eta = \eta_R$) one can find the power spectrum $h(n,\eta)$ at that instant of time. For the today's spectrum in terms of frequency ν measured in Hz, $\nu = nH_0/4\pi$, we use the notation $h_{rms}(\nu)$.

In our further applications we will also need the power spectrum of the first time-derivative of metric perturbations:

$$\langle 0|\, \frac{\partial h_{ij}(\eta,\mathbf{x})}{\partial\eta}\frac{\partial h^{ij}(\eta,\mathbf{x})}{\partial\eta}\,|0\rangle = \frac{1}{2}\int\limits_0^\infty \sum_{s=1,2}\left|\frac{d\,\overset{s}{h}(n,\eta)}{d\eta}\right|^2 \frac{dn}{n}. \tag{2.16}$$

To simplify calculations, in our further analysis we will be using a 'classical' version of the theory, whereby the quantum-mechanical operators $\overset{s}{c}_{\mathbf{n}}$ and $\overset{s\dagger}{c}_{\mathbf{n}}$ are treated as classical random complex numbers $\overset{s}{c}_{\mathbf{n}}$ and $\overset{s*}{c}_{\mathbf{n}}$. It is assumed that they satisfy the relationships analogous to (2.12):

$$\langle \overset{s}{c}_{\mathbf{n}}\rangle = \langle \overset{s'*}{c}_{\mathbf{n}'}\rangle = 0,\quad \langle \overset{s}{c}_{\mathbf{n}}\overset{s'*}{c}_{\mathbf{n}'}\rangle = \langle \overset{s*}{c}_{\mathbf{n}}\overset{s'}{c}_{\mathbf{n}'}\rangle = \delta_{ss'}\delta^{(3)}(\mathbf{n}-\mathbf{n}'),\quad \langle \overset{s}{c}_{\mathbf{n}}\overset{s'}{c}_{\mathbf{n}'}\rangle = \langle \overset{s*}{c}_{\mathbf{n}}\overset{s'*}{c}_{\mathbf{n}'}\rangle = 0, \tag{2.17}$$

where the averaging is performed over the ensemble of all possible realizations of the random field (2.11).

The relationships (2.17) are the only statistical assumptions that we make. They fully determine all the expectations values and correlation functions that we will calculate, both for cosmological perturbations and for the induced CMB fluctuations. For example, the metric power spectrum (2.14) follows now from the calculation:

$$\frac{1}{2}\left\langle h_{ij}(\eta,\mathbf{x})h^{ij}(\eta,\mathbf{x})\right\rangle = \frac{\mathcal{C}^2}{2\pi^2}\int\limits_0^\infty n^2 \sum_{s=1,2} |\overset{s}{h}_n(\eta)|^2 \frac{dn}{n}. \tag{2.18}$$

The quantities $|\overset{s}{h}_n(\eta)|^2$ are responsible for the magnitude of the mean-square fluctuations of the field in the corresponding polarization states s. In general, the assumption of statistical independence of two linear polarization components in one polarization basis is not equivalent to this assumption in another polarization basis. As we show in Appendix C, statistical properties are independent of the basis (i.e. independent of ψ, Eq. (2.8)), if the condition

$$|\overset{+}{h}_n(\eta)|^2 = |\overset{\times}{h}_n(\eta)|^2 \tag{2.19}$$

is satisfied. As for the discrete transformations (2.9), they leave the g.w. field correlation functions unchanged.

In our further discussion of the CMB fluctuations it will be convenient to use also the expansion of h_{ij} over circular, rather than linear, polarization states. In terms of definitions (2.2), the left ($s = L$) and right ($s = R$) circular polarization states are described by the complex polarization tensors

$$\begin{array}{ll} \overset{L}{p}_{ij} = \frac{1}{\sqrt{2}}\left(\overset{1}{p}_{ij} + i\,\overset{2}{p}_{ij}\right), & \overset{R}{p}_{ij} = \frac{1}{\sqrt{2}}\left(\overset{1}{p}_{ij} - i\,\overset{2}{p}_{ij}\right), \\ \overset{L}{p}{}^{*}_{ij} = \overset{R}{p}_{ij}, & \overset{R}{p}{}^{*}_{ij} = \overset{L}{p}_{ij}, \end{array} \tag{2.20}$$

satisfying the conditions (for $s = L, R$)

$$\overset{s}{p}_{ij}\,\delta^{ij} = 0, \quad \overset{s}{p}_{ij}\,n^i = 0, \quad \overset{s'}{p}_{ij}\,\overset{s}{p}{}^{ij*} = 2\delta_{s's}. \tag{2.21}$$

A continuous transformation (2.6) brings the tensors (2.20) to the form

$$\overset{L}{p}{}'_{ij} = \overset{L}{p}_{ij}\,e^{-i2\psi}, \qquad \overset{R}{p}{}'_{ij} = \overset{R}{p}_{ij}\,e^{i2\psi}. \tag{2.22}$$

Functions transforming according to the rule (2.22) are called the spin-weighted functions of spin +2 and spin -2, respectively [38, 39, 40]. A discrete transformation (2.7) applied to (2.20) interchanges the left and right polarization states:

$$\overset{L}{p}{}'_{ij} = \overset{R}{p}_{ij}, \qquad \overset{R}{p}{}'_{ij} = \overset{L}{p}_{ij}\ . \tag{2.23}$$

The assumption of statistical independence of two linear polarization states is, in general, not equivalent to the assumption of statistical independence of two circular polarization states. Moreover, it is shown in Appendix C that symmetry between left and right is violated, unless

$$|\overset{L}{h}_n(\eta)|^2 = |\overset{R}{h}_n(\eta)|^2. \tag{2.24}$$

However, if conditions (2.19), (2.24) are satisfied, statistical properties of the random g.w. field remain unchanged under transformations from one basis to another, including the transitions between linear and circular polarizations. The summation over s in the power spectra such as (2.18) can be replaced by the multiplicative factor 2. Moreover, the mode functions $\overset{s}{h}_n(\eta)$ for two independent polarization states will be equal up to a constant complex factor $e^{i\alpha}$. This factor can be incorporated in the redefinition of random coefficients $\overset{s}{c}_{\mathbf{n}}$ without violating the statistical assumptions (2.17). After this, the index s over the mode functions can be dropped:

$$\overset{s}{h}_n(\eta) = h_n(\eta). \tag{2.25}$$

There is no special reason for the quantum-mechanical generating mechanism to prefer one polarization state over another. It is natural to assume that the conditions (2.19), (2.24) hold true for relic gravitational waves, but in general they could be violated. In calculations below we often use these equalities, but we do not enforce them without warning.

2.2.2 Mode functions and power spectra

The perturbed Einstein equations give rise to the g.w. equation for the mode functions $\overset{s}{h}_n(\eta)$ [41]:

$$\overset{s}{h}{}''_n + 2\frac{a'}{a}\overset{s}{h}{}'_n + n^2\overset{s}{h}_n = 0. \tag{2.26}$$

This equation can be transformed to the equation for a parametrically disturbed oscillator [17]:

$$\overset{s}{\mu}{}''_n + \overset{s}{\mu}_n\left[n^2 - \frac{a''}{a}\right] = 0, \tag{2.27}$$

where $\overset{s}{\mu}_n(\eta) \equiv a(\eta)\overset{s}{h}_n(\eta)$ and $' = d/d\eta = (a/c)d/dt$. (In this work, we ignore anisotropic stresses. For the most recent account of this subject, which includes earlier references, see [42].) Clearly, the behaviour of the mode functions depend on the gravitational 'pumping' field $a(\eta)$, regardless of the physical nature of the matter sources driving the cosmological scale factor $a(\eta)$. Observational data about relic gravitational waves allow us to make direct inferences about $H(\eta)$ and $a(\eta)$ [43], and it is only through extra assumptions that we can make inferences about such things as, say, the scalar field potential (if it is relevant at all).

Previous analytical calculations (see, for example, [44, 36] and references there) were based on models where $a(\eta)$ consists of pieces of power-law evolution

$$a(\eta) = l_o|\eta|^{1+\beta}, \tag{2.28}$$

where l_o and β are constants. The functions $a(\eta)$, $a'(\eta)$, $\overset{s}{h}_n(\eta)$, $\overset{s}{h}{}'_n(\eta)$ were continuously joined at the transition points between various power-law eras.

It is often claimed in the literature that this method of joining the solutions is unreliable, unless the wavelength is "much longer than the time taken for the transition to take place". Specifically, it is claimed that the joining procedure leads to huge errors in the g.w. power spectrum for short waves. It is important to show that these claims

are incorrect. As an example, we will consider the transition between the radiation-dominated and matter-dominated eras.

The exact scale factor, which accounts for the simultaneous presence of matter, $\rho_m \propto a(\eta)^{-3}$, and radiation, $\rho_\gamma \propto a(\eta)^{-4}$, has the form

$$a(\eta) = 2l_H \left(\frac{1+z_{eq}}{2+z_{eq}}\right) \eta \left(\eta + \frac{2\sqrt{2+z_{eq}}}{1+z_{eq}}\right), \tag{2.29}$$

where z_{eq} is the redshift of the era of equality of energy densities in matter and radiation $\rho_m(z_{eq}) = \rho_\gamma(z_{eq})$,

$$1 + z_{eq} = \frac{a(\eta_R)}{a(\eta_{eq})} = \frac{\Omega_m}{\Omega_\gamma}.$$

For this model, the values of parameter η at equality and today are given by the expressions

$$\eta_{eq} = \left(\sqrt{2}-1\right)\frac{\sqrt{2+z_{eq}}}{1+z_{eq}}, \qquad \eta_R = 1 - \frac{\sqrt{2+z_{eq}}}{1+z_{eq}} + \frac{1}{1+z_{eq}}.$$

The current observations favour the value $z_{eq} \approx 3 \times 10^3$ [45].

The piece-wise approximation to the scale factor (2.29) has the form

$$a(\eta) = \frac{4l_H}{\sqrt{1+z_{eq}}}\eta, \quad \eta \le \eta_{eq}; \qquad a(\eta) = 2l_H\left(\eta + \eta_{eq}\right)^2, \quad \eta \ge \eta_{eq}, \tag{2.30}$$

where η_{eq} and η_R for this joined $a(\eta)$ are given by $\eta_{eq} = 1/2\sqrt{1+z_{eq}}$ and $\eta_R = 1 - 1/2\sqrt{1+z_{eq}}$. It can be seen from (2.29) and (2.30) that the relative difference between the two scale factors is very small in the deep radiation-dominated era, $\eta \ll 1/\sqrt{z_{eq}}$, and in the deep matter-dominated era, $\eta \gg 1/\sqrt{z_{eq}}$. But the difference reaches about 25% at times near equality.

The initial conditions for the g.w. equation (2.27) are the same in the models (2.29), (2.30) and they are determined by quantum-mechanical assumptions at the stage (which we call the i-stage) preceding the radiation epoch. The i-stage has finished, and the radiation-dominated stage has started, at some η_i with a redshift z_i. The numerical value of z_i should be somewhere near 10^{29} (see below).

The initial conditions at the radiation-dominated stage can be specified at that early time η_i or, in practice, for numerical calculations, at much latter time, as long as the appropriate g.w. solution is taken as [36]

$$\overset{s}{\mu}_n(\eta) = -2iB\sin n\eta, \quad \overset{s}{\mu}_n{}'(\eta) = -2inB\cos n\eta, \tag{2.31}$$

where

$$B = F(\beta)\left(\frac{n\sqrt{1+z_{eq}}}{1+z_i}\right)^{\beta},$$

and $F(\beta)$ is a slowly varying function of the constant parameter β, $|F(-2)| = 2$. Parameter β describes the power-law evolution at the i-stage and determines the primordial spectral index n, $n = 2\beta + 5$. In particular, $\beta = -2$ corresponds to the flat (scale-invariant) primordial spectrum $n = 1$.

For numerical calculations we use the constant B in the form:

$$B = 2\left(\frac{4\pi\sqrt{1+z_{eq}}}{1+z_i}\right)^{\beta}\left(\frac{n}{n_H}\right)^{\beta}. \tag{2.32}$$

The wave-equation (2.27) with the scale factor (2.29) can not be solved in elementary functions. However, it can be solved numerically using the initial data (2.31). Concretely, we have imposed the initial data (2.31) at $\eta_r = 10^{-6}$, which corresponds to the redshift $z \approx 3 \times 10^7$, and have chosen $z_{eq} = 6 \times 10^3$ for illustration. Numerical solutions for $h_n(\eta)/h_n(\eta_r)$ characterized by different wavenumbers n are shown by solid lines in Fig. 2.1. We should compare these solutions with the joined solutions found on the joined evolution (2.30) for the same wavenumbers.

The piece-wise scale factor (2.30) allows one to write down the piece-wise analytical solutions to the g.w. equation (2.27):

$$\mu_n(\eta) = \begin{cases} -2iB\sin n\eta, & \eta \le \eta_{eq} \\ \sqrt{n(\eta+\eta_{eq})}\left[A_n J_{3/2}\left(n(\eta+\eta_{eq})\right) - iB_n J_{-3/2}\left(n(\eta+\eta_{eq})\right)\right], & \eta \ge \eta_{eq}, \end{cases} \tag{2.33}$$

where $J_{3/2}, J_{-3/2}$ are Bessel functions. The coefficients A_n and B_n are calculated from the condition of continuous joining of μ_n and μ_n' at η_{eq} [36]:

$$A_n = -i\sqrt{\tfrac{\pi}{2}}\tfrac{B}{4y_2^2}\left[(8y_2^2-1)\sin y_2 + 4y_2\cos y_2 + \sin 3y_2\right],$$
$$B_n = -\sqrt{\tfrac{\pi}{2}}\tfrac{B}{4y_2^2}\left[(8y_2^2-1)\cos y_2 - 4y_2\sin y_2 + \cos 3y_2\right],$$

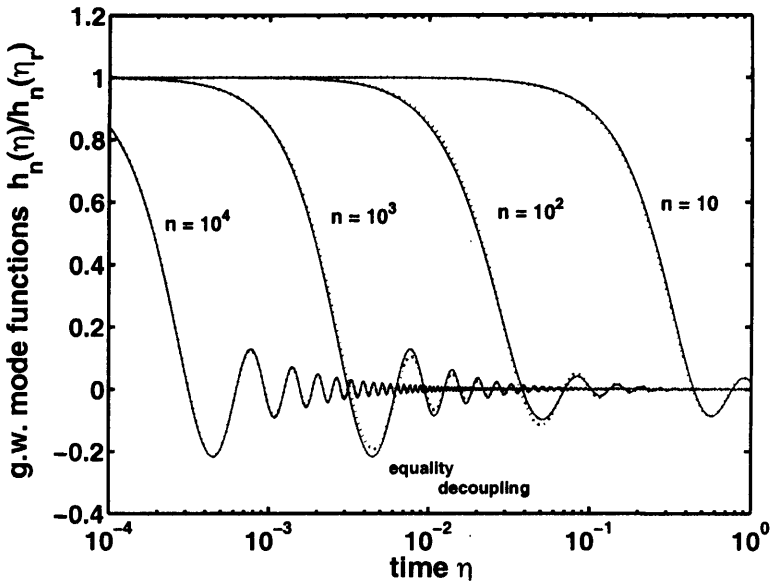

Figure 2.1: The g.w. mode functions $h_n(\eta)/h_n(\eta_r)$ in a matter-radiation universe. The solid curves are numerically calculated solutions on the scale factor (2.29), while the dotted curves are analytical solutions on the scale factor (2.30).

where $y_2 = n\eta_{eq}$. In Fig. 2.1 we show the joined solutions (2.33) by dotted curves.

It is clear from Fig. 2.1 that the g.w. solutions as functions of η are pretty much similar in the two models. The solid and dotted curves are slightly different near equality (where the relative difference between the scale factors is noticeably large) and only for modes that entered the Hubble radius around or before equality. Moreover, the g.w. amplitudes of the modes that entered the Hubble radius before equality gradually equalize in course of later evolution. There is nothing like a huge underestimation or overestimation of the high-frequency g.w. power that was alleged to happen in the joined model.

It is easy to understand these features. Let us start from waves that entered the Hubble radius well after equality, i.e. waves with wavenumbers $n/n_H \ll \sqrt{1+z_{eq}}$. As long as these waves are outside the Hubble radius, their amplitudes remain constant and equal in the two models, despite the fact that the scale factors are somewhat different near equality. The waves start oscillating in the regime where the relative difference between (2.29) and (2.30) is small, and therefore the mode functions, as

functions of η, coincide.

The waves with wavenumbers $n/n_H \gg \sqrt{1+z_{eq}}$ enter the Hubble radius well before the equality. They oscillate in the WKB regime according to the law $h_n(\eta) \propto e^{-in\eta}/a(\eta)$, having started with equal amplitudes in the two models. Near equality, the mode functions are different in the two models, as much as the scale factors are different. But the relative difference between (2.29) and (2.30) decreases with time, and therefore the mode functions in the two models gradually equalize. The amplitudes of these mode functions, as well as the scale factors (2.29), (2.30), are exactly equal today. The only difference between these high-frequency mode functions is in phase, that is, in different numbers of cycles that they experienced by today. This is because the moment of time defined as 'today' in the two models is given, in terms of the common parameter η, by slightly different values of η_R.

Finally, for intermediate wavenumbers $n/n_H \approx \sqrt{1+z_{eq}}$, the modes enter the Hubble radius when the scale factors differ the most. Therefore, they start oscillating with somewhat different amplitudes. The difference between these mode functions is noticeable by the redshift of decoupling z_{dec} (characterized by somewhat different values of η_{dec}), as shown in Fig. 2.1. The difference survives until today, making the graph for the g.w. power spectrum (2.14) a little smoother (in comparison with that derived from the joined model) in the region of frequencies 10^{-16} Hz that correspond to the era of equality.

Having demonstrated that the use of joined analytical solutions is well justified, and the previously plotted graphs for $h_{rms}(\nu)$ and $\Omega_{gw}(\nu)$ are essentially correct, we shall now exhibit the more accurate graphs based on numerical calculations with the initial conditions (2.31), (2.32). We adopt $z_{eq} = 3 \times 10^3$ and $H_0 = 75\frac{km}{s}/Mpc$ [45]. We adjust the remaining free constant z_i in such a way that the temperature correlation function $\ell(\ell+1)C_\ell/2\pi$ at $\ell = 2$ is equal to 211 μK^2 [46]. This requires us to take $z_i = 1.0 \times 10^{29}$ for $\beta = -2$ and $z_i = 2.4 \times 10^{30}$ for $\beta = -1.9$.

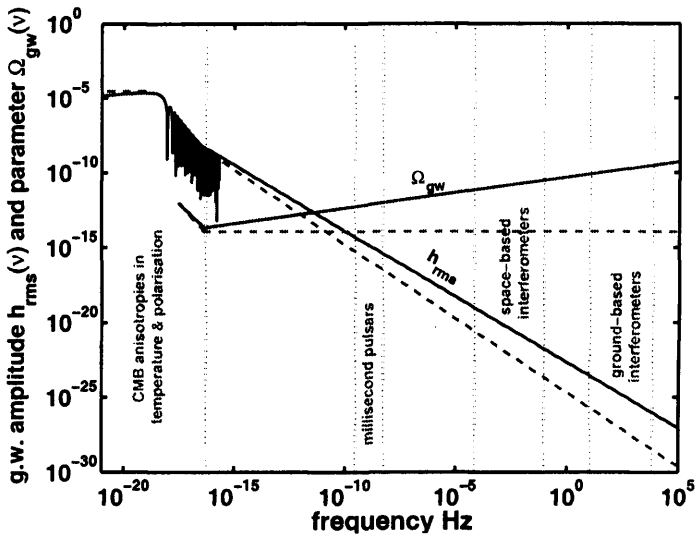

Figure 2.2: The present-day spectra for $h_{rms}(\nu)$ and $\Omega_{gw}(\nu)$. The solid lines correspond to the primordial spectral index $\beta = -1.9$, i.e. n = 1.2, while the dashed lines are for $\beta = -2$, i.e. n = 1.

The graphs for today's spectra, normalised as stated above, are shown in Fig. 2.2. In order to keep the figure uncluttered, the oscillations of $h_{rms}(\nu)$ are shown only at low frequencies, while the oscillations of $\Omega_{gw}(\nu)$ are not shown at all. We have also indicated possible detection techniques in various frequency bands.

The function $\Omega_{gw}(\nu)$ is the spectral value of the cosmological parameter Ω_{gw} [44]:

$$\Omega_{gw}(\nu_1, \nu_2) = \frac{\rho_{gw}(\nu_1, \nu_2)}{\rho_c} = \frac{1}{\rho_c} \int_{\nu_1}^{\nu_2} \rho_{gw}(\nu) \frac{d\nu}{\nu} = \int_{\nu_1}^{\nu_2} \Omega_{gw}(\nu) \frac{d\nu}{\nu},$$

that is,

$$\Omega_{gw}(\nu) = \frac{1}{\rho_c} \rho_{gw}(\nu).$$

Using the high-frequency definition of $\rho_{gw}(\nu)$ (valid only for waves which are significantly shorter than l_H) we derive [44]:

$$\Omega_{gw}(\nu) = \frac{\pi^2}{3} h_{rms}^2(\nu) \left(\frac{\nu}{\nu_H}\right)^2. \tag{2.34}$$

It is this definition of $\Omega_{gw}(\nu)$ that is used for drawing the curves in Fig. 2.2.

We have to warn the reader that a great deal of literature on stochastic g.w. back-

grounds uses the incorrect definition

$$\Omega_{gw}(\nu) = \frac{1}{\rho_c}\frac{d\rho_{gw}(\nu)}{d\ ln\nu},$$

which suggests that the $\Omega_{gw}(\nu)$ parameter is zero if the g.w. energy density $\rho_{gw}(\nu)$ is frequency-independent, regardless of the numerical value of $\rho_{gw}(\nu)$. Then, from this incorrect definition, a formula similar to Eq. (2.34) is often being derived by making further compensating errors.

The higher-frequency part of $h_{rms}(\nu)$ is relevant for direct searches for relic gravitational waves, while the lower-frequency part is relevant to the CMB calculations that we turn to in chapter 5. The direct and indirect methods of detecting relic gravitational waves are considered in a large number of papers (see, for example, [47, 48, 16, 49, 50, 51, 52, 53]). It is important to keep in mind that according to the inflationary theory the horizontal dashed line for $\Omega_{gw}(\nu)$ in Fig. 2.2 should be at a zero level, because it describes the g.w. background with a flat primordial spectrum $\beta = -2$, n = 1. The 'consistency relation' of the inflationary theory demands $r = 0$, i.e. vanishingly small g.w. background, in the limit n = 1.

Chapter 3

Components of the gravitational force in the field of a gravitational wave

3.1 Motion of free charges in the field of electromagnetic wave

To understand the motion of test particles in the field of a gravitational wave it is convenient to start the analysis with the similar problem in electrodynamics. Let us consider the motion of a charged particle in the field of a monochromatic electromagnetic wave. It is known [1] that a charged particle in the electromagnetic field is subject to the electromagnetic Lorentz force $\mathbf{F}$ given by

$$\mathbf{F} = e\mathbf{E} + \frac{e}{c}(\mathbf{v} \times \mathbf{H}). \tag{3.1}$$

The first term in Eq. (3.1) is the electric contribution to the force, while the second term is the magnetic contribution. The ratio of the second term to the first one is of the order of v/c. This means that in the field of a weak electromagnetic wave, i.e. in the field of a wave that gives rise to a small velocity $v/c \ll 1$ of the charged particle, the magnetic contribution to the force F is also small. To find the trajectory of the particle, one has to solve the equations

$$m\frac{d^2\mathbf{x}}{dt^2} = e\mathbf{E} + \frac{e}{c}\left(\frac{d\mathbf{x}}{dt} \times \mathbf{H}\right). \tag{3.2}$$

The character of the trajectory depends on the wave's polarization.

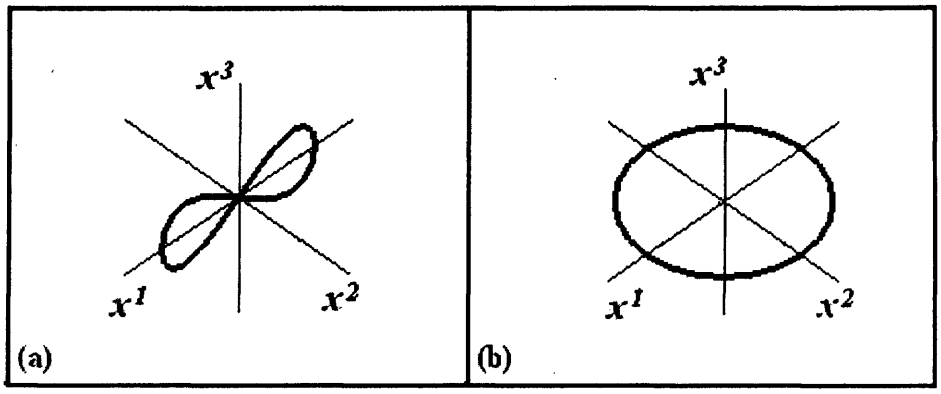

Figure 3.1: The figure a) on the left shows the trajectory of a charged particle in the field of a linearly polarized electromagnetic wave, whereas the figure b) on the right shows the trajectory in the field of a circularly polarized wave.

Let us start with a linearly polarized monochromatic wave of angular frequency ω, propagating in the x^3 direction, with the electric field E oscillating along the x^1 axis. The trajectory of the particle, which is on average at rest, is given by [1]

$$x^1 = -\tfrac{eE}{m\omega^2}\cos\omega t, \quad x^2 = 0, \quad x^3 = \tfrac{eE}{8m\omega^2}\left(\tfrac{eE}{mc\omega}\right)\sin 2\omega t. \tag{3.3}$$

The particle moves in the (x^1, x^3) plane along a symmetric curve, shaped as figure 8, with its main axis oriented in the x^1 direction, see Fig. 3.1a. The electric component of the Lorentz force is dominant, and it drives the particle in the plane of the wave-front, while the magnetic component is responsible for the movement of the particle back and forth in the x^3 direction. For a weak electromagnetic wave, the size of the x^1-amplitude is small in comparison with the wavelength: $\frac{x^1}{\lambda} \sim \frac{eE}{mc\omega} \ll 1$, but the size of the x^3-amplitude is even smaller: $x^3 \sim x^1\left(\frac{x^1}{\lambda}\right)$. The ratio of x^3 and x^1 amplitudes is of the order of $\frac{eE}{mc\omega} \sim \frac{v}{c}$, where v is the characteristic value of the particle's velocity.

A circularly polarized wave provides an exceptional case wherein the magnetic component of the force is inactive; the particle does not have an x^3-component of motion. The trajectory of the particle, which is on average at rest, is given by [1],

$$x^1 = -\tfrac{eE}{m\omega^2}\cos\omega t, \quad x^2 = -\tfrac{eE}{m\omega^2}\sin\omega t, \quad x^3 = 0. \tag{3.4}$$

The particle moves in the (x^1, x^2) plane along a circle, as shown in Fig. 3.1b. In the

general case of an elliptically-polarized wave, the x^3-component of motion is always present. The projection of the trajectory onto the (x^1, x^2) plane forms an ellipse. The ellipse degenerates into a straight line or a circle for a linearly-polarized or a circularly-polarized wave, respectively. We shall see below that there exists an analogy between the considered motion of charged particles in the field of an electromagnetic wave and the motion of test masses in the field of a gravitational wave.

3.2 Motion of a free test mass in the field of a weak gravitational wave

Weak gravitational waves belong to the class of weak gravitational fields:

$$ds^2 = -c^2dt^2 + [\delta_{ij} + h_{ij}]\, dx^i dx^j. \tag{3.5}$$

A general expression for a plane wave incoming from the positive x^3 direction is given by

$$h_{ij} = \overset{1}{p}_{ij} a + \overset{2}{p}_{ij} b, \tag{3.6}$$

where

$$a = h_+ \sin\left(k(x^0 + x^3) + \psi_+\right), \quad b = -h_\times \sin\left(k(x^0 + x^3) + \psi_\times\right), \tag{3.7}$$

and $k = \frac{2\pi}{\lambda} = \frac{2\pi\nu}{c} = \frac{\omega}{c}$ is the wavenumber [1], $x^0 = ct$; ψ_+ and $\psi_\times$ are arbitrary phases. The polarization tensors $\overset{s}{p}_{ij}$ $(s = 1, 2)$ are given by (2.2).

One still has the freedom of turning the coordinate system in the (x^1, x^2) plane by some angle. This transformation mixes the components of the matrix (3.6). Using this freedom (see Appendix A) one can simplify the functions (3.7) in such a way that in the new coordinate system they take the form

$$a = h_+ \sin\left(k(x^0 + x^3) + \psi\right), \quad b = -h_\times \cos\left(k(x^0 + x^3) + \psi\right), \tag{3.8}$$

[1] In this chapter we use k (instead of n) to denote the wavenumber.

where h_+, $h_\times$ are arbitrary amplitudes and ψ is an arbitrary phase. The mutually orthogonal unit vectors l_i, m_i figuring in the expression for the polarization tensors $\overset{s}{p}_{ij}$ (2.2) are orthogonal to the direction of wave propagation (i.e. lie in the (x^1, x^2) plane). They can be chosen to have the components $l_i = (1, 0, 0)$ and $(m_i = 0, 1, 0)$ [2]. We shall call this special coordinate system a frame based on principal axes. Two independent linear polarization states are defined by the conditions $h_+ = 0$ or $h_\times = 0$, and two independent states of circular polarization are defined by $h_+ = h_\times$ or $h_+ = -h_\times$. Specifically, we will be working with the metric

$$ds^2 = -c^2dt^2 + (1+a)dx^{1\,2} + (1-a)dx^{2\,2} - 2b\, dx^1dx^2 + dx^{3\,2}, \tag{3.9}$$

where the functions a and b are given by Eq. (3.8).

The metric (3.9) is written in synchronous coordinates. Therefore, the world lines $x^1, x^2, x^3 = \text{const}$ are time-like geodesics, they represent the histories of free test masses. To be as close as possible to the framework of laboratory physics, and specifically to electrodynamic examples considered in the previous section, we have to introduce a local inertial coordinate system $(\bar{t}, \bar{x}^1, \bar{x}^2, \bar{x}^3)$. Let us associate it with the central world line $x^1 = x^2 = x^3 = 0$. By definition, in the local inertial frame, and along the central geodesic line, the metric tensor takes on the Minkowski values and all first derivatives of the metric tensor vanish. The transformed metric takes on the form

$$\bar{g}_{\mu\nu} = \eta_{\mu\nu} + \textit{terms of the order of } \left(h\frac{\bar{x}^{1\,2} + \bar{x}^{2\,2} + \bar{x}^{3\,2}}{\lambda^2} \right). \tag{3.10}$$

A local inertial frame realizes, as good as we can do in the presence of the gravitational field, a rigid freely falling "box" with a clock in it [2]. The required coordinate

[2]The unit vector l_i, used here and in chapter 2, should not be confused with the the coordinate position of the free test particle also denoted l_i further on in this chapter.

transformation $\bar{x}^\mu = \bar{x}^\mu(x^\nu)$ is given by [29]:

$$\begin{aligned}
\bar{x}^0 &= x^0 + \tfrac{1}{4}\dot{a}\,\left(x^{1\,2} - x^{2\,2}\right) - \tfrac{1}{2}\dot{b}\,x^1x^2,\\
\bar{x}^1 &= x^1 + \tfrac{1}{2}a\,x^1 - \tfrac{1}{2}b\,x^2 + \tfrac{1}{2}\dot{a}\,x^3x^1 - \tfrac{1}{2}\dot{b}\,x^3x^2,\\
\bar{x}^2 &= x^2 - \tfrac{1}{2}a\,x^2 - \tfrac{1}{2}b\,x^1 - \tfrac{1}{2}\dot{a}\,x^3x^2 - \tfrac{1}{2}\dot{b}\,x^3x^1,\\
\bar{x}^3 &= x^3 - \tfrac{1}{4}\dot{a}\,\left(x^{1\,2} - x^{2\,2}\right) + \tfrac{1}{2}\dot{b}\,x^1x^2.
\end{aligned} \tag{3.11}$$

In the above transformation, the functions a, b and their time derivatives $\dot{a} = \frac{1}{c}\frac{\partial a}{\partial t}$, $\dot{b} = \frac{1}{c}\frac{\partial b}{\partial t}$ are evaluated along the world line $x^1 = x^2 = x^3 = 0$. The linear and quadratic terms, as powers of x^α, are unambiguously determined by the conditions of local inertial frame, but the cubic and higher-order corrections are not determined by these conditions. In principle, transformations (3.11) can be used for all values of x^α, but they are physically useful when the values of x^α are sufficiently small, that is, when the cubic and higher-order terms can be neglected.

Let us consider a free test mass riding on a time-like geodesic ($x^1 = l_1$, $x^2 = l_2$, $x^3 = l_3$). Equations (3.11) define the behaviour of this mass with respect to the introduced local inertial frame. Concretely, we have

$$\begin{aligned}
\bar{x}^1(t) &= l_1 + \tfrac{1}{2}\left[h_+ l_1 \sin(\omega t + \psi) - h_\times l_2 \cos(\omega t + \psi)\right]\\
&\quad + \tfrac{1}{2}k\left[h_+ l_3 l_1 \cos(\omega t + \psi) + h_\times l_3 l_2 \sin(\omega t + \psi)\right],\\
\bar{x}^2(t) &= l_2 - \tfrac{1}{2}\left[h_+ l_2 \sin(\omega t + \psi) + h_\times l_1 \cos(\omega t + \psi)\right]\\
&\quad - \tfrac{1}{2}k\left[h_+ l_3 l_2 \cos(\omega t + \psi) - h_\times l_3 l_1 \sin(\omega t + \psi)\right],\\
\bar{x}^3(t) &= l_3 - \tfrac{1}{4}k\left[h_+\left(l_1^{\,2} - l_2^{\,2}\right)\cos(\omega t + \psi) + 2h_\times l_1 l_2 \sin(\omega t + \psi)\right].
\end{aligned} \tag{3.12}$$

Obviously, the unperturbed (*i.e.* in the absence of the gravitational wave) position of the nearby mass is (l_1, l_2, l_3). The action of the wave drives the mass in an oscillatory fashion around the unperturbed position. In general, all three components of motion are present.

If one neglects in Eq. (3.12) the terms with k, thus effectively sending the wavelength

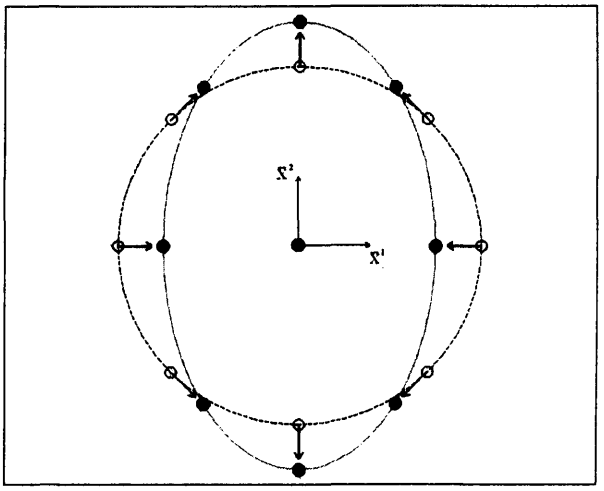

Figure 3.2: Motion of free test masses in the field of a linearly polarized ($h_+ \neq 0, h_\times = 0$) g.w. in the lowest approximation, that is, when the wave number k is effectively set to zero.

λ to infinity, one arrives at the often cited statement about the particle's motion:

$$\begin{aligned} \bar{x}^1(t) &= l_1 + \tfrac{1}{2}\left[h_+ l_1 \sin(\omega t + \psi) - h_\times l_2 \cos(\omega t + \psi)\right], \\ \bar{x}^2(t) &= l_2 - \tfrac{1}{2}\left[h_+ l_2 \sin(\omega t + \psi) + h_\times l_1 \cos(\omega t + \psi)\right], \\ \bar{x}^3(t) &= l_3. \end{aligned} \tag{3.13}$$

Clearly, this is the analog of the electric component of motion in electrodynamics; moving particles remain in the plane of the wave-front. The oscillations of individual particles, for the particular case of a linearly polarized g.w., are shown in Fig. 3.2.

A circular disk, consisting of particles that are located in the plane of the wave-front, stretches and squeezes in an oscillatory fashion, as shown in Fig. 3.3.

Now, let us take into account the terms with k in Eq. (3.12). If $l_3 = 0$, these terms do not change the $\bar{x}^1, \bar{x}^2$ components of motion, but nevertheless they introduce oscillations along the $\bar{x}^3$ direction. In analogy with electrodynamics, it is reasonable to call these terms the "magnetic" components of motion. The trajectories of free masses are, in general, ellipses, and they are not confined to the plane of the wave-front. In Fig. 3.4 (taken from [29]) we show the trajectories of some individual particles. The "magnetic" contribution is smaller than the "electric" one. In analogy with electrodynamics, the major axis of the individual ellipse is small in comparison with λ and l, but the size of

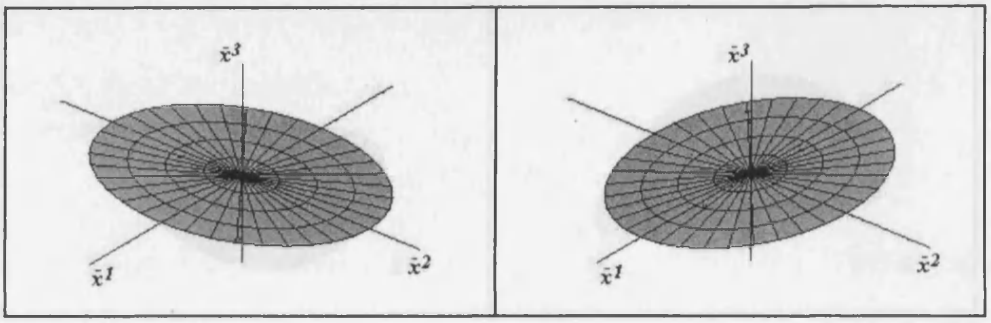

Figure 3.3: Deformation of a disk of free test particles in the field of a linearly polarized ($h_+ \neq 0, h_\times = 0$) g.w. in the limit of $k = 0$. The two figures show the displacements at the moments of time separated by a half period.

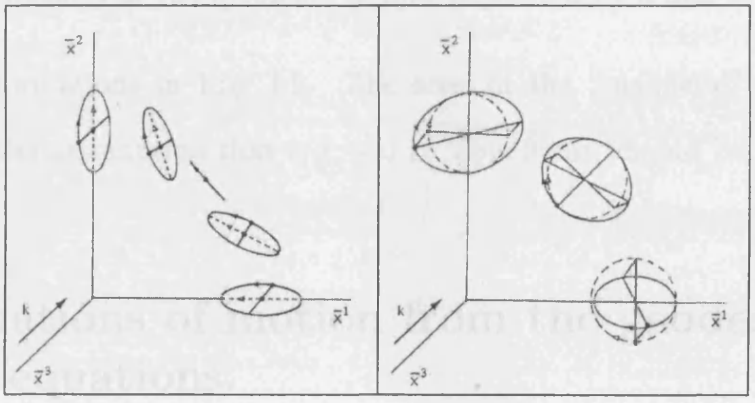

Figure 3.4: Solid lines show 3-dimensional motion of particles, while dashed lines show projections of the trajectories onto the $\bar{x}^1, \bar{x}^2$ plane. In the left picture the wave is linearly polarized ($h_+ \neq 0, h_\times = 0$), whereas in the right picture the wave is circularly polarized ($h_+ = h_\times$).

the $\bar{x}^3$-amplitude is even smaller than the $\bar{x}^1$-amplitude. Their ratio is typically of the order of $kl = 2\pi(l/\lambda)$, where $l = \sqrt{{l_1}^2 + {l_2}^2 + {l_3}^2}$ is the mean (unperturbed) distance of the test particle from the origin. In analogy with electrodynamics, the "magnetic" component of motion will be present even if the particle is initially at rest with respect to the local inertial frame.

A circular disk, consisting of free test particles, also behaves differently, as compared with the lowest order "electric" approximation. The disk does not remain flat while being stretched and squeezed. In addition to being stretched and squeezed it bends, in an oscillatory manner, forward and backward in the $\bar{x}^3$ direction. We show these

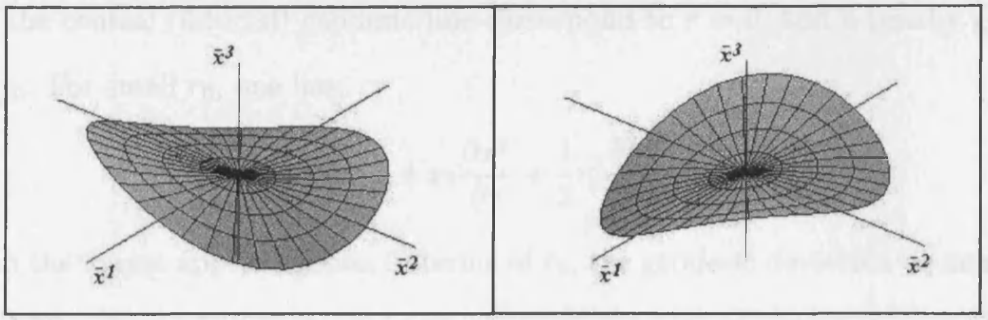

Figure 3.5: The figure shows the deformations of a circular disk of free test particles under the action of a linearly polarized g.w. ($h_+ \neq 0, h_\times = 0$). The "magnetic" contribution is responsible for the displacements along the $\bar{x}^3$ axis. The two pictures show the configurations at the moments of time separated by a half of period.

complicated deformations in Fig. 3.5. The level of the "magnetic" contribution is determined by the assumption that $l/\lambda = 0.1$. This figure should be compared with Fig. 3.3.

3.3 Equations of motion from the geodesic deviation equations.

In this section we shall consider the motion of free masses from a different perspective. The geodesic deviation equations will be used in order to derive the analog of the Lorentz force Eq. (3.1) and the analog of the Newtonian equations of motion Eq. (3.2). We shall see that the "magnetic" component of motion is contained in the higher-order geodesic deviation equations.

3.3.1 Geodesic deviation equations in general

The derivation of the geodesic deviation equations is usually based on a 2-parameter family of time-like geodesics $x^\mu(\tau, r)$. For each value of r, the line $x^\mu(\tau, r)$ is a time-like geodesic with a proper time parameter τ. The vector u^μ is the unit tangent vector to the geodesic, and n^μ is the "separation" vector between the geodesics (see Fig. 3.6):

$$u^\mu(\tau, r) = \frac{\partial x^\mu}{\partial \tau}|_{r=\text{const}} , \quad n^\mu(\tau, r) = \frac{\partial x^\mu}{\partial r}|_{\tau=\text{const}} . \tag{3.14}$$

Let the central (fiducial) geodesic line correspond to $r = 0$, and a nearby geodesic to $r = r_0$. For small r_0, one has:

$$x^\mu(\tau, r_0) = x^\mu(\tau, 0) + r_0 \frac{\partial x^\mu}{\partial r} + \frac{1}{2} r_0^2 \frac{\partial^2 x^\mu}{\partial r^2} + O(r_0^3). \tag{3.15}$$

Then, in the lowest approximation in terms of r_0, the geodesic deviation equations are given by [2]:

$$\frac{D^2 n^\mu}{d\tau^2} = R^\mu_{\alpha\beta\gamma} u^\alpha u^\beta n^\gamma, \tag{3.16}$$

where $R^\mu_{\alpha\beta\gamma}$ is the curvature tensor calculated along the geodesic line $r = 0$, and $\frac{D}{d\tau}$ is the covariant derivative calculated along that line.

To discuss the "magnetic" component of motion in the field of a gravitational wave we will need the geodesic deviation equations extended to the next approximation. These equations were derived by Bazanski [54]. A modified derivation can be found in [55]. In the required approximation, one needs the information on the second derivatives of x^μ: $\frac{\partial^2 x^\mu}{\partial r^2}$. These quantities do not form a vector. It is convenient to introduce a closely related vector w^μ:

$$w^\mu = \frac{Dn^\mu}{dr} = n^\mu_{;\alpha} n^\alpha = \frac{\partial^2 x^\mu}{\partial r^2} + \Gamma^\mu_{\alpha\beta} n^\alpha n^\beta. \tag{3.17}$$

This vector obeys the equations [54] (see also [55]):

$$\frac{D^2 w^\mu}{d\tau^2} = R^\mu_{\alpha\beta\gamma} u^\alpha u^\beta w^\gamma + \left(R^\mu_{\alpha\beta\gamma;\delta} - R^\mu_{\gamma\delta\alpha;\beta}\right) u^\alpha u^\beta n^\gamma n^\delta + 4 R^\mu_{\alpha\beta\gamma} u^\beta \frac{Dn^\alpha}{d\tau} n^\gamma. \tag{3.18}$$

To combine equations (3.16) and (3.18) into a single formula, valid up to and including the terms of the order of r_0^2, it is convenient to construct a vector N^μ:

$$N^\mu = r_0 n^\mu + \frac{1}{2} r_0^2 w^\mu. \tag{3.19}$$

Taking the sum of Eq. (3.16), multiplied by r_0, and Eq. (3.18) multiplied by $r_0^2/2$, we obtain the equation whose solution we will need,

$$\begin{aligned} \frac{D^2 N^\mu}{d\tau^2} = {} & R^\mu_{\alpha\beta\gamma} u^\alpha u^\beta N^\gamma + \tfrac{1}{2}\left(R^\mu_{\alpha\beta\gamma;\delta} - R^\mu_{\gamma\delta\alpha;\beta}\right) u^\alpha u^\beta N^\gamma N^\delta \\ & + 2 R^\mu_{\alpha\beta\gamma} u^\beta \tfrac{DN^\alpha}{d\tau} N^\gamma + O(r_0^3). \end{aligned} \tag{3.20}$$

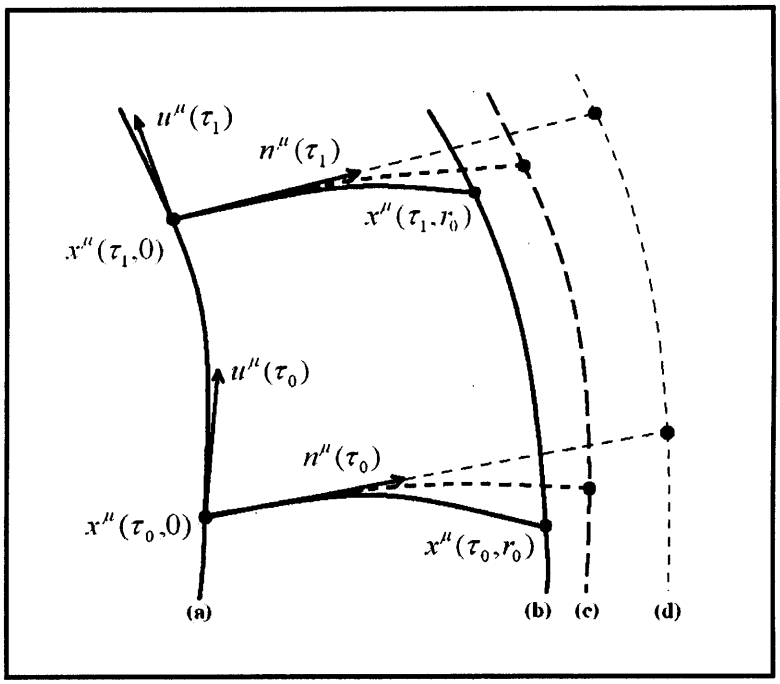

Figure 3.6: Deviation of two nearby geodesics in a gravitational field. Line (a) represents the central geodesic $r = 0$ and line (b) represents the nearby geodesic $r = r_0$. u^μ is the unit tangent vector to the central world line, n^μ is the tangent vector to the curve $\tau = \text{const}$. The lines (d) and (c) are the corresponding first and second order approximations to the exact nearby geodesic (b).

In terms of N^μ, the expansion (3.15) takes the form

$$x^\mu(\tau, r_0) = x^\mu(\tau, 0) + N^\mu - \Gamma^\mu_{\alpha\beta} N^\alpha N^\beta + O(r_0^3). \tag{3.21}$$

Formula (3.21) shows that in the local inertial frame (in which case $\Gamma^\mu_{\alpha\beta} = 0$ along the central geodesic line) the spatial components N^i will directly give the time-dependent positions of the nearby particle. According to Eq. (3.20), these positions include the next order corrections, as compared with solutions to Eq. (3.16).

In Fig 3.6 we show the successive approximations to the exact position of the nearby geodesic (*b*). The line (*d*) represents the first order approximation (*i.e.* $x^\mu(\tau, r_0) = x^\mu(\tau, 0) + r_0 \frac{\partial x^\mu}{\partial r}$), the line (*c*) takes into account the second order approximation (*i.e.* $x^\mu(\tau, r_0) = x^\mu(\tau, 0) + r_0 \frac{\partial x^\mu}{\partial r} + \frac{1}{2} r_0^2 \frac{\partial^2 x^\mu}{\partial r^2}$), according to (3.15).

3.3.2 Geodesic deviation in the field of a gravitational wave

We now specialize to the g.w. metric (3.5), (3.6), where a and b are given by (3.8). We take account only of linear perturbations in terms of g.w. amplitude h. The first particle is described by the central time-like geodesic $x^i(t) = 0$, its tangent vector is $u^\alpha = (1, 0, 0, 0)$. The second particle resides at the unperturbed position $x^i(0) = l^i$ and has zero unperturbed velocity. It is assumed that the local inertial frame is realized along the central geodesic. The objective is to find the trajectory of the second particle using the geodesic deviation equation (3.20).

The deviation vector N^i has the form

$$N^i(t) = l^i + \xi^i(t), \tag{3.22}$$

where $\xi^i(t)$ is the perturbation caused by the gravitational wave. The choice of the local inertial frame allows one to replace all covariant derivatives in Eq. (3.20) by ordinary derivatives. In particular, covariant time derivative $\frac{D^2}{d\tau^2}$ is being replaced by ordinary time derivative $\frac{d^2}{c^2dt^2}$. In the lowest approximation, Eqs. (3.20) reduce to Eqs. (3.16) and specialize to

$$\frac{d^2\xi^i}{dt^2} = -\frac{1}{2}l^j\frac{\partial^2}{\partial t^2}\left(h^i_j\right) = \frac{1}{2}\omega^2 l^j\left[\overset{1}{p}{}^i_j h_+ \sin(\omega t + \psi) - \overset{2}{p}{}^i_j h_\times \cos(\omega t + \psi)\right]. \tag{3.23}$$

As expected, the relevant solution to this equation coincides exactly with the usual "electric" part of the motion, which is given by Eq. (3.13).

In order to identify the "magnetic" part of the gravitational force, one has to consider all the terms in Eq. (3.20). Since $DN^\alpha/d\tau$ is of the order of h, the third term in Eq. (3.20) is of the order of h^2 and should be neglected. Working out the derivatives of the curvature tensor and substituting them into (3.20), we arrive at the accurate equations of motion:

$$\frac{d^2\xi^i}{dt^2} = -\frac{1}{2}l^j\frac{\partial^2}{\partial t^2}\left(h^i_j\right) - \frac{1}{2}l^k l^l\frac{\partial^2}{\partial t^2}\left(\frac{\partial}{\partial x^l}\left(h^i_k\right) - \frac{1}{2}\delta^{ij}\frac{\partial}{\partial x^j}\left(h_{kl}\right)\right). \tag{3.24}$$

The second term of this formula is responsible for the "magnetic" component of motion

and can be interpreted as the gravitational analog of the magnetic part of the Lorentz force (3.1).

Specifically, in the field of the gravitational wave (3.9), the full equations of motion (3.24) take the form:

$$\begin{aligned}\frac{d^2\xi^i}{dt^2} &= \frac{1}{2}\omega^2 l^j \left[\overset{1}{p}{}^i{}_j h_+ \sin(\omega t+\psi) - \overset{2}{p}{}^i{}_j h_\times \cos(\omega t+\psi)\right] \\ &\quad -\frac{1}{2}\omega^2 l^k l^l \left[k_l\delta^{ij} + \frac{1}{2}k^i\delta^j_l\right]\left[\overset{1}{p}{}_{kj} h_+ \cos(\omega t+\psi) + \overset{2}{p}{}_{kj} h_\times \sin(\omega t+\psi)\right].\end{aligned} \tag{3.25}$$

This equation clearly exhibits two contributions:

$$m\frac{d^2\xi^i}{dt^2} = F^i_{(e)} + F^i_{(m)}. \tag{3.26}$$

The "electric" component of the gravitational force $F^i_{(e)}/m$ is given by the first term in Eq. (3.25). The second term - the "magnetic" component $F^i_{(m)}/m$ of the gravitational force - can be written, demonstrating certain analogy with electrodynamics, in the form involving the (lowest order non-vanishing) velocity $\frac{d\xi^i}{dt}$ of the test particle:

$$\frac{F^i_{(m)}}{m} = \omega l^l \left[k_l\delta^i_j + \frac{1}{2}k^i\delta_{jl}\right]\frac{d\xi^j}{dt}. \tag{3.27}$$

The right hand side of Eq. (3.25) is exactly the acceleration $\frac{d^2\bar{x}^i}{dt^2}$ which can be derived by taking the time derivatives of Eq. (3.12). Not surprisingly, by integrating equations of motion (3.25), one arrives exactly at the time-dependent positions of the particles, Eq. (3.12), which we have already derived by the direct coordinate transformation. Therefore, the gravitational Lorentz force, identified above, leads exactly to the expected result.

It should be noted that Eqs. (3.25) depend only on the so-called transverse traceless (TT) components of the g.w. field. This happens not only because we have explicitly started from them in Eq. (3.9). Even if we have started from the general form of the g.w. field, which includes also the non-TT components, we would have ended up with equations containing only the TT components. This happens because Eqs. (3.20)

involve the curvature tensor (and its derivatives) in which the non-TT components automatically cancel out.

It is interesting to compare the components of the gravitational force derived here with what would follow from the concept of "gravitomagnetism". In general, the concept of "gravitomagnetism" is a helpful analogy which was successfully used in studies of stationary gravitational fields [3], [56]. However, its application to the gravitational-wave problem considered here requires certain care. For example, in the local inertial frame, the leading terms of the equations of motion derived in the framework of "gravitomagnetism" [56] read (in notations consistent with this thesis):

$$\frac{d^2N^i}{dt^2} = R^i_{00j}N^j + 2R^i_{j0k}\frac{dN^j}{dt}N^k. \tag{3.28}$$

This equation should be compared with our Eq. (3.20), also specialized to the local inertial frame:

$$\frac{d^2N^i}{dt^2} = R^i_{00j}N^j + \frac{1}{2}\left(R^i_{00j;k} - R^i_{jk0;0}\right)N^jN^k + 2R^i_{j0k}\frac{dN^j}{dt}N^k. \tag{3.29}$$

Clearly, the last term in both equations is common, and it resembles the magnetic part of the electromagnetic Lorentz force. However, as was shown above, for particles which do not have large unperturbed velocities and are (on average) at rest in the local inertial frame, this term is quadratic in h and should be neglected. At the same time, the second term in Eq. (3.29) (which we provisionally call "magnetic") is linear in h and cannot be neglected. Regardless of terminology, the correct results exhibited in Eq. (3.12) can only be obtained if one proceeds with Eq. (3.29) and not with Eq. (3.28).

3.4 Variation of the distance between test masses

We have used a local inertial frame and completely specified the time-dependent positions of test particles acted upon by a gravitational wave. As was already mentioned, this description is as close as possible to the description of laboratory physics. Having

answered all the questions with regard to particles's positions, we can now discuss the variation of distances between them. We are mostly interested in the distance between the central particle and the particle located, on average, at some position (l_1, l_2, l_3). This is a model for the central mirror and the end-mirror placed in one of the arms of an interferometer. We will later use these results for the derivation of the response function of the laser interferometer.

In the local inertial frame, metric tensor (3.10) has the Minkowski values up to small terms of order of $h(\frac{l}{\lambda})^2$. The Euclidian expression

$$d(t) = \sqrt{\bar{x}^{1\,2} + \bar{x}^{2\,2} + \bar{x}^{3\,2}} + O\left(hl(l/\lambda)^2\right), \tag{3.30}$$

gives the distance between particles, which is accurate up to terms of the order of hl and $hl\frac{l}{\lambda}$ inclusive. Obviously, we neglect the terms quadratic in h. Denoting $\bar{x}^i = l_i + \Delta\bar{x}^i$, one gets

$$d(t) \approx l + \frac{1}{l}\left(l_1\Delta\bar{x}^1 + l_2\Delta\bar{x}^2 + l_3\Delta\bar{x}^3\right). \tag{3.31}$$

Using the time-dependent positions (3.12), we obtain the distance $d(t)$ with the required accuracy:

$$\begin{aligned} d(t) \;=\; & l + \frac{1}{2l}\left[h_+({l_1}^2 - {l_2}^2)\sin(\omega t + \psi) - 2h_\times l_1 l_2 \cos(\omega t + \psi)\right] \\ & + \frac{1}{4l}kl_3\left[h_+({l_1}^2 - {l_2}^2)\cos(\omega t + \psi) + 2h_\times l_1 l_2 \sin(\omega t + \psi)\right] + O\left(hl(l/\lambda)^2\right). \end{aligned} \tag{3.32}$$

Clearly, the first correction to l is due to the "electric" contribution, whereas the second correction to l is due to the "magnetic" contribution.

According to Eqs. (3.12), the "magnetic" component of motion is present even if the mean position of the second mass is such that $l_3 = 0$. However, this motion is in the direction orthogonal to the line joining the masses and therefore it does not lead to a (first order in terms of h) change of distance between them. This fact is reflected in Eq. (3.32) in the form of disappearance of the "magnetic" contribution to the distance

when $l_3 = 0$. In other words, "magnetic" contribution to the distance is present only if the interferometer's arm is not orthogonal to the wave's propagation.

The distance (3.32) was calculated in the local inertial frame. It was assumed that $l/\lambda \ll 1$. It is important to show that the approximate expression (3.32) follows also from exact definitions of distance. One of them is based on the measurement of time that it takes for a light ray to travel from one free particle to another and back. [This is a part of a more general problem of finding light-like geodesics in the presence of a weak gravitational wave [2],[57], [58].] This definition is applicable regardless of the relationship between l and λ and does not require the introduction of a local inertial frame. If a photon is sent out from the first particle-mirror at the moment of time t_0, gets reflected off the second particle-mirror, and then returns back to the first particle-mirror at t_2, the proper distance $d(t)$ between the mirrors at time t is defined as

$$d\,(t) = c\frac{t_2 - t_0}{2}, \tag{3.33}$$

where $t = (t_0 + t_2)/2$ is the mean time between the departure of the photon and its arrival back.

In the field of the gravitational wave (3.9), the light rays, $ds^2 = 0$, are described by the equation

$$c^2dt^2 = (1+a)dx^{1^2} + (1-a)dx^{2^2} - 2b\; dx^1dx^2 + dx^{3^2}. \tag{3.34}$$

To calculate the time delay effects, in the framework of perturbation theory valid up to linear order in h, it is sufficient to consider an unperturbed geodesic (see, for example, §40.4 in [2]). Let the (unperturbed) outgoing light ray be parameterized as

$$x^0 = ct_0 + l\tau, \quad x^1 = l_1\tau, \quad x^2 = l_2\tau, \quad x^3 = l_3\tau, \tag{3.35}$$

where the parameter τ changes from 0 to 1. Then, according to Eq. (3.34), we have along the ray:

$$cdt = l\left[1 + \frac{1}{2}a(\tau)\frac{l_1^2 - l_2^2}{l^2} - b(\tau)\frac{l_1l_2}{l^2}\right]d\tau. \tag{3.36}$$

Integrating both parts of this equation, we can find the time t of arrival of the photon to the second particle. The calculated time includes the g.w. corrections proportional to h_+ and $h_\times$. Similarly, the (unperturbed) reflected light ray can be parameterized as

$$x^0 = ct + l\tau, \quad x^1 = l_1 - l_1\tau, \quad x^2 = l_2 - l_2\tau, \quad x^3 = l_3 - l_3\tau, \tag{3.37}$$

where τ is again changing from 0 to 1. A similar integration of Eq. (3.36) allows us to find the time t_2 of arrival of the photon back to the first particle, including the g.w. corrections.

Combining two pieces of the light travel time, we derive the exact formula for the distance:

$$d(t) = l + \frac{1}{2l}\left[h_+\frac{l_1^2 - l_2^2}{2}\Phi_c + h_\times l_1 l_2 \Phi_s\right], \tag{3.38}$$

where

$$\begin{aligned}\Phi_c &= -\frac{1}{k(l+l_3)}\left[\cos\left(\omega t + \psi + kl_3\right) - \cos\left(\omega t + \psi - kl\right)\right] \\ &\quad + \frac{1}{k(l-l_3)}\left[\cos\left(\omega t + \psi + kl_3\right) - \cos\left(\omega t + \psi + kl\right)\right],\end{aligned} \tag{3.39}$$

and Φ_s is obtained from Φ_c by the replacement of all cos-functions with sin-functions of the same arguments. Exactly the same formula (3.38) follows also from the direct joining of the perturbed light-like geodesic lines, derived in reference [57].

Formula (3.32) is sufficient for ground-based interferometers, for which the condition $l \ll \lambda$ is usually satisfied. Formula (3.38) is appropriate for space-based interferometers for which the above condition is not satisfied in the higher-frequency portion of the sensitivity band (see, for example, [9], [59], [60], [61]). However, it is important that formula (3.32), including its "magnetic" terms, follows also from exact definition (3.38), when the appropriate approximation is taken. Assuming that $k(l + l_3) \ll 1$ and $k(l - l_3) \ll 1$ and retaining only the first two terms in the expansion of Φ_c and Φ_s, one derives Eq. (3.32) from Eq. (3.38). As expected, the "magnetic" contribution to the distance is a universal phenomenon. It is most easily identified and interpreted in the local

inertial frame, but conclusions about the distance do not depend on the introduction of this frame.

It is known that there is no unique definition of spatial distance in curved space-time. We have considered the definition based on measuring the round-trip time of a light ray. One more definition is based on measuring the length of a spatial geodesic line joining the particles at a fixed moment of time. This is the length of the geodesic joining the particles, in three dimensional time slice $t = \text{const}$, described by metric 3.9 with $dt = 0$. It can be shown that this definition leads to the formula

$$d(t) = l + \frac{1}{2l}\left[h_+ \frac{l_1^2 - l_2^2}{2}\tilde{\Phi}_c + h_\times l_1 l_2 \tilde{\Phi}_s\right], \tag{3.40}$$

where

$$\tilde{\Phi}_c = -\frac{2}{kl_3}\left[\cos(\omega t + \psi + kl_3) - \cos(\omega t + \psi)\right], \tag{3.41}$$

and $\tilde{\Phi}_s$ is obtained from $\tilde{\Phi}_c$ by the replacement of all cos-functions with sin-functions of the same arguments. In general, the distance (3.40) differs from the distance (3.38). However, they do coincide in the first order approximation in terms of small parameter kl. This can be shown by expanding Eq. (3.40) in powers of kl and retaining the linear terms. It is satisfying that the exact definitions (3.38) and (3.40) lead precisely to the Euclidean result (3.32) in the appropriate approximation.

3.5 Response of an interferometer to the incoming plane gravitational wave

Laser interferometer measures the difference of distances travelled by light in two arms. We describe interferometer in the local inertial frame, with the origin of the frame at the corner mirror. The unperturbed coordinates of the end-mirrors are given by $(l_1^{(a)},\ l_2^{(a)},\ l_3^{(a)})$, where $a = 1, 2$ labels the arms. We consider an interferometer whose unperturbed arms have equal lengths, $l = \sqrt{l_1^{(a)^2} + l_2^{(a)^2} + l_3^{(a)^2}}$, and the arms are orthogonal to each other. A detailed introduction to interferometers in gravitational-wave research can be found in [8], [24], [9].

It was shown in the previous section that the distance variation in one of the arms is given by Eq. (3.32). Then, the response of a 2-arm interferometer is given by

$$\Delta d(t) = d(t)^{(1)} - d(t)^{(2)}. \tag{3.42}$$

The derivation of formula (3.32) is based on the coordinate system adjusted to the gravitational wave. Specifically, it is assumed that the x^3 axis is the direction from which the incoming plane wave propagates, while the x^1, x^2 directions are defining the principal axes of the wave, see Eq. (3.9). Then, the response function (3.42) is characterized by six free parameters ($l_1^{(a)}$, $l_2^{(a)}$, $l_3^{(a)}$).. Among these six parameters only four are independent (one of which is l), because the arms have equal unperturbed lengths l and are orthogonal to each other.

When it comes to the observer, it is more convenient to associate coordinate system with the interferometer's arms, rather than with one particular wave. Let the observer's coordinate system (X^1, X^2, X^3) be chosen in such a way that the arms are located along the X^1 and X^2 directions. Then, the response function is characterized by l and three angles : Θ, Φ and Ψ. The angles Θ, Φ describe the direction of a particular incoming wave, and the third angle Ψ describes the orientation of the principal axes of the wave with respect to the observer's meridian (see, for example, [8], [24], [62]). The relationship between these two coordinate systems is shown in Fig. 3.7 and is described in detail in Appendix B.

The parameters ($l_1^{(a)}$, $l_2^{(a)}$, $l_3^{(a)}$) are expressible in terms of the parameters Θ, Φ, Ψ according to the relationships (see Appendix B):

$$\begin{aligned} l_1^{(1)} &= l(\cos\Phi\cos\Theta\cos\Psi - \sin\Phi\sin\Psi), \\ l_2^{(1)} &= l(-\sin\Phi\cos\Psi - \cos\Phi\cos\Theta\sin\Psi), \\ l_3^{(1)} &= l(\cos\Phi\sin\Theta), \end{aligned} \tag{3.43}$$

and

$$\begin{aligned} l_1^{(2)} &= l(\sin\Phi\cos\Theta\cos\Psi + \cos\Phi\sin\Psi), \\ l_2^{(2)} &= l(\cos\Phi\cos\Psi - \sin\Phi\cos\Theta\sin\Psi), \\ l_3^{(2)} &= l(\sin\Phi\sin\Theta). \end{aligned} \tag{3.44}$$

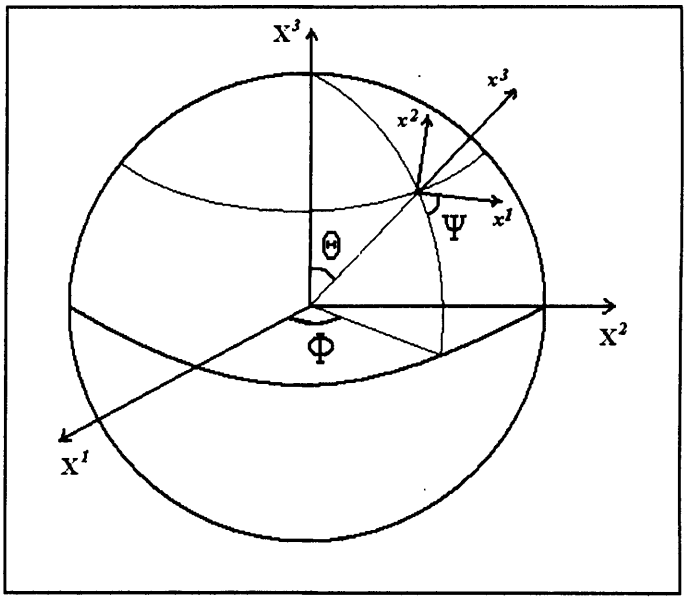

Figure 3.7: The relationship between the coordinate system (x^1, x^2, x^3) adjusted to the wave and the coordinate system (X^1, X^2, X^3) adjusted to the interferometer. The two arms of the interferometer lie along the axes X^1 and X^2.

Using (3.43) and (3.44) in (3.42), the response function can be written in the form

$$\begin{aligned}\Delta d(t) = \; l \; \Big[& h_+ \left\{ F_+^E(\Theta,\Phi,\Psi)\sin(\omega t+\psi) + (kl) F_+^H(\Theta,\Phi,\Psi)\cos(\omega t+\psi) \right\} \\ & + h_\times \left\{ F_\times^E(\Theta,\Phi,\Psi)\cos(\omega t+\psi) + (kl) F_\times^H(\Theta,\Phi,\Psi)\sin(\omega t+\psi) \right\} \Big] ,\end{aligned} \tag{3.45}$$

where the "electric" (E) components of $F_{+,\times}(\Theta,\Phi,\Psi)$ are given by

$$F_+^E(\Theta,\Phi,\Psi) = \cos 2\Phi \left(\frac{1+\cos^2\Theta}{2} \right) \cos 2\Psi - \sin 2\Phi \cos\Theta \sin 2\Psi, \tag{3.46}$$

$$F_\times^E(\Theta,\Phi,\Psi) = -\cos 2\Phi \left(\frac{1+\cos^2\Theta}{2} \right) \sin 2\Psi - \sin 2\Phi \cos\Theta \cos 2\Psi, \tag{3.47}$$

and the "magnetic" (H) components of $F_{+,\times}(\Theta,\Phi,\Psi)$ are given by

$$\begin{aligned} F_+^H(\Theta,\Phi,\Psi) = \; & \tfrac{1}{4}\sin\Theta \left[\left(\cos^2\Theta + \sin 2\Phi \left(\tfrac{1+\cos^2\Theta}{2} \right) \right) (\cos\Phi - \sin\Phi) \cos 2\Psi \right. \\ & \left. - \sin 2\Phi \, (\cos\Phi + \sin\Phi) \cos\Theta \sin 2\Psi \right] , \end{aligned} \tag{3.48}$$

$$\begin{aligned} F_\times^H(\Theta,\Phi,\Psi) = \; & \tfrac{1}{4}\sin\Theta \left[\left(\cos^2\Theta + \sin 2\Phi \left(\tfrac{1+\cos^2\Theta}{2} \right) \right) (\cos\Phi - \sin\Phi) \sin 2\Psi \right. \\ & \left. + \sin 2\Phi \, (\cos\Phi + \sin\Phi) \cos\Theta \cos 2\Psi \right] . \end{aligned} \tag{3.49}$$

Our response function is more accurate than the previously derived expressions [8], [24], [62], [63], because our Eq. (3.45) includes the "magnetic" contribution. In equation (3.45) it is given by the terms proportional to the factor (kl).

In general, the response function (3.45) contains two independent polarization amplitudes, h_+ and $h_\times$. To simplify the analysis of Eq. (3.45), we will separately consider circularly polarized ($h_+ = \pm h_\times$), and linearly polarized ($h_\times = 0$ or $h_+ = 0$), waves. We start with the analysis of the response function as a function of time, assuming that a circularly polarized or a linearly polarized wave arrives from a fixed direction Θ, Φ on the sky.

In the case of a circularly polarized wave ($h_+ = \pm h_\times$) we obtain

$$\Delta d(t) = l h_+ \left[F_+^{E\,2} + F_\times^{E\,2}\right]^{\frac{1}{2}} \left[1 \pm (kl)\left(\frac{F_+^E F_\times^H + F_\times^E F_+^H}{F_+^{E\,2} + F_\times^{E\,2}}\right)\right] \sin\left(\omega t + \psi \pm \Delta\psi\right), \quad (3.50)$$

where the phase shift $\Delta\psi$ is given by

$$\tan\left(\Delta\psi\right) = \frac{F_\times^E}{F_+^E}\left[1 \pm (kl)\left(\frac{F_+^E F_+^H - F_\times^E F_\times^H}{F_+^E F_\times^E}\right)\right]. \quad (3.51)$$

Clearly, the inclusion of "magnetic" terms changes the amplitude and the phase of $\Delta d(t)$. As an illustration, we show in Fig. 3.8 the response of an interferometer, as a function of time, to a circularly polarized wave $h_+ = h_\times$, coming from the direction $\Theta = 2\pi/3, \Phi = \pi/3$ (we have also set $\Psi = 0$ to fix the phase of the response function; the amplitude of the response function does not depend on Ψ). The dashed curve shows the "electric" response alone, while the solid curve shows the total response, including the "magnetic" part. We have taken $l/\lambda = 0.1$.

The response of an interferometer to any elliptically polarized wave is qualitatively similar to Fig. 3.8, that is, in general, the "magnetic" component contributes, both, to the amplitude and to the phase of $\Delta d(t)$. However, "magnetic" contribution to the amplitude may be very small for linearly polarized waves. If one puts $h_\times = 0$ or $h_+ = 0$ in Eq. (3.45), one finds that the correction to the amplitude $\Delta d(t)$ is quadratic in $(kl)^2$ (and, hence, can be neglected) with the exception of directions on the sky where F_+^E

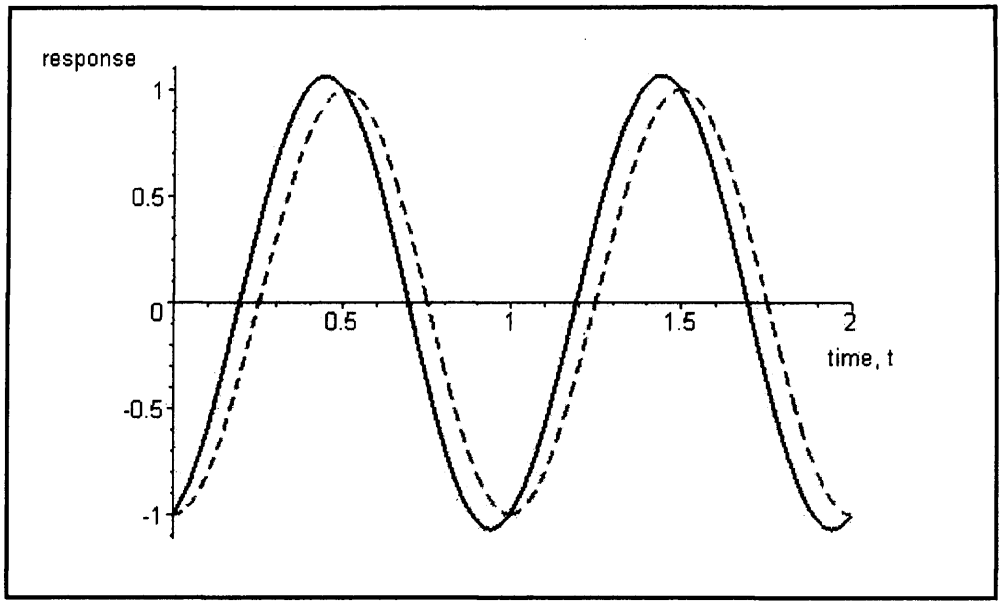

Figure 3.8: A typical response of an interferometer, as a function of time, to the monochromatic circularly polarized gravitational wave coming from a fixed direction on the sky. The solid line shows the total response, while the dashed line is purely "electric" part.

or $F_\times^E$ vanish. Specifically, for the linearly polarized wave $h_\times = 0$, we obtain

$$\Delta d(t) = l\ h_+\ \sqrt{F_+^{E\,2} + (kl)^2 F_+^{H\,2}}\ \sin\left(\omega t + \psi + \Delta\psi\right), \tag{3.52}$$

where the phase shift $\Delta\psi$ is given by

$$\tan\left(\Delta\psi\right) = kl\left(\frac{F_+^H}{F_+^E}\right). \tag{3.53}$$

(The case when $h_+ = 0$ is given by the above expressions in which all the "plus" indices are replaced by "cross" indices, and the sin-function in expression (3.52) is replaced by a cos-function.)

We now turn to the amplitude of $\Delta d(t)$ as a function of the angles Θ, Φ. It is usually called the beam pattern. In general, the amplitude of $\Delta d(t)$ depends also on Ψ, but we will consider, for simplicity, circularly polarized waves, in which case the parameter Ψ does not participate in the amplitude of $\Delta d(t)$. We consider circularly polarized waves, with one and the same amplitude h_R, coming from arbitrary directions on the sky. The beam pattern is shown in Fig. 3.9. The left figure shows the purely

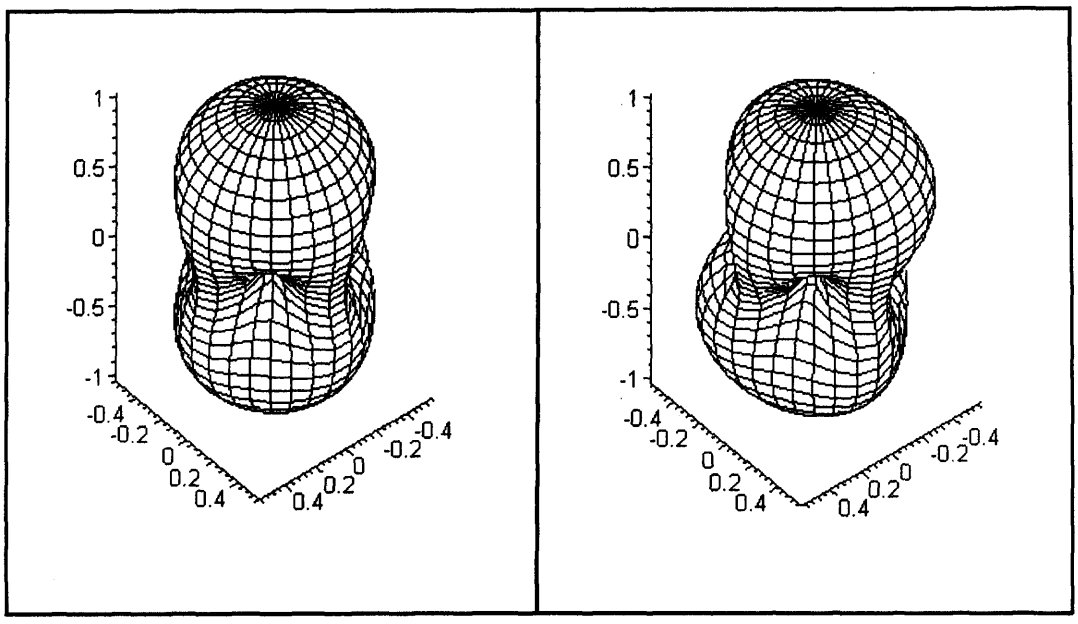

Figure 3.9: The amplitude of the interferometer's response to circularly polarized waves. The graphs are normalized in such a way that the amplitude is equal 1 for $\Theta = 0$. The left figure ignores the "magnetic" effect, whereas the right figure shows the total response.

"electric" contribution, whereas the right figure shows the total beam pattern, with the "magnetic" contribution included. We have taken $l/\lambda = 0.1$. It is clearly seen that the "magnetic" component breaks the characteristic quadrupole symmetry of the "electric" beam pattern (more detail - in the next Section).

3.6 Response function in terms of spin-weighted spherical harmonics

The response function (3.45) allows an elegant invariant representation in terms of the spin-weighted spherical harmonics. This description is also helpful for physical interpretation of the response function.

First, let us introduce the amplitudes of circularly polarized gravitational waves,

$$h_R = \frac{1}{2}(h_+ + h_\times), \quad h_L = \frac{1}{2}(h_+ - h_\times), \tag{3.54}$$

and the complex functions

$$\begin{aligned} F_R &= \left(F_+^E + (kl)F_\times^H\right) + i\left(F_\times^E + (kl)F_+^H\right), \\ F_L &= \left(F_+^E - (kl)F_\times^H\right) + i\left(-F_\times^E + (kl)F_+^H\right). \end{aligned} \tag{3.55}$$

In terms of the introduced notations, the response function (3.45) can be identically rewritten as

$$\Delta d(t) = l\left(-\frac{i}{2}\right)\left[e^{i(\omega t+\psi)}\left(h_R F_R + h_L F_L\right) - e^{-i(\omega t+\psi)}\left(h_R F_R^* + h_L F_L^*\right)\right]. \tag{3.56}$$

Clearly, the $\Delta d(t)$ has been separated in two components associated with the left (L) and right (R) polarization states of the gravitational wave. Only the $L(R)$ component of the response function is present, when the $R(L)$ g.w. amplitude is set to zero.

Using the explicit expressions (3.46), (3.47), (3.48) and (3.49), one can show that the newly defined functions F_R, F_L can be rearranged to read

$$F_R = \widetilde{F}_R(\Theta,\Phi)e^{-2i\Psi}, \qquad F_L = \widetilde{F}_L(\Theta,\Phi)e^{2i\Psi}, \tag{3.57}$$

where $\widetilde{F}_L$ and $\widetilde{F}_R$ are given by

$$\begin{aligned} \widetilde{F}_L &= \frac{1}{4}\left[(1+\cos\Theta)^2 e^{2i\Phi} + (1-\cos\Theta)^2 e^{-2i\Phi}\right] \\ &+\frac{ikl}{32}\left[(1-i)(1+\cos\Theta)^2\sin\Theta e^{3i\Phi} + (1+i)(3\cos\Theta-1)(\cos\Theta+1)\sin\Theta e^{i\Phi}\right. \\ &\left.+(1-i)(3\cos\Theta+1)(\cos\Theta-1)\sin\Theta e^{-i\Phi} + (1+i)(1-\cos\Theta)^2\sin\Theta e^{-3i\Phi}\right], \end{aligned} \tag{3.58}$$

$$\begin{aligned} \widetilde{F}_R &= \frac{1}{4}\left[(1-\cos\Theta)^2 e^{2i\Phi} + (1+\cos\Theta)^2 e^{-2i\Phi}\right] \\ &+\frac{ikl}{32}\left[(1-i)(1-\cos\Theta)^2\sin\Theta e^{3i\Phi} + (1+i)(3\cos\Theta+1)(\cos\Theta-1)\sin\Theta e^{i\Phi}\right. \\ &\left.+(1-i)(3\cos\Theta-1)(\cos\Theta+1)\sin\Theta e^{-i\Phi} + (1+i)(1+\cos\Theta)^2\sin\Theta e^{-3i\Phi}\right]. \end{aligned} \tag{3.59}$$

For a given direction (Θ,Φ) on the sky, the functions F_R and F_L transform under the rotation of Ψ, specified by the transformation $\Psi \to \Psi+\Psi_0$, according to $\widetilde{F}_R \to \widetilde{F}_R e^{-2i\Psi_0}$

and $\widetilde{F}_L \rightarrow \widetilde{F}_L e^{2i\Psi_0}$. A function ${}_sf(\Theta,\Phi)$ is said to be a spin-s function, if under the transformation $\Psi \rightarrow \Psi + \Psi_0$ it transforms like ${}_sf(\Theta,\Phi) \rightarrow {}_sf(\Theta,\Phi)e^{-is\Psi_0}$. Therefore, our functions F_L and F_R represent the $s=-2$ and $s=+2$ functions, respectively.

A scalar function on a 2-sphere can be expanded over a set of ordinary spherical harmonics $Y^\ell_m(\Theta,\Phi)$, which form a complete and orthonormal basis. These harmonics are not appropriate for the expansion of spin-weighted functions with $s \neq 0$. The spin-weighted functions can be expanded over a set of harmonics called the spin-weighted spherical harmonics ${}_sY^\ell_m(\Theta,\Phi)$ [39], [40], [64], [65]. The spin-weighted spherical harmonics satisfy the completeness and othonormality conditions similar to those of ordinary spherical harmonics. The functions ${}_sY^\ell_m(\Theta,\Phi)$ can be derived from $Y^\ell_m(\Theta,\Phi)$ according to the rules:

$$ {}_sY^\ell_m = \begin{cases} \left[\frac{(\ell-s)!}{(\ell+s)!}\right]^{1/2} \eth^s Y^\ell_m, & (0 \leq s \leq \ell) \\ (-1)^s \left[\frac{(\ell+s)!}{(\ell-s)!}\right]^{1/2} \bar{\eth}^{-s} Y^\ell_m, & (0 \geq s \geq -\ell) \end{cases}, \tag{3.60} $$

where the differential operators $\eth$ and $\bar{\eth}$ [acting on a spin s function ${}_sf(\Theta,\Phi)$] are given by

$$ \begin{aligned} \eth\ {}_sf(\Theta,\Phi) &= -\sin^s\Theta \left(\tfrac{\partial}{\partial\Theta} + \tfrac{i}{\sin\Theta}\tfrac{\partial}{\partial\Phi}\right) \sin^{-s}\Theta\ {}_sf(\Theta,\Phi), \\ \bar{\eth}\ {}_sf(\Theta,\Phi) &= -\sin^{-s}\Theta \left(\tfrac{\partial}{\partial\Theta} - \tfrac{i}{\sin\Theta}\tfrac{\partial}{\partial\Phi}\right) \sin^{s}\Theta\ {}_sf(\Theta,\Phi). \end{aligned} \tag{3.61} $$

Using the spin-weighted spherical harmonics, the functions $\widetilde{F}_L$ and $\widetilde{F}_R$ can be expanded as follows:

$$ \begin{aligned} \widetilde{F}_L &= \sqrt{2\pi}\left[{}_{-2}Y^2_{+2}(\Theta,\Phi) + {}_{-2}Y^2_{-2}(\Theta,\Phi)\right] \\ &\quad + ikl\sqrt{\frac{\pi}{46}}\left[\frac{(1-i)}{\sqrt{3}}{}_{-2}Y^3_{+3}(\Theta,\Phi) + \frac{(1+i)}{\sqrt{5}}{}_{-2}Y^3_{+1}(\Theta,\Phi)\right. \\ &\qquad \left. + \frac{(1-i)}{\sqrt{5}}{}_{-2}Y^3_{-1}(\Theta,\Phi) + \frac{(1+i)}{\sqrt{3}}{}_{-2}Y^3_{-3}(\Theta,\Phi)\right], \end{aligned} \tag{3.62} $$

$$ \begin{aligned} \widetilde{F}_R &= \sqrt{2\pi}\left[{}_{+2}Y^2_{+2}(\Theta,\Phi) + {}_{+2}Y^2_{-2}(\Theta,\Phi)\right] \\ &\quad + ikl\sqrt{\frac{\pi}{46}}\left[\frac{(1-i)}{\sqrt{3}}{}_{+2}Y^3_{+3}(\Theta,\Phi) + \frac{(1+i)}{\sqrt{5}}{}_{+2}Y^3_{+1}(\Theta,\Phi)\right. \\ &\qquad \left. + \frac{(1-i)}{\sqrt{5}}{}_{+2}Y^3_{-1}(\Theta,\Phi) + \frac{(1+i)}{\sqrt{3}}{}_{+2}Y^3_{-3}(\Theta,\Phi)\right]. \end{aligned} \tag{3.63} $$

As one could expect, the "electric" components of the response function are described by the spin ± 2 quadrupole ($\ell = 2$) terms ${}_{\pm 2}Y^2_m$, whereas the "magnetic" components are described by the spin ± 2 octupole ($\ell = 3$) terms ${}_{\pm 2}Y^3_m$. The "magnetic" components can be viewed as the higher-order terms in the multipole expansion of the response function.

3.7 Astrophysical example

The "magnetic" component in the motion of free masses will have serious practical implications for the current gravitational wave observations. For example, the LIGO interferometers have the arm length of $l = 4km$ and are most sensitive to g.w. in the interval of frequencies between $30Hz$ and 10^4Hz. This means that the "magnetic" component, whose relative contribution is of the order of kl, may provide a correction at the level of 5% to the response function in the frequency region of $600Hz$, and up to 10% in the frequency region of $1200Hz$. This contribution may significantly affect the determination of the source's parameters.

The high frequency region, $600Hz - 1200Hz$, will be extensively studied with the help of the "narrow-band tuning" of advanced interferometers [12]. The signal recycling technique allows reshaping of the sensitivity curve in such a way that it reduces noise within a chosen narrow band, while weakening sensitivity in other frequency regions. This region of high frequencies is populated by various periodic and quasi-periodic astrophysical sources, such as neutron stars in low-mass X-ray binaries, including Sco X-1, slightly deformed rotating neutron stars, neutron star and black hole binaries in the last moments of their inspiral. For a more detailed list of high frequency sources and the prospects of their detection see [12].

To better understand the role of the "magnetic" components in estimation of the g.w. source parameters, we shall briefly consider an idealized example of a compact binary system. Let the binary consist of objects of equal mass M orbiting each other

in a circular orbit of size $2r$. The distance of the binary to the observer is R. For simplicity, we assume that the orbital plane is orthogonal to the line of sight defined by Θ, Φ. Then, the gravitational wave at Earth has the form of Eq. (3.8) with the amplitudes given by [24], [11]:

$$h_+ = h_\times = h_R = \frac{32\pi^2 G}{Rc^4} M r^2 \omega^2, \tag{3.64}$$

where the g.w. angular frequency $\omega = \sqrt{\frac{GM}{r^3}}$ is twice the orbital frequency. The angle Ψ can be taken as $\Psi = 0$, and the phase ψ is the angle between the observer's meridian and the line joining the components of the binary at some initial moment of time.

The response of the interferometer to the incoming wave is determined by Eq. (3.45):

$$\begin{aligned}\Delta d(t) = \; & l h_R \left[\left\{ \cos 2\Phi \left(\frac{1+\cos^2\Theta}{2} \right) - \frac{1}{4}\frac{\omega l}{c} \sin 2\Phi \left(\cos\Phi + \sin\Phi\right) \cos\Theta \sin\Theta \right\} \right. \\ & \times \sin\left(\omega t + \psi\right) \\ & - \left\{ \sin 2\Phi \cos\Theta - \frac{1}{4}\frac{\omega l}{c} \left(\cos^2\Theta + \sin 2\Phi \left(\frac{1+\cos^2\Theta}{2} \right) \right) \left(\cos\Phi - \sin\Phi\right) \sin\Theta \right\} \\ & \left. \times \cos\left(\omega t + \psi\right) \right] . \end{aligned} \tag{3.65}$$

The terms with ωl represent "magnetic" contribution. If the observed $\Delta d(t)$ is incorrectly interpreted as the "electric" contribution only, then the parameters of source (for example, its mass $2M$) would be estimated from the relationship:

$$\Delta d(t) = l \; h_R \left[\cos 2\Phi \left(\frac{1+\cos^2\Theta}{2} \right) \sin\left(\omega t + \psi\right) - \sin 2\Phi \cos\Theta \cos\left(\omega t + \psi\right) \right] . \tag{3.66}$$

Clearly, this would have resulted in a significant error in the estimated M (of the order $\frac{2\pi l}{\lambda}$). The correct procedure is the comparison of the observed $\Delta d(t)$ with the full response function, consisting of "electric" and "magnetic" contributions. A concrete value of the error depends on the direction Θ, Φ.

3.8 Conclusions

In this chapter we have considered the motion of free test particles in the field of a gravitational wave. We have shown that this motion is similar to the motion of charged

test particles in the field of an electromagnetic wave. Using different methods we have demonstrated the presence and importance of what we call the "magnetic" components of motion. Regardless of interpretation and terminology, these terms contribute to the variation of distance between the interferometer's mirrors and, hence, they contribute to the total response function of the interferometer. The "magnetic" contribution must be taken into account in advanced data analysis programs.

Chapter 4

Radiation field and the general equation of radiative transfer

4.1 Characterization of a radiation field

We shall now shift our attention to the imprints of gravitational waves on the CMB radiation. In order to study the fluctuations in the CMB, along with knowledge about gravitational wave field developed in chapter 2, we shall require the knowledge about the electromagnetic radiation field and the equations of radiative transfer. We shall begin, in this section, with a general description of the radiation field. In the following sections we shall analyze the Thomson scattering mechanism, and then proceed to study the equations of radiative transfer in a slightly perturbed FLRW universe.

Every monochromatic wave is, by definition, necessarily polarized. However one usually has to deal with waves which are only approximately monochromatic, and which contain frequencies in a small interval $\Delta\nu$. Following [1], let us consider such a wave, and let $\omega = 2\pi\nu$ be some average frequency for it. Then, at a fixed point in space, the electric field for this wave can be written in the form

$$\mathbf{E}(t) = \mathbf{E_0}(t)e^{-i\omega t},$$

where the complex amlitude $\mathbf{E_0}(t)$ is some slowly (compared with the frequency ω) varying function of time. Since $\mathbf{E_0}$ determines the polarization of the wave, this means that at each point of the wave, its polarization changes with time; such a wave is said to be partially polarized.

The polarization properties of electromagnetic waves are observed experimentally by passing the light to be investigated through various bodies and then observing the intensity of the transmitted light. From the mathematical point of view this means that we draw conclusions concerning the polarization properties of the light from the values of certain quadratic functions of the its field.

The possible quadratic functions of the field are made up of terms proportional to the products $E_a E_b$, $E_a^* E_b^*$ or $E_a E_b^*$. The first two to of these products contain a rapidly oscillating factor $e^{\pm 2i\omega t}$, thus giving zero when their time average is taken. Hence we see that the polarization properties are completely characterized by the tensor

$$P_{ab} = \overline{E_{0a} E_{0b}^*},$$

where the overline denotes the time averaging. Since $\mathbf{E}_0$ always lies in a plane perpendicular to the direction of the wave, P_{ab} is a tensor lying in the plane of the wavefront (i.e. P_{ab} is a two by two tensor with $a, b = 1, 2$). We shall take z as the direction of wave propogation, and x, y to be the two orthogonal directions in the plane of the wavefront. From the definition it also follows that P_{ab} is an Hermitian tensor ($P_{ab} = P_{ba}^*$). A Herimitian two by two tensor is completely characterized by four real numbers. The four numbers characterizing the polarization properties are conventionally taken to be the Stokes parameters (I, Q, U, V) [66, 1], and are related to the components of P_{ab} by

$$\begin{aligned} I &= \overline{E_{0x} E_{0x}^*} + \overline{E_{0y} E_{0y}^*}, \\ Q &= \overline{E_{0x} E_{0x}^*} - \overline{E_{0y} E_{0y}^*}, \\ U &= -\overline{E_{0x} E_{0y}^*} - \overline{E_{0y} E_{0x}^*}, \\ V &= -i\left(\overline{E_{0x} E_{0y}^*} - \overline{E_{0y} E_{0x}^*}\right). \end{aligned}$$

Out of the four Stokes parameters, the parameter I describes the total intensity of radiation, Q and U describe the magnitude and direction of linear polarization, and V describes the circular polarization. The intensity P and direction (characterized by angle ψ between the axis of linear polarization and the x axis) of linear polarization

are given in terms of the parameters Q and U as follows

$$P = \sqrt{Q^2 + U^2}, \quad \tan 2\psi = -\frac{U}{Q}.$$

The quantity $\Pi = \sqrt{Q^2 + U^2 + V^2}/I$ is known as the polarization fraction. For completely polarized light (i.e. $\mathbf{E}_0(t) = \text{const}$) the polarization fraction equals unity. On the other hand, for the opposite case, known as unpolarized or natural (ordinary) light, the polarization fraction is zero. In the general case of partially polarized light, the polarization fraction lies between the above limiting cases, i.e. $0 \leq \Pi \leq 1$. When several independent streams of light (i.e. streams of light which have no permanent phase relations between themselves) are combined, the Stokes parameters for the mixture is the sum of the respective Stokes parameters of the separate streams. In this way natural light can be thought of as a sum of independent completely polarized light streams such that the sum total of their three Stokes parameters Q, U and V equal zero.

Until now we have been dealing with almost monochromatic light incoming from a single direction z, and restricted our analysis to coordinate origin. In the cosmological context we deal with a radiation field at every point in spacetime characterized by a frequency spectra and incoming from all the directions on the sky. Thus, in this case, the Stokes parameters characterizing the radiation field become functions of (t, x^i, ν, e^i), where ν is the photon's frequency, and e^i is a unit vector in the direction of observation (opposite to the photon's propagation). Equivalently, the Stokes parameters can be viewed as functions of photons' coordinates and momenta (x^α, p^α). Since photons propagate with the speed of light c, the momenta satisfy the condition $p_\alpha p^\alpha = 0$, this implies that Stokes parameters become functions of seven variables (t, x^i, ν, e^i) (time variable, three spatial position variables, frequency, two variables characterizing the direction of photon propagation).

In a given space-time point (t, x^i), the Stokes parameters are functions of ν, θ, ϕ,

where θ, ϕ are coordinates on a unit sphere:

$$d\sigma^2 = g_{ab}dx^a dx^b = d\theta^2 + \sin^2\theta d\phi^2. \tag{4.1}$$

The radial direction is the direction of observation.

The Stokes parameters form the components of the two by two polarization tensor P_{ab} on the sphere, which can be written as

$$P_{ab}(\theta,\phi) = \frac{1}{2}\begin{pmatrix} I+Q & -(U-iV)\sin\theta \\ -(U+iV)\sin\theta & (I-Q)\sin^2\theta \end{pmatrix}. \tag{4.2}$$

(We do not indicate the dependence of Stokes parameters on ν.)

It follows that $I \pm Q$ describe the intensity of radiation field observed in the direction (θ, ϕ) on the sky with the linear polarimeter directed along meridian (θ-direction) and latitude (ϕ-direction) respectively. The quantity $I \pm U$ describes the intensity from the same direction with the polarimeter directed at $\pm 45°$ to the meridian. The parameter V, as usual, describes the intensity of circularly polarized radiation.

Under arbitrary transformations of (θ, ϕ), the components of $P_{ab}(\theta, \phi)$ transform as components of a tensor, but some quantities remain invariant. We want to build linear invariants from P_{ab} and its derivatives, using the metric tensor $g_{ab}(\theta, \phi)$ and a completely antisymmetric pseudo-tensor $\epsilon^{ab}(\theta, \phi)$,

$$\epsilon^{ab} = \begin{pmatrix} 0 & -\sin^{-1}\theta \\ \sin^{-1}\theta & 0 \end{pmatrix}.$$

The first two invariants are easy to build:

$$I(\theta,\phi) = g^{ab}(\theta,\phi)P_{ab}(\theta,\phi), \quad V(\theta,\phi) = i\epsilon^{ab}(\theta,\phi)P_{ab}(\theta,\phi). \tag{4.3}$$

Then, it is convenient to single out the trace and antisymmetric parts of P_{ab}, and introduce the symmetric trace-free (STF) part P^{STF}_{ab}:

$$P_{ab}(\theta,\phi) = \frac{1}{2}I g_{ab} - \frac{i}{2}V\epsilon_{ab} + P^{STF}_{ab},$$

$$P^{STF}_{ab} = \frac{1}{2}\begin{pmatrix} Q & -U\sin\theta \\ -U\sin\theta & -Q\sin^2\theta \end{pmatrix}.$$

Clearly, the construction of other linear invariants requires the use of covariant derivatives of the tensor P_{ab}^{STF}. There are no invariants that can be built from the first derivatives $P_{ab;c}^{STF}$, so we need to go to the second derivatives. One can check that there are only two linearly independent invariants that can be built from the second derivatives:

$$E(\theta,\phi) = -2\left(P_{ab}^{STF}\right)^{;a;b}, \quad B(\theta,\phi) = -2\left(P_{ab}^{STF}\right)^{;b;d}\epsilon^{a}{}_{d}, \tag{4.4}$$

The quantities I and E are scalars, while V and B are pseudoscalars. V and B change sign under flips of directions (coordinate transformations with negative determinants). This is also seen from the fact that their construction involves the pseudo-tensor ϵ_{ab}.

The invariant quantities (I, V, E, B), as functions of (θ, ϕ), can be expanded over ordinary spherical harmonics $Y_{\ell m}(\theta,\phi)$, $Y_{\ell m}^{*} = (-1)^{m} Y_{\ell,-m}$:

$$I(\theta,\phi) = \sum_{\ell=0}^{\infty}\sum_{m=-\ell}^{\ell} a_{\ell m}^{T} Y_{\ell m}(\theta,\phi), \tag{4.5a}$$

$$V(\theta,\phi) = \sum_{\ell=0}^{\infty}\sum_{m=-\ell}^{\ell} a_{\ell m}^{V} Y_{\ell m}(\theta,\phi), \tag{4.5b}$$

$$E(\theta,\phi) = \sum_{\ell=2}^{\infty}\sum_{m=-\ell}^{\ell} \left[\frac{(\ell+2)!}{(\ell-2)!}\right]^{\frac{1}{2}} a_{\ell m}^{E} Y_{\ell m}(\theta,\phi), \tag{4.5c}$$

$$B(\theta,\phi) = \sum_{\ell=2}^{\infty}\sum_{m=-\ell}^{\ell} \left[\frac{(\ell+2)!}{(\ell-2)!}\right]^{\frac{1}{2}} a_{\ell m}^{B} Y_{\ell m}(\theta,\phi). \tag{4.5d}$$

The set of multipole coefficients $(a_{\ell m}^{T}, a_{\ell m}^{V}, a_{\ell m}^{E}, a_{\ell m}^{B})$ completely characterizes the radiation field. We will use these quantities in our further discussion.

To make contact with previous work, we note that the multipole coefficients $a_{\ell m}^{E}, a_{\ell m}^{B}$ can also be expressed in terms of the tensor P_{ab} itself, rather than its derivatives. This is possible because one can interchange the order of differentiation under the integrals that define $a_{\ell m}^{E}, a_{\ell m}^{B}$ in terms of the right hand side (r.h.s.) of Eq. (4.4). This leads to the appearance of the spin-weighted spherical harmonics or tensor spherical harmonics

[38, 39, 40, 65, 68]. For example, the tensor P_{ab} can be written as

$$P_{ab} = \frac{1}{2}\sum_{\ell=0}^{\infty}\sum_{m=-\ell}^{\ell}\left(g_{ab}a^{T}_{\ell m} - i\epsilon_{ab}a^{V}_{\ell m}\right)Y_{\ell m}(\theta,\phi) + \frac{1}{\sqrt{2}}\sum_{\ell=2}^{\infty}\sum_{m=-l}^{l}\left(-a^{E}_{\ell m}Y^{G}_{(\ell m)ab}(\theta,\phi) + a^{B}_{\ell m}Y^{C}_{(\ell m)ab}(\theta,\phi)\right),$$

where $Y^{G}_{(\ell m)ab}(\theta,\phi)$ and $Y^{C}_{(\ell m)ab}(\theta,\phi)$ are the "gradient" and "curl" tensor spherical harmonics forming a set of orthonormal functions for STF tensors [68]. The invariants E and B can also be written in terms of the spin raising and lowering operators $\eth$ and $\bar{\eth}$ [65]:

$$E = -\frac{1}{2}\left[\bar{\eth}^2\left(Q+iU\right) + \eth^2\left(Q-iU\right)\right], \qquad B = \frac{i}{2}\left[\bar{\eth}^2\left(Q+iU\right) - \eth^2\left(Q-iU\right)\right].$$

The quantities E and B are called the E (or "gradient") and B (or "curl") modes of polarization. The ℓ-dependent numerical coefficients in (4.5c) and (4.5d) were introduced in order to make the definitions of this work fully consistent with the previous literature [65, 68].

4.2 Physics of Thomson scattering

The main physical process determining the coupling of matter to radiation prior to recombination ($z \lesssim 1100$) is Thomson scattering of radiation on free electrons. Before proceeding further it is thus helpful to gain some physical intuition into the physics of Thomson scattering. We shall analyze this on a simple idealized example of a single act of scattering. In the next section we shall write down the equation of radiative transfer which, heuristically speaking, takes into account all the possible acts of scattering in a medium filled with radiation and free electrons.

The Thomson scattering obeys the Rayleigh's law of scattering [66]. It states that when a pencil of natural light of wavelength λ, intensity I, and solid angle $d\Omega$, is incident on a particle of polarizability α, energy at the rate of

$$\frac{128\pi^5}{3\lambda^4}\alpha^2 I d\Omega \times \frac{3}{4}\left(1+\cos^2\Theta\right)\frac{d\Omega'}{4\pi},$$

is scattered in a direction making an angle Θ with the direction of incidence and in a solid angle $d\Omega'$; that the scattered light is partially plane polarized; that the angle of polarization is at right angles to the plane of scattering (i.e. the plane that contains the direction of the incident and the scattering light); and finally, that the intensity of the scattered light in directions parallel and perpendicular respectively to the plane of scattering are in the ratio of $\cos^2\Theta : 1$.

For the case of Thomson scattering the coefficient α is given by

$$\alpha^2 = \frac{3\lambda^4}{128\pi^5}\sigma_T,$$

where σ_T is the Thomson scattering cross section

$$\sigma_T = \frac{8\pi e^4}{3m_e^2c^4} \approx 6.65 \cdot 10^{-24}\ \mathrm{cm}^2.$$

Heuristically, the incident radiation sets up oscillations of the scattering free electron in the direction of the electric field of the falling radiation. The projection of this oscillations onto the plane orthogonal to the direction of scattering determines the polarization properties of the scattered radiation.

Following Chandrasekhar [66] let us introduce a symbolic vector $\hat{\mathbf{I}}$ to denote the components of radiation field

$$\hat{\mathbf{I}} = \begin{pmatrix} I_l \\ I_r \\ U \\ V \end{pmatrix},$$

where $I_l = (I+Q)/2$, $I_r = (I-Q)/2$, and (I, Q, U, V) are the Stokes parameters discussed in the previous section.

Denoting by subscripts *in* and *sc* the incoming and scattered components of the radiation respectively, the radiation field scattered in the direction (θ, ϕ) by a single act of scattering of an incident pencil of radiation incoming from direction (θ', ϕ') is given by [66]

$$d\hat{\mathbf{I}}_{sc}(\theta,\phi) = \hat{\mathbf{P}}(\theta,\phi;\theta',\phi')\hat{\mathbf{I}}_{in}(\theta',\phi')\frac{d\Omega'}{4\pi},$$

where $\hat{\mathbf{P}}(\theta, \phi; \theta', \phi')$ is the Chandrasekhar matrix for Thomson scattering [66].

In order to calculate the scattered field due an arbitrary incoming radiation field $\hat{\mathbf{I}}_{in}(\theta, \phi)$ we need to integrate the above expression over all possible directions of the incoming radiation

$$\hat{\mathbf{I}}_{sc}(\theta, \phi) = \frac{1}{4\pi} \oint d\Omega' \; \hat{\mathbf{P}}(\theta, \phi; \theta', \phi') \hat{\mathbf{I}}_{in}(\theta', \phi').$$

In order to gain further physical insight into Thomson scattering it is convenient to introduce the symbolic vector $\tilde{\mathbf{I}}$, whose components are $(I, Q + iU, Q - iU, V)$, by the following linear transformation

$$\tilde{\mathbf{I}} = \begin{pmatrix} I \\ Q + iU \\ Q - iU \\ V \end{pmatrix} = \mathbf{A}\hat{\mathbf{I}}, \quad \text{where } \mathbf{A} = \begin{pmatrix} 1 & 1 & 0 & 0 \\ 1 & -1 & i & 0 \\ 1 & -1 & -i & 0 \\ 0 & 0 & 0 & 1 \end{pmatrix}.$$

The convenience of introducing the vector $\tilde{\mathbf{I}}$ lies in the fact that its components correspond to spin weighted quantities, with I and V having spin weight 0, while $Q \pm iU$ have the spin weight ± 2 [65, 67]. Spin weighted quantities allow for an elegant mathematical formalism using decomposition into spin weighted spherical harmonics [38, 39, 40]. From a physical point of view the vector $\tilde{\mathbf{I}}$ is convenient since its components $(I, Q + iU, Q - iU, V)$ correspond to unpolarized component of radiation, two degrees of linear polarization, and circular polarization respectively.

The scattering of radiation in terms of $\tilde{\mathbf{I}}$ takes the form similar to the form written above for $\hat{\mathbf{I}}$

$$\tilde{\mathbf{I}}_{sc}(\theta, \phi) = \frac{1}{4\pi} \oint d\Omega' \; \tilde{\mathbf{P}}(\theta, \phi; \theta', \phi') \tilde{\mathbf{I}}_{in}(\theta', \phi'), \quad \tilde{\mathbf{P}}(\theta, \phi; \theta', \phi') = \mathbf{A}\hat{\mathbf{P}}(\theta, \phi; \theta', \phi')\mathbf{A}^{-1}.$$

The matrix $\tilde{\mathbf{P}}(\theta, \phi; \theta', \phi')$ can be elegantly written in terms of spin weighted spherical harmonics in the form [67]

$$\tilde{\mathbf{P}}(\theta, \phi; \theta', \phi') = \tilde{\mathbf{P}}_{(0)}(\theta, \phi; \theta', \phi') + \tilde{\mathbf{P}}_{(1)}(\theta, \phi; \theta', \phi') + \tilde{\mathbf{P}}_{(2)}(\theta, \phi; \theta', \phi'),$$

where

$$\tilde{\mathbf{P}}_{(0)}(\theta,\phi;\theta',\phi') = \begin{pmatrix} 1 & 0 & 0 & 0 \\ 0 & 0 & 0 & 0 \\ 0 & 0 & 0 & 0 \\ 0 & 0 & 0 & 0 \end{pmatrix},$$

$$\tilde{\mathbf{P}}_{(1)}(\theta,\phi;\theta',\phi') = 2\pi \sum_{m=-1}^{m=+1} Y_{1m}\, Y_{1m}^{*'} \begin{pmatrix} 0 & 0 & 0 & 0 \\ 0 & 0 & 0 & 0 \\ 0 & 0 & 0 & 0 \\ 0 & 0 & 0 & 1 \end{pmatrix},$$

$$\tilde{\mathbf{P}}_{(2)}(\theta,\phi;\theta',\phi') = \frac{2\pi}{5} \sum_{m=-2}^{m=+2} \begin{pmatrix} Y_{2m}\, Y_{2m}^{*'} & -\sqrt{\frac{3}{2}} Y_{2m}\, {}_{+2}Y_{2m}^{*'} & -\sqrt{\frac{3}{2}} Y_{2m}\, {}_{-2}Y_{2m}^{*'} & 0 \\ -\sqrt{6}\, {}_{+2}Y_{2m}\, Y_{2m}^{*'} & 3\, {}_{+2}Y_{2m}\, {}_{+2}Y_{2m}^{*'} & 3\, {}_{+2}Y_{2m}\, {}_{-2}Y_{2m}^{*'} & 0 \\ -\sqrt{6}\, {}_{-2}Y_{2m} Y_{2m}^{*'} & 3\, {}_{-2}Y_{2m}\, {}_{+2}Y_{2m}^{*'} & 3\, {}_{-2}Y_{2m}\, {}_{-2}Y_{2m}^{*'} & 0 \\ 0 & 0 & 0 & 0 \end{pmatrix},$$

where the arguments of funtions ${}_sY_{\ell m}$ are (θ,ϕ), and arguments of ${}_sY_{\ell m}^{*'}$ are (θ',ϕ').

The individual terms $\tilde{\mathbf{P}}_{(i)}$ of the scattering matrix have a clear physical meaning. $\tilde{\mathbf{P}}_{(0)}$ describes the isotropic unpolarized scattering of the isotropic and unpolarized part of the incoming radiation field. $\tilde{\mathbf{P}}_{(1)}$ describes the scattering of circularly polarized radiation and has a dipole ($\ell = 1$) structure. It follows that since the scattering matrix is diagonal in its last element (corresponding to the V Stokes parameter), circular polarization is produced only when the incoming radiation field has a circularly polarized dipole component. Finally, $\tilde{\mathbf{P}}_{(2)}$ term describes scattering of anisotropic and linearly polarized component of radiation. This term has a quadrupole structure ($\ell = 2$), and thus produces an anisotropic and polarized quadrupole radiation field.

As an illustration, let us consider an arbitrary incoming radiation field $\tilde{\mathbf{I}}_{in}(\theta,\phi)$. The components of this field can be decomposed into their appropriate spin-weighted harmonics as follows (below, for brevity, we do not write the arguments (θ,ϕ))

$$\tilde{\mathbf{I}}_{in} = \begin{pmatrix} I_{in} \\ Q_{in} + iU_{in} \\ Q_{in} - iU_{in} \\ V_{in} \end{pmatrix} = \sum_{\ell,m} \begin{pmatrix} a_{\ell m}^{T}\, Y_{\ell m} \\ {}_{+2}a_{\ell m}\, {}_{+2}Y_{\ell m} \\ {}_{-2}a_{\ell m}\, {}_{-2}Y_{\ell m} \\ a_{\ell m}^{V}\, Y_{\ell m} \end{pmatrix}.$$

The scattered radiation field has the form

$$\tilde{\mathbf{I}}_{sc} = \begin{pmatrix} I_{sc} \\ Q_{sc} + iU_{sc} \\ Q_{sc} - iU_{sc} \\ V_{sc} \end{pmatrix} = \begin{pmatrix} a_{00}^T\, Y_{00} \\ 0 \\ 0 \\ 0 \end{pmatrix} + \frac{1}{2} \sum_{m=-1}^{+1} \begin{pmatrix} 0 \\ 0 \\ 0 \\ a_{1m}^V\, Y_{1m} \end{pmatrix} + \frac{1}{10} \sum_{m=-2}^{+2} \begin{pmatrix} \left(a_{2m}^T - \sqrt{\frac{3}{2}}\,{}_{+2}a_{2m} - \sqrt{\frac{3}{2}}\,{}_{-2}a_{2m}\right) Y_{2m} \\ \left(-\sqrt{6}a_{2m}^T + 3\,{}_{+2}a_{2m} + 3\,{}_{-2}a_{2m}\right)\, {}_{+2}Y_{2m} \\ \left(-\sqrt{6}a_{2m}^T + 3\,{}_{+2}a_{2m} + 3\,{}_{-2}a_{2m}\right)\, {}_{-2}Y_{2m} \\ 0 \end{pmatrix}.$$

For our purpose it is important to notice a few things. Firstly, in order to produce a linearly polarized scattered radiation field ($Q_{sc} \pm iU_{sc}$ components), the incoming field must have a quadrupole component in anisotropy or polarization (i.e. $a_{2m}^T \neq 0$ or ${}_{\pm 2}a_{2m} \neq 0$). Secondly, the scattered radiation field (ignoring the isotropic component) has a quadrupole ($\ell = 2$) structure in anisotropy and linear polarization.

The analysis of a single act of scattering considered in this section are important to keep in mind in the subsequent sections where we write the radiative transfer equation. Many of the general statements about the solution to the radiative transfer equation follow directly from the physics and geometry of an individual act of scattering considered above.

4.3 Radiative transfer in a perturbed universe

We now shift our attention to cosmology. We need to work out the radiative transfer equation in a slightly perturbed FLRW universe described by metric (2.4). As was mentioned in the previous section, the Thomson scattering of initially unpolarized light cannot generate circular polarization, so we shall not consider the V Stokes parameter. Following [69, 70], we shall write the radiative transfer equation in terms of a 3-component quantity (symbolic vector) $\hat{\mathbf{n}}(x^\alpha, p^\alpha)$. The components $(\hat{n}_1, \hat{n}_2, \hat{n}_3)$ are related to the Stokes parameters by

$$\hat{\mathbf{n}} = \begin{pmatrix} \hat{n}_1 \\ \hat{n}_2 \\ \hat{n}_3 \end{pmatrix} = \frac{1}{2}\frac{c^2}{h\nu^3} \begin{pmatrix} I + Q \\ I - Q \\ -2U \end{pmatrix}, \tag{4.6}$$

where h is the Planck constant. The quantities $\hat{n}_1, \hat{n}_2, (\hat{n}_1+\hat{n}_2+\hat{n}_3)/2$ are the numbers of photons of frequency ν coming from the direction (θ, ϕ) on the sky and passing through a polarimeter oriented in the directions of the meridian, parallel, and their bisection respectively.

The equation of radiative transfer can be treated as a Boltzmann equation in a phase space. The general form of this equation is as follows [71]

$$\frac{D\hat{\mathbf{n}}}{ds} = \hat{\mathbf{C}}\left[\hat{\mathbf{n}}\right], \tag{4.7}$$

where s is a parameter along the world-line of a photon, $\frac{D}{ds}$ is a total derivative along this world-line, and $\hat{\mathbf{C}}$ is a collision term. We shall explain each term of this equation separately.

The total derivative in Eq. (4.7) reads:

$$\frac{D\hat{\mathbf{n}}}{ds} = \left[\frac{dx^\alpha}{ds}\frac{\partial}{\partial x^\alpha} + \frac{dp^\alpha}{ds}\frac{\partial}{\partial p^\alpha}\right]\hat{\mathbf{n}}, \tag{4.8}$$

where dx^α/ds and dp^α/ds are determined by the light-like geodesic world-line,

$$\frac{dx^\alpha}{ds} = p^\alpha, \quad \frac{dp^\alpha}{ds} = -\Gamma^\alpha_{\beta\gamma}p^\beta p^\gamma, \quad g_{\alpha\beta}p^\alpha p^\beta = 0. \tag{4.9}$$

Strictly speaking, the square bracket in Eq. (4.8) should also include the additive matrix term $\hat{\mathbf{R}}$. This term is responsible for the rotation of polarization axes that may take place in course of parallel transport along the photon's geodesic line [72]. In the perturbation theory that we are working with, this matrix does not enter the equations in the zeroth and first order approximations [69], and therefore we neglect $\hat{\mathbf{R}}$.

In our problem, the collision term $\hat{\mathbf{C}}$ describes the Thomson scattering of light on free (not combined in atoms) electrons [66]. We assume that the electrons are at rest with respect to one of synchronous coordinate systems (2.4). We work with this coordinate system, so that it is not only synchronous but also 'comoving' with the electrons. (This choice is always possible when the functions h_{ij} in (2.4) are gravitational waves. Certain complications in the case of density perturbations will be considered later,

Appendix F.) Thus, the collision term $\hat{\mathbf{C}}$ is given by the expression

$$\hat{\mathbf{C}}\left[\hat{\mathbf{n}}\right] = -\sigma_T N_e(x^\alpha)\left(\frac{cdt}{ds}\right)\left[\hat{\mathbf{n}}(t,x^i,\nu,\theta,\phi) - \frac{1}{4\pi}\int d\Omega'\hat{\mathbf{P}}(\theta,\phi;\theta',\phi')\hat{\mathbf{n}}(t,x^i,\nu,\theta',\phi')\right], \tag{4.10}$$

where σ_T is the Thomson cross section, N_e is the density of free electrons, and $\hat{\mathbf{P}}(\theta,\phi;\theta',\phi')$ is the Chandrasekhar scattering matrix. (The explicit form of the scattering matrix is discussed in Appendix E.) The factor cdt/ds arises because of our use of the element ds, instead of cdt, in the left hand side (l.h.s.) of Eq. (4.7). In accord with the meaning of the scattering term, the quantity $\sigma_T N_e(x^\alpha)(cdt/ds)$ is the averaged number of electrons that could participate in the scattering process when the photon traversed the element ds along its path.

Let us now write down the equations of radiative transfer in the presence of the gravitational field (2.4). First, we write down the equations for the light-like geodesic line $x^\alpha(s) = (\eta(s), x^i(s))$:

$$p^0 = \frac{d\eta}{ds} = \frac{\nu}{ca}, \quad p^i = \frac{dx^i}{ds} = \frac{\nu}{ca}e^i, \quad \frac{d\nu}{ds} = -\nu\left[\frac{1}{a}\frac{da}{d\eta} + \frac{1}{2}e^i e^j\frac{\partial h_{ij}}{\partial\eta}\right]\frac{d\eta}{ds}, \tag{4.11}$$

$$\left(\delta_{ij} + h_{ij}\right)e^i e^j = 1.$$

We do not need the expression for de^i/ds, because it is a first-order (in terms of metric perturbations) quantity, and this quantity enters the equations of radiative transfer only in products with other first-order terms. We neglect such second-order corrections.

Second, we write for the 'vector' $\hat{\mathbf{n}}$:

$$\hat{\mathbf{n}} = \hat{\mathbf{n}}^{(0)} + \hat{\mathbf{n}}^{(1)}, \tag{4.12}$$

where $\hat{\mathbf{n}}^{(0)}$ is the zeroth order solution, and $\hat{\mathbf{n}}^{(1)}$ is the first order correction arising because of the presence of metric perturbations. We shall now formulate the equation for $\hat{\mathbf{n}}^{(1)}$, taking into account the zero-order solution to Eq. (4.7).

In the zero-order approximation we assume that $h_{ij} = 0$ and that the radiation field is fully homogeneous, isotropic, and unpolarized. Therefore,

$$\hat{\mathbf{n}}^{(0)} = n^{(0)}(\eta, \nu)\hat{\mathbf{u}}, \tag{4.13}$$

where

$$\hat{\mathbf{u}} = \begin{pmatrix} 1 \\ 1 \\ 0 \end{pmatrix}.$$

Since the scattering matrix $\hat{\mathbf{P}}$ does not couple to the radiation field if it has no quadrupole anisotropy, the collision term (4.10) vanishes, $\hat{\mathbf{C}}\left[\hat{\mathbf{n}}^{(0)}\right] = 0$, and the equation for $n^{(0)}(\eta, \nu)$ reads

$$\frac{\partial n^{(0)}}{\partial \eta} - \frac{\nu}{a}\frac{da}{d\eta}\frac{\partial n^{(0)}}{\partial \nu} = 0.$$

The general solution to this equation is $n^{(0)} = n_0\left(\nu a(\eta)\right)$, which makes it convenient to use a new variable

$$\tilde{\nu} = \nu a(\eta).$$

In the zero-order approximation, $\nu = \text{const}/a(\eta)$ and therefore $\tilde{\nu}$ is a constant along the light ray.

We are now in a position to write down the first-order approximation to the Boltzmann equation (4.7). We take $(\eta, x^i, \tilde{\nu}, e^i)$ as independent variables, i.e. $n^{(0)} = n_0\left(\tilde{\nu}\right)$, $\hat{\mathbf{n}}^{(1)} = \hat{\mathbf{n}}^{(1)}(\eta, x^i, \tilde{\nu}, e^i)$, and use the identity

$$\frac{dp^\alpha}{ds}\frac{\partial}{\partial p^\alpha} = \frac{d\tilde{\nu}}{ds}\frac{\partial}{\partial \tilde{\nu}} + \frac{de^i}{ds}\frac{\partial}{\partial e^i}$$

in the first-order approximation to (4.8). Taking also into account the geodesic equation (4.11) we arrive at the equation

$$\left[\frac{\partial \hat{\mathbf{n}}^{(1)}}{\partial \eta} + e^i\frac{\partial \hat{\mathbf{n}}^{(1)}}{\partial x^i} - \frac{1}{2}\tilde{\nu}e^i e^j\frac{\partial h_{ij}}{\partial \eta}\frac{\partial \hat{\mathbf{n}}^{(0)}}{\partial \tilde{\nu}}\right]\frac{d\eta}{ds} = \hat{\mathbf{C}}\left[\hat{\mathbf{n}}^{(1)}\right].$$

Introducing new notations $q(\eta) = \sigma_T a(\eta) N_e(\eta)$ and $f(\tilde{\nu}) = \partial \ln n_0 / \partial \ln \tilde{\nu}$ [69] (the astrophysical meaning and numerical values of the functions $q(\eta)$ and $f(\tilde{\nu})$ are discussed in Appendix D) we write down the final form of the transfer equation:

$$\left[\frac{\partial}{\partial \eta} + q(\eta) + e^i \frac{\partial}{\partial x^i}\right] \hat{\mathbf{n}}^{(1)}(\eta, x^i, \tilde{\nu}, e^i) =$$
$$= \frac{f(\tilde{\nu}) n_0(\tilde{\nu})}{2} e^i e^j \frac{\partial h_{ij}}{\partial \eta} \hat{\mathbf{u}} + q(\eta) \frac{1}{4\pi} \int d\Omega' \, \hat{\mathbf{P}}(e^i; e'^j) \hat{\mathbf{n}}^{(1)}(\eta, x^i, \tilde{\nu}, e'^j). \quad (4.14)$$

It is seen from Eq. (4.14) that the 'source' for the generation of $\hat{\mathbf{n}}^{(1)}$ consists of two terms on the r.h.s. of this equation. First, it is the gravitational field perturbation h_{ij}, participating in the combination $e^i e^j \partial h_{ij} / \partial \eta$. It directly generates a structure proportional to $\hat{\mathbf{u}}$, i.e. a variation in the I Stokes parameter and a temperature anisotropy. In this process, a quadrupole component of the temperature anisotropy necessarily arises due to the presence of the term $e^i \partial / \partial x^i$, even if the above-mentioned combination itself does not have angular dependence. The second term on the r.h.s. of Eq. (4.14) generates polarization, i.e. a structure different from $\hat{\mathbf{u}}$. This happens because of the mixing of different components of $\hat{\mathbf{n}}^{(1)}$, including those proportional to $\hat{\mathbf{u}}$, in the product term $\hat{\mathbf{P}}\hat{\mathbf{n}}^{(1)}$. In other words, polarization is generated by the scattering of anisotropic radiation field. Clearly, polarization is generated only in the intervals of time when $q(\eta) \neq 0$, i.e. when free electrons are available for the Thomson scattering (see, for example, [73]).

Chapter 5

Imprints of Relic Gravitational waves in the CMB

5.1 The radiative transfer equations for a single gravitational wave

In this chapter, using the results on relic gravitational waves from chapter 2, and the general formalism of radiative transfer in a slightly perturbed FLRW universe developed in chapter 4, we shall consider the imprints of gravitational waves on the anisotropies in temperature and polarization of CMB radiation.

We work with a random gravitational field h_{ij} expanded over spatial Fourier components (2.11). It is convenient to make similar expansion for the quantities $\hat{\mathbf{n}}^{(1)}(\eta, x^i, \tilde{\nu}, e^i)$. Since Eq. (4.14) is linear, the Fourier components of $\hat{\mathbf{n}}^{(1)}$ inherit the same random coefficients $\overset{s}{c}_{\mathbf{n}}$ that enter Eq. (2.11):

$$\hat{\mathbf{n}}^{(1)}(\eta, x^i, \tilde{\nu}, e^i) = \frac{\mathcal{C}}{(2\pi)^{3/2}} \int_{-\infty}^{+\infty} \frac{d^3\mathbf{n}}{\sqrt{2n}} \sum_{s=1,2} \left[\hat{\mathbf{n}}^{(1)}_{\mathbf{n},s}(\eta, \tilde{\nu}, e^i) e^{i\mathbf{n}\cdot\mathbf{x}} \overset{s}{c}_{\mathbf{n}} + \hat{\mathbf{n}}^{(1)*}_{\mathbf{n},s}(\eta, \tilde{\nu}, e^i) e^{-i\mathbf{n}\cdot\mathbf{x}} \overset{s*}{c}_{\mathbf{n}} \right]. \tag{5.1}$$

Equation (4.14) for a particular Fourier component takes the form:

$$\left[\frac{\partial}{\partial\eta} + q(\eta) + i e^i n_i \right] \hat{\mathbf{n}}^{(1)}_{\mathbf{n},s}(\eta, \tilde{\nu}, e^i) =$$
$$= \frac{f(\tilde{\nu}) n_0(\tilde{\nu})}{2} e^i e^j \overset{s}{p}_{ij}(\mathbf{n}) \frac{d\,\overset{s}{h}_n(\eta)}{d\eta} \hat{\mathbf{u}} + \frac{q(\eta)}{4\pi} \int d\Omega'\, \hat{\mathbf{P}}(e^i; e'^j) \hat{\mathbf{n}}^{(1)}_{\mathbf{n},s}(\eta, \tilde{\nu}, e'^j). \tag{5.2}$$

To simplify technical details, we start with a single gravitational wave propagating exactly in the direction of z, i.e. $\mathbf{n}$ is parallel to z axis. The $(\mathbf{l}, \mathbf{m})$ vectors, figuring in the expression for polarization tensors (2.2) and (2.20), are specified by $\theta = 0$, $\phi = 0$ in (2.5). This simplifies the polarization tensors (2.20) and makes them constant matrices. At the same time, the observation direction is arbitrary and is defined by $e^i = (\sin\theta\cos\phi,\ \sin\theta\sin\phi,\ \cos\theta)$. We consider circularly polarized states with $s = 1 = L$, $s = 2 = R$. Then, we find

$$e^i e^j \overset{s}{p}_{ij}(\mathbf{n}) = (1-\mu^2)e^{\pm 2i\phi}, \tag{5.3}$$

where $\mu = \cos\theta$, and the $\pm$ signs correspond to $s = L, R$, respectively. This simplification of the angular dependence is possible only for one Fourier component, but not for all of them together. We shall still need the results for a wave propagating in an arbitrary direction. The necessary generalization will be done in Sec. 5.3.2.

The $\pm 2\phi$ angular dependence of the source term in Eq. (5.2) generates the $\pm 2\phi$ angular dependence in the solution [69, 70]. We show in Appendix E that the terms in $\hat{\mathbf{n}}^{(1)}_{\mathbf{n},s}(\eta, \tilde{\nu}, \mu, \phi)$ with any other ϕ-dependence satisfy homogeneous differential equations, and therefore they vanish if they were not present initially (which we always assume). Similarly, the $\tilde{\nu}$ dependence of the solution can be factored out. Finally, we show in Appendix E that one linear combination of the three components of $\hat{\mathbf{n}}^{(1)}_{\mathbf{n}}$ always satisfies a homogeneous equation and therefore vanishes at zero initial data. Thus, the problem of solving Eq. (5.2) reduces to the problem of finding two functions of the arguments η, μ.

Explicitly, we can now write

$$\hat{\mathbf{n}}^{(1)}_{n,s}(\eta, \tilde{\nu}, \mu, \phi) = \\ = \frac{f(\tilde{\nu})n_0(\tilde{\nu})}{2}\left[\alpha_{n,s}(\eta,\mu)(1-\mu^2)\begin{pmatrix}1\\1\\0\end{pmatrix} + \beta_{n,s}(\eta,\mu)\begin{pmatrix}(1+\mu^2)\\-(1+\mu^2)\\\mp 4i\mu\end{pmatrix}\right]e^{\pm 2i\phi}. \tag{5.4}$$

Clearly, function α is responsible for temperature anisotropy (I Stokes parameter), while function β is responsible for polarization (Q and U Stokes parameters).

Temporarily dropping out the labels n, s and introducing the auxiliary function $\xi(\eta,\mu) = \alpha(\eta,\mu) + \beta(\eta,\mu)$, we get from Eqs. (5.2),(5.4) a pair of coupled equations [70]:

$$\frac{\partial\beta(\eta,\mu)}{\partial\eta} + (q(\eta) + in\mu)\,\beta(\eta,\mu) = \frac{3}{16}q(\eta)\mathcal{I}(\eta), \tag{5.5}$$

$$\frac{\partial\xi(\eta,\mu)}{\partial\eta} + (q(\eta) + in\mu)\,\xi(\eta,\mu) = \frac{dh(\eta)}{d\eta}, \tag{5.6}$$

where

$$\mathcal{I}(\eta) = \int_{-1}^{1} d\mu' \left[(1+\mu'^2)^2\beta(\eta,\mu') - \frac{1}{2}(1-\mu'^2)^2\xi(\eta,\mu')\right]. \tag{5.7}$$

5.2 Radiative transfer equations as a single integral equation

In some previous studies [74, 65, 75], equations (5.5), (5.6) are being solved by first expanding the μ-dependence in terms of Legendre polynomials. This generates an infinite series of coupled ordinary differential equations. Then, the series is being truncated at some order.

We go by a different road. We demonstrate that the problem can be reduced to a single mathematically consistent integral equation. There are technical and interpretational advantages in this approach. The integral equation enables us to derive physically transparent analytical solutions and make reliable estimates of the generated polarization. The numerical implementation of the integral equation considerably saves computing time and allows simple control of accuracy.

5.2.1 Derivation of the integral equation

In order to show that the solutions of Eqs. (5.5), (5.6) for $\alpha(\eta,\mu)$ and $\beta(\eta,\mu)$ are completely determined by a single integral equation, we first introduce new quantities

[76]

$$\Phi(\eta) = \frac{3}{16} g(\eta) \mathcal{I}(\eta), \tag{5.8}$$

$$H(\eta) = e^{-\tau(\eta)} \frac{dh(\eta)}{d\eta}. \tag{5.9}$$

Solutions to Eqs. (5.5), (5.6) can be written as

$$\beta(\eta, \mu) = e^{\tau(\eta) - in\mu\eta} \int_0^\eta d\eta' \; \Phi(\eta') e^{in\mu\eta'}, \tag{5.10}$$

$$\xi(\eta, \mu) = e^{\tau(\eta) - in\mu\eta} \int_0^\eta d\eta' \; H(\eta') e^{in\mu\eta'}, \tag{5.11}$$

Expression (5.10) is a formal solution to Eq. (5.5) in the sense that $\beta(\eta, \mu)$ is expressed in terms of $\Phi(\eta)$ which itself depends on $\beta(\eta, \mu)$ (see (5.7) and (5.8)).

We now put (5.10) and (5.11) into Eq. (5.7) to get a new formulation for $\mathcal{I}(\eta)$:

$$\mathcal{I}(\eta) = e^{\tau(\eta)} \int_{-1}^{1} \int_0^\eta d\mu d\eta' \left[\left(1 + \mu^2\right)^2 \Phi(\eta') - \frac{1}{2} \left(1 - \mu^2\right)^2 H(\eta') \right] e^{in\mu(\eta' - \eta)}. \tag{5.12}$$

Using the kernels $K_\pm(\eta - \eta')$,

$$K_\pm(\eta - \eta') = \int_{-1}^{1} d\mu (1 \pm \mu^2)^2 e^{in\mu(\eta - \eta')}, \tag{5.13}$$

Eq. (5.12) can be rewritten as

$$\mathcal{I}(\eta) = e^{\tau(\eta)} \int_0^\eta d\eta' \left[K_+(\eta - \eta') \Phi(\eta') - \frac{1}{2} K_-(\eta - \eta') H(\eta') \right]. \tag{5.14}$$

Multiplying both sides of this equality by $(3/16) q(\eta) e^{-\tau(\eta)}$ and recalling the definition (5.8) we arrive at a closed form equation for $\Phi(\eta)$:

$$\Phi(\eta) = \frac{3}{16} q(\eta) \int_0^\eta d\eta' \Phi(\eta') K_+(\eta - \eta') + F(\eta), \tag{5.15}$$

where $F(\eta)$ is the known gravitational-field term given by the metric perturbations,

$$F(\eta) = -\frac{3}{32} q(\eta) \int_0^\eta d\eta' H(\eta') K_-(\eta - \eta'), \tag{5.16}$$

The derived equation (5.15) for $\Phi(\eta)$ is the integral equation of Voltairre type. As soon as $\Phi(\eta)$ is found from this equation, we can find $\beta(\eta,\mu)$ from Eq. (5.10). Then, Eqs. (5.11) and (5.10) completely determine all the components of $\hat{\mathbf{n}}^{(1)}$ according to Eq. (5.4).

Clearly, we are mainly interested in temperature and polarization anisotropies seen at the present time $\eta = \eta_R$. Introducing $\zeta = n(\eta_R - \eta)$ and restoring the indices n and s, we obtain the present-day values of α and β:

$$\alpha_{n,s}(\mu) \equiv \alpha_{n,s}(\eta_R,\mu) = \int_0^{\eta_R} d\eta \left(H_{n,s}(\eta) - \Phi_{n,s}(\eta)\right) e^{-i\mu\zeta}, \tag{5.17a}$$

$$\beta_{n,s}(\mu) \equiv \beta_{n,s}(\eta_R,\mu) = \int_0^{\eta_R} d\eta\ \Phi_{n,s}(\eta) e^{-i\mu\zeta}. \tag{5.17b}$$

The integrals can safely be taken from $\eta = 0$ as the optical depth τ quickly becomes very large in the early Universe, and the 'source' functions $H_{n,s}(\eta)$ and $\Phi_{n,s}(\eta)$ quickly vanish there. We will work with expressions (5.17) in our further calculations.

5.2.2 Analytical solution to the integral equation

The integral equation (5.15) can be solved analytically in the form of a series expansion. Although our graphs and physical conclusions in this work are based on the exact numerical solution to Eq. (5.15), it is important to have a simple analytical approximation to the exact numerical solution. We will show below why the infinite series can be accurately approximated by its first term and how this simplification helps in physical understanding of the derived numerical results.

We start with the transformation of kernels (5.13) of the integral equation (5.15). Using the identity $\mu^k e^{ix\mu} = (d/idx)^k e^{ix\mu}$, the kernels can be written as

$$K_{\pm}(\eta - \eta') = \int_{-1}^{+1} d\mu\ (1 \pm \mu^2)^2 e^{in\mu(\eta-\eta')} = 2\left(1 \mp \frac{d^2}{dx^2}\right)^2 \frac{\sin x}{x},$$

where $x = n(\eta - \eta')$. Now, taking into account the expansion

$$\frac{\sin x}{x} = \sum_{m=0}^{\infty} \frac{(-1)^m}{(2m+1)!} x^{2m},$$

the r.h.s. of Eq. (5.15) can be presented in the form of a series:

$$\Phi(\eta) = \frac{3}{2} q(\eta) \sum_{m=0}^{\infty} n^{2m} \int_0^{\eta} d\eta' \ (\eta - \eta')^{2m} \left[\lambda_+(m) \Phi(\eta') - \lambda_-(m) H(\eta') \right], \qquad (5.18)$$

where

$$\lambda_+(m) = \frac{(-1)^m}{(2m+1)!} \left[1 - 4 \frac{(m+2)}{(2m+3)(2m+5)} \right],$$
$$\lambda_-(m) = \frac{(-1)^m}{(2m+1)!(2m+3)(2m+5)}.$$

Since the r.h.s. of Eq. (5.18) is a series in even powers of the wavenumber n, the l.h.s. of the same equation can also be expanded in powers of n^{2m}:

$$\Phi(\eta) = \sum_{m=0}^{\infty} \Phi^{(m)}(\eta) n^{2m}. \qquad (5.19)$$

Using expansion (5.19) in both sides of Eq. (5.18) we transform this equation to

$$\sum_{m=0}^{\infty} \Phi^{(m)}(\eta) n^{2m} = \frac{3}{2} q(\eta) \left[\sum_{m=0}^{\infty} \sum_{j=0}^{\infty} \lambda_+(m) n^{2(m+j)} \int_0^{\eta} d\eta' \Phi^{(j)}(\eta') (\eta - \eta')^{2m} \right.$$
$$\left. - \sum_{m=0}^{\infty} \lambda_-(m) n^{2m} \int_0^{\eta} d\eta' H(\eta') (\eta - \eta')^{2m} \right]. \qquad (5.20)$$

The left side and the second term in the right side of Eq. (5.20) are series in n^{2m}, but the first sum on the r.h.s. of Eq. (5.20) is still a mixture of different powers. This sum can be rearranged to be manifestly a series in n^{2m}:

$$\sum_{m=0}^{\infty} \sum_{j=0}^{\infty} \lambda_+(m) n^{2(m+j)} \int_0^{\eta} d\eta' \Phi^{(j)}(\eta') (\eta - \eta')^{2m} =$$
$$= \sum_{m=0}^{\infty} n^{2m} \left[\sum_{k=0}^{m} \lambda_+(k) \int_0^{\eta} d\eta' \Phi^{(m-k)}(\eta') (\eta - \eta')^{2k} \right]. \qquad (5.21)$$

According to Eq. (5.20) we have to make equal the coefficients of terms with the same power n^{2m} in both sides of the equation. This produces a set of integral equations

$$\Phi^{(m)}(\eta) = q(\eta) S^{(m)}(\eta) + \frac{7}{10} q(\eta) \int_0^{\eta} d\eta' \ \Phi^{(m)}(\eta'), \qquad (5.22)$$

where functions $S^{(m)}(\eta)$ depend only on the known function $H(\eta)$ and functions $\Phi^{(m-k)}(\eta)$ presumed to be found from equations of previous orders:

$$S^{(m)}(\eta) = -\frac{3}{2}\lambda_-(m)\int_0^\eta d\eta'\ H(\eta')(\eta-\eta')^{2m} + \frac{3}{2}\sum_{k=1}^{m}\lambda_+(k)\int_0^\eta d\eta'\ \Phi^{(m-k)}(\eta')(\eta-\eta')^{2k}. \tag{5.23}$$

The important advantage of the performed expansion in powers of n^{2m} is that Eq. (5.22) of any order m is now a self-contained analytically solvable integral equation.

Exact solution to the integral equation (5.22) is given by the formula

$$\Phi^{(m)}(\eta) = q(\eta)\int_0^\eta d\eta' \frac{dS^{(m)}(\eta')}{d\eta'} e^{\frac{7}{10}\tau(\eta,\eta')}. \tag{5.24}$$

We can further simplify this formula. Taking an η-derivative of expression (5.23) we find

$$\frac{dS^{(m)}(\eta)}{d\eta} = -\frac{1}{10}H(\eta)\delta_{0m} - \omega_-(m)\int_0^\eta d\eta' H(\eta')(\eta-\eta')^{2m-1} + \sum_{k=1}^{m}\omega_+(k)\int_0^\eta d\eta'\Phi^{(m-k)}(\eta')(\eta-\eta')^{2k-1},$$

where $\omega_\pm(m) = 3m\lambda_\pm(k)$. Substituting this expression into Eq. (5.24), we arrive at the final result

$$\Phi^{(m)}(\eta) = q(\eta)e^{-\frac{7}{10}\tau(\eta)}\int_0^\eta d\eta' e^{\frac{7}{10}\tau(\eta')}\left[-H(\eta')\left(\frac{1}{10}\delta_{0m} + \omega_-(m)\Psi_{(m)}(\eta,\eta')\right) + \sum_{k=1}^{m}\omega_+(k)\Phi^{(m-k)}(\eta')\Psi_{(k)}(\eta,\eta')\right], \tag{5.25}$$

where

$$\Psi_{(k)}(\eta,\eta') = \int_{\eta'}^\eta d\eta''\ e^{-\frac{7}{10}\tau(\eta'',\eta')}(\eta''-\eta')^{2k-1}. \tag{5.26}$$

Functions $\Psi_{(k)}(\eta,\eta')$ depend only on the ionization history of the background cosmological model described by $q(\eta)$. These functions can be computed in advance.

Complete determination of the function $\Phi(\eta)$, Eq. (5.19), requires only one integration by η at each level m in Eq. (5.25), starting from $m = 0$. The zero-order term $\Phi^{(0)}(\eta)$ does not depend on functions $\Psi_{(k)}$ and is determined exclusively by $H(\eta)$, Eq. (5.9). The zero-order term can be presented as

$$\Phi_n^{(0)}(\eta) = -\frac{1}{10} g(\eta) \int_0^\eta d\eta' \frac{dh_n(\eta')}{d\eta} e^{-\frac{3}{10}\tau(\eta,\eta')}. \tag{5.27}$$

It is crucial to remember that the function $\Phi(\eta)$, Eq. (5.8), always contains the narrow visibility function $g(\eta)$ (see Appendix D). In particular, function $\Phi^{(0)}(\eta)$ is nonzero only for η within the width of $g(\eta)$, and is proportional to this width. In the era of decoupling, we denote the characteristic width of $g(\eta)$ by $\Delta\eta_{dec}$. With $\Delta\eta_{dec}$ we associate the characteristic wavenumber n_*:

$$n_* = \frac{2\pi}{\Delta\eta_{dec}}.$$

Numerically, $\Delta\eta_{dec} \approx 3 \times 10^{-3}$ and $n_* \approx 2 \times 10^3$. In what follows, we will be interested in CMB multipoles $\ell \lesssim 10^3$. They are mostly generated by perturbations with wavenumbers $n \lesssim 10^3$. Therefore, for wavenumbers of interest, we regard n/n_* as a small parameter.

We shall now show that $\Phi^{(0)}(\eta)$ is the dominant term of the series (5.19). The next term, $\Phi^{(1)}(\eta)n^2$, is at least a factor $(n/n_*)^2$ smaller than $\Phi^{(0)}(\eta)$, and so on. The explicit expression for $\Phi^{(1)}$ is as follows

$$\Phi^{(1)}(\eta) = -g(\eta) \int_0^\eta d\eta' \left[\omega_-(1)\frac{dh(\eta')}{d\eta'} - \omega_+(1)e^{\tau(\eta')}\Phi^{(0)}(\eta')\right] e^{-\frac{3}{10}\tau(\eta,\eta')}\Psi_{(1)}(\eta,\eta').$$

Effectively, function $\Phi^{(1)}(\eta)$, in comparison with $\Phi^{(0)}(\eta)$, contains an extra factor $\Psi_{(1)}(\eta,\eta')$. Taking into account the fact that the functions $g(\eta)$ and $e^{-\frac{7}{10}\tau(\eta'',\eta')}$ are localized in the interval of arguments not larger than $\Delta\eta_{dec}$, this factor evaluates to a number not larger than $(\Delta\eta_{dec})^2$. Therefore, the $m = 1$ term in Eq. (5.19) is at least a factor $(n/n_*)^2$ smaller than the $m = 0$ term.

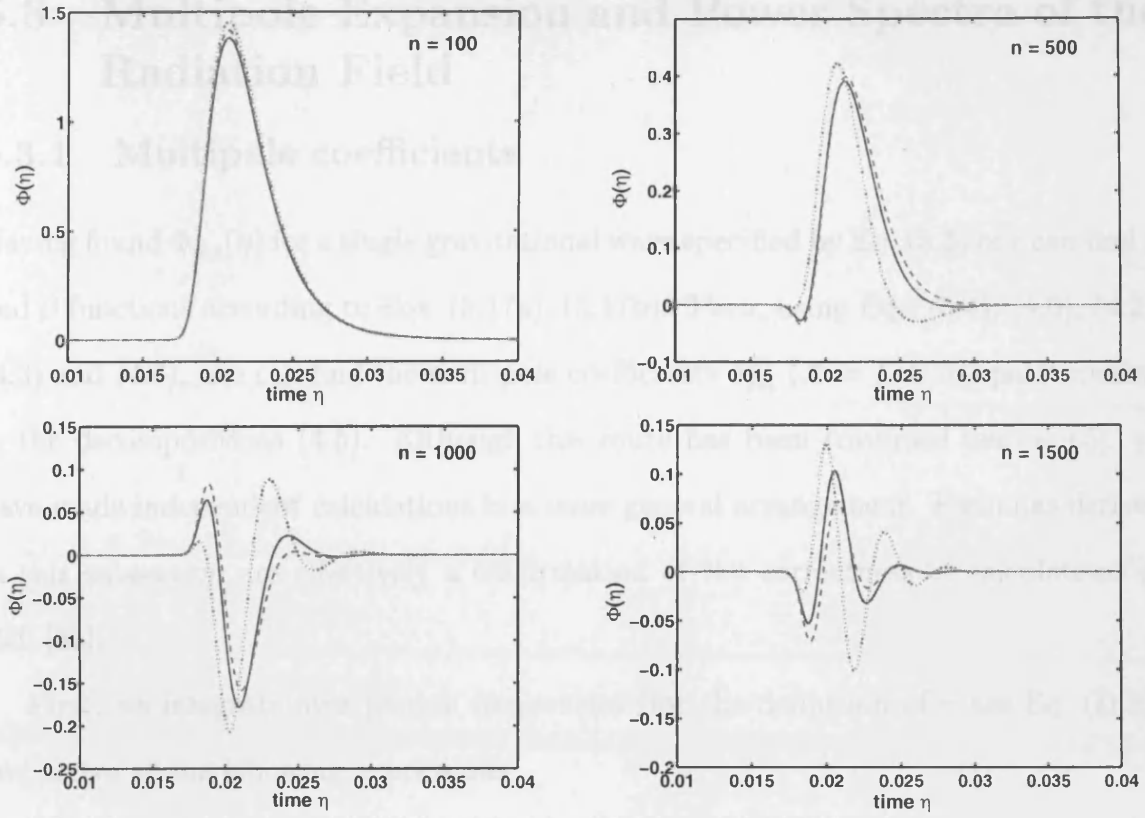

Figure 5.1: Function $\Phi_n(\eta)$ for different values of n. The solid line is exact numerical solution to Eq. (5.15). The dashed line is the zero order approximation (5.27). The dotted line shows the approximation (5.45) (see below). The g.w. mode functions are normalized such that $h_n(\eta_r) = 1$.

These analytical evaluations are confirmed by numerical analysis as shown in Fig. 5.1. The solid line shows the exact numerical solution found from Eq. (5.15) for $h_n(\eta)$ and $q(\eta)$ described in Sec. 2.2.2 and Appendix D respectively. The dashed line is plotted according to formula (5.27), with the same $h_n(\eta)$ and $q(\eta)$. It is seen from Fig. 5.1 that the zero-order term $\Phi^{(0)}(\eta)$ is a good approximation. The deviations are significant, they reach (20-25)%, only for the largest wavenumbers n in the domain of our interest.

5.3 Multipole Expansion and Power Spectra of the Radiation Field

5.3.1 Multipole coefficients

Having found $\Phi_{n,s}(\eta)$ for a single gravitational wave specified by Eq. (5.3) one can find α and β functions according to Eqs. (5.17a), (5.17b). Then, using Eqs. (5.4), (4.6), (4.2), (4.3) and (4.4), one can find the multipole coefficients $a^X_{\ell m}$ $(X = I, E, B)$ participating in the decompositions (4.5). Although this route has been traversed before [65], we have made independent calculations in a more general arrangement. Formulas derived in this subsection are effectively a confirmation of the correctness of calculations in Ref. [65].

First, we integrate over photon frequencies (for the definition of γ see Eq. (D.3)) and arrive at the following expressions

$$I_{n,s}(\mu,\phi) = \gamma\left[\left(1-\mu^2\right)\alpha_{n,s}(\mu)\, e^{\pm 2i\phi}\right], \tag{5.28a}$$

$$E_{n,s}(\mu,\phi) = -\gamma\left[\left(1-\mu^2\right)\left(\left(1+\mu^2\right)\frac{d^2}{d\mu^2} + 8\mu\frac{d}{d\mu} + 12\right)\beta_{n,s}(\mu)\, e^{\pm 2i\phi}\right], \tag{5.28b}$$

$$B_{n,s}(\mu,\phi) = \mp\gamma\left[2\left(1-\mu^2\right)\left(i\mu\frac{d^2}{d\mu^2} + 4i\frac{d}{d\mu}\right)\beta_{n,s}(\mu)\, e^{\pm 2i\phi}\right], \tag{5.28c}$$

where, as before, the upper and lower signs correspond to $s = 1 = L$ and $s = 2 = R$, respectively. The $\pm 2\phi$ dependence in Eqs. (5.28) implies that only the $m = \pm 2$ multipoles are nonzero.

Then, we integrate Eqs. (5.28) over angular variables in order to find $a^X_{\ell m}$ according to Eq. (4.5). Using the notations $T_\ell(\zeta)$, $E_\ell(\zeta)$, $B_\ell(\zeta)$ for the functions arising in course of calculations (and called multipole projection functions)

$$T_\ell(\zeta) = \sqrt{\frac{(\ell+2)!}{(\ell-2)!}}\,\frac{j_\ell(\zeta)}{\zeta^2}, \tag{5.29a}$$

$$E_\ell(\zeta) = \left[\left(2 - \frac{l(l-1)}{\zeta^2}\right)j_\ell(\zeta) - \frac{2}{\zeta}j_{\ell-1}(\zeta)\right], \tag{5.29b}$$

$$B_\ell(\zeta) = 2\left[-\frac{(\ell-1)}{\zeta}j_\ell(\zeta) + j_{\ell-1}(\zeta)\right], \tag{5.29c}$$

and replacing $\alpha(\mu)$ and $\beta(\mu)$ by their expressions (5.17), we finally arrive at

$$a^T_{\ell m}(n,s) = (-i)^{\ell-2}\left(\delta_{2,m}\delta_{1,s} + \delta_{-2,m}\delta_{2,s}\right) a^T_\ell(n,s), \tag{5.30a}$$

$$a^E_{\ell m}(n,s) = (-i)^{\ell-2}\left(\delta_{2,m}\delta_{1,s} + \delta_{-2,m}\delta_{2,s}\right) a^E_\ell(n,s), \tag{5.30b}$$

$$a^B_{\ell m}(n,s) = (-i)^{\ell-2}\left(\delta_{2,m}\delta_{1,s} - \delta_{-2,m}\delta_{2,s}\right) a^B_\ell(n,s), \tag{5.30c}$$

where

$$a^T_\ell(n,s) = \gamma\sqrt{4\pi(2\ell+1)}\int_0^{\eta_R} d\eta\ \left(H_{n,s}(\eta) - \Phi_{n,s}(\eta)\right) T_\ell(\zeta), \tag{5.31a}$$

$$a^E_\ell(n,s) = \gamma\sqrt{4\pi(2\ell+1)}\int_0^{\eta_R} d\eta\ \Phi_{n,s}(\eta) E_\ell(\zeta), \tag{5.31b}$$

$$a^B_\ell(n,s) = \gamma\sqrt{4\pi(2\ell+1)}\int_0^{\eta_R} d\eta\ \Phi_{n,s}(\eta) B_\ell(\zeta). \tag{5.31c}$$

5.3.2 Superposition of gravitational waves with arbitrary wavevectors

It is important to remember that the result (5.30) is valid only for a special wave, with the wavevector $\mathbf{n}$ oriented exactly along the coordinate axis z. Since the perturbed gravitational field is a random collection of waves with all possible wavevectors $\mathbf{n}$, and we are interested in their summarized effect as seen in some fixed observational direction (θ,ϕ), we have to find the generalization of Eq. (5.30) to an arbitrary wave, and then to sum them up.

To find the effect of an arbitrary wave, there is no need to do new calculations. It is convenient to treat calculations in Sec. 5.3.1 as done in a (primed) coordinate system specially adjusted to a given wave in such a manner that the wave propagates along z', $\mathbf{n}' = (0,0,n)$. The observational direction e^i is characterized by (θ',ϕ'). The quantities $X = I, E, B$ calculated in Sec. 5.3.1 are functions of (θ',ϕ') expanded over $Y_{\ell m}(\theta',\phi')$,

$$X_{\mathbf{n}',s}(\theta,\phi') = \sum_{\ell=0}^{\infty}\sum_{m=-\ell}^{\ell} \mathsf{a}^X_{\ell m}(n,s) Y_{\ell m}(\theta',\phi'), \tag{5.32}$$

where $\mathsf{a}^X_{\ell m}$ is a set of coefficients (compare with Eq. (4.5)): $a^T_{\ell m}$, $[(\ell+2)!/(\ell-2)!]^{1/2}\, a^E_{\ell m}$, $[(\ell+2)!/(\ell-2)!]^{1/2}\, a^B_{\ell m}$.

Now, imagine that this special (primed) coordinate system is rotated with respect to the observer's (unprimed) coordinate system by some Euler angles

$$\alpha = \phi_{\mathbf{n}}, \quad \beta = \theta_{\mathbf{n}}, \quad \gamma = 0$$

(see, for example [77]). The same observational direction e^i is now characterized by (θ, ϕ), and the same wavevector $\mathbf{n}'$ is now characterized by the unit vector

$$\tilde{\mathbf{n}} = \mathbf{n}/n = (\sin\theta_{\mathbf{n}} \cos\phi_{\mathbf{n}}, \sin\theta_{\mathbf{n}} \sin\phi_{\mathbf{n}}, \cos\theta_{\mathbf{n}}).$$

Obviously, the already calculated numerical values of the invariants $X(\theta', \phi')$ do not depend on the rotation of the coordinate system. Being expressed in terms of (θ, ϕ), the invariants describe the effect produced by a wave with a given (arbitrary) unit wavevector $\tilde{\mathbf{n}}$, as seen in the direction (θ, ϕ).

The transformation between coordinate systems (θ', ϕ') and (θ, ϕ) is accompanied by the transformation of spherical harmonics,

$$Y_{\ell m}(\theta', \phi') = \sum_{m'=-\ell}^{\ell} D^{\ell}_{m',m}(\tilde{\mathbf{n}})\, Y_{\ell m'}(\theta, \phi),$$

where

$$D^{\ell}_{m',m}(\tilde{\mathbf{n}}) \equiv D^{\ell}_{m',m}(\phi_{\mathbf{n}}, \theta_{\mathbf{n}}, 0)$$

are the Wigner symbols [78]. Later, we will need their orthogonality relationship

$$\int d\Omega D^{\ell}_{m,p}(\tilde{\mathbf{n}}) D^{\ell'*}_{m',p}(\tilde{\mathbf{n}}) = \frac{4\pi}{2\ell+1} \delta_{\ell\ell'} \delta_{mm'}, \tag{5.33}$$

where $d\Omega = \sin\theta_{\mathbf{n}} d\theta_{\mathbf{n}} d\phi_{\mathbf{n}}$.

We can now rewrite Eq. (5.32) in terms of θ, ϕ, and thus find the contribution of a single arbitrary Fourier component,

$$X_{\mathbf{n},s}(\theta, \phi) = \sum_{\ell=0}^{\infty} \sum_{m=-\ell}^{\ell} \left(\sum_{m'=-\ell}^{\ell} \mathsf{a}^X_{\ell m'}(n, s) D^{\ell}_{mm'}(\tilde{\mathbf{n}}) \right) Y_{\ell m}(\theta, \phi). \tag{5.34}$$

The superposition of all Fourier components of the perturbed gravitational field gives, at the observer's position $\mathbf{x} = 0$ and at $\eta = \eta_R$ (see (5.1)), the final result:

$$X(\theta,\phi) = \frac{\mathcal{C}}{(2\pi)^{3/2}} \int_{-\infty}^{+\infty} \frac{d^3\mathbf{n}}{\sqrt{2n}} \sum_{s=1,2} \left[X_{\mathbf{n},s}(\theta,\phi)\, \overset{s}{c}_{\mathbf{n}} + X^*_{\mathbf{n},s}(\theta,\phi)\, \overset{s*}{c}_{\mathbf{n}} \right]. \tag{5.35}$$

From this expression, combined with Eq. (5.34), one can read off the random multipole coefficients $a^X_{\ell m}$ that participate in the expansions (4.5):

$$a^X_{\ell m} = \frac{\mathcal{C}}{(2\pi)^{3/2}} \int_{-\infty}^{+\infty} \frac{d^3\mathbf{n}}{\sqrt{2n}} \sum_{s=1,2} \sum_{m'=-\ell}^{\ell} \left[a^X_{\ell m'}(n,s) D^{\ell}_{m,m'}(\tilde{\mathbf{n}})\, \overset{s}{c}_{\mathbf{n}} + (-1)^m a^{X*}_{\ell -m'}(n,s) D^{\ell *}_{m,-m'}(\tilde{\mathbf{n}})\, \overset{s*}{c}_{\mathbf{n}} \right]. \tag{5.36}$$

Since X is a real field, the multipole coefficients $a^X_{\ell m}$ obey the reality conditions

$$a^{X*}_{\ell m} = (-1)^m a^X_{\ell,-m}, \tag{5.37}$$

as is seen directly from (5.36). The gravitational-wave nature of metric perturbations is encoded in concrete values of the coefficients (5.31), (4.5). But in all other aspects the argumentation presented here is general.

5.3.3 Angular power spectra of temperature and polarization anisotropies

It follows from Eq. (5.36) that the statistical properties of the multipole coefficients $a^X_{\ell m}$ are fully determined by the statistical properties of the gravitational field perturbations represented by the random coefficients $\overset{s}{c}_{\mathbf{n}}$. A particular realization of $\overset{s}{c}_{\mathbf{n}}$ is responsible for the particular realization of $a^X_{\ell m}$ actually observed in the sky. Having derived the distribution function for $\overset{s}{c}_{\mathbf{n}}$ from some fundamental considerations (for example, from the assumption of the initial quantum-mechanical vacuum state of perturbations) we could estimate the probability of the observed set $a^X_{\ell m}$ within the ensemble of all possible sets. We could also evaluate the inevitable uncertainty in the observational determination of the parameters of the underlying random process. This uncertainty is associated with the inherent absence of ergodicity of any random process on a 2-sphere

(i.e. sky) [79]. In this work, however, we adopt a minimalistic approach; we postulate only the relationships (2.17) and calculate only the quadratic correlation functions for $a^X_{\ell m}$.

Clearly, the mean values of the multipole coefficients are zeros,

$$\langle a^X_{\ell m} \rangle = \langle a^{X\,*}_{\ell m} \rangle = 0.$$

To calculate the variances and cross-correlation functions, we have to form the products $a^{X*}_{\ell m} a^{X'}_{\ell' m'}$ and then take their statistical averages. First, we find

$$\begin{aligned}\langle a^{X*}_{\ell m} a^{X'}_{\ell' m'} \rangle = \frac{C^2}{(2\pi)^3} \int \frac{n^2 dn d\Omega}{2n} \sum_{s=1,2} \sum_{m_1=-\ell}^{\ell} \sum_{m'_1=-\ell}^{\ell} \\ \Big[a^{X*}_{\ell m_1}(n,s) a^{X'}_{\ell' m'_1}(n,s) D^{\ell *}_{m m_1}(\tilde{\mathbf{n}}) D^{\ell'}_{m' m'_1}(\tilde{\mathbf{n}}) \\ + a^{X}_{\ell m_1}(n,s) a^{X'*}_{\ell' m'_1}(n,s) D^{\ell}_{-m, m_1}(\tilde{\mathbf{n}}) D^{\ell' *}_{-m', m'_1}(\tilde{\mathbf{n}}) \Big] . \end{aligned} \tag{5.38}$$

We now take into account the fact (compare with Eq. (5.30)) that

$$a^X_{\ell m_1}(n,s) a^{X'}_{\ell' m'_1}(n,s) \propto \delta_{m_1 m'_1}.$$

This property allows us to get rid of summation over m'_1 in Eq. (5.38). Then, we perform integration over $d\Omega$ and use the orthogonality relationships (5.33). We finally arrive at

$$\langle a^{X*}_{\ell m} a^{X'}_{\ell' m'} \rangle = C^{XX'}_{\ell} \delta_{\ell \ell'} \delta_{m m'}, \tag{5.39}$$

where

$$C^{XX'}_{\ell} = \frac{C^2}{4\pi^2 (2\ell+1)} \int n dn \sum_{s=1,2} \sum_{m=-\ell}^{\ell} \Big(a^X_{\ell m}(n,s) a^{X'*}_{\ell m}(n,s) + a^{X*}_{\ell m}(n,s) a^{X'}_{\ell m}(n,s) \Big) . \tag{5.40}$$

Other quadratic averages, such as $\langle a^X_{\ell m} a^{X'}_{\ell' m'} \rangle$, $\langle a^{X*}_{\ell m} a^{X'*}_{\ell' m'} \rangle$, follow from (5.39) and the reality condition (5.37).

The angular correlation and cross-correlation functions of the fields I, E, B are directly expressible in terms of Eq. (5.40). For example,

$$\langle I(\theta_1, \phi_1) I(\theta_2, \phi_2) \rangle = \Gamma(\delta) = \sum_{\ell=0}^{\infty} \frac{2\ell+1}{4\pi} C^{TT}_{\ell} P_{\ell}(\cos\delta),$$

where δ is the angular separation between the directions (θ_1, ϕ_1) and (θ_2, ϕ_2) on the sky. For a particular realization of the gaussian random process, represented by the actually measured values of $\tilde{a}^X_{\ell m}$, the quantities

$$\tilde{C}^{XX'}_{\ell} = \frac{1}{2\ell+1} \sum_{m=-\ell}^{+\ell} \tilde{a}^X_{\ell m} \tilde{a}^{X'*}_{\ell m}$$

are the best unbiased estimates of the underlying power spectrum $C^{XX'}_{\ell}$ [79].

One can note that the final result (5.39), (5.40) is the integral of individual contributions (5.30) from single gravitational waves given in a special frame discussed in Sec. 5.3.1. However, one cannot jump directly from (5.30) to (5.40) (which is often done in the literature). In general, Eq. (5.40) does not follow from Eq. (5.30). By calculations given in this subsection we have rigorously shown that Eq. (5.40) is justified only if special statistical assumptions (2.17) are adopted.

One can also note that the correlation functions containing the label B once, i.e. C^{TB}_{ℓ} and C^{EB}_{ℓ}, vanish if the extra assumptions (2.19), (2.24) are made. Indeed, under these assumptions one can use one and the same mode function for both polarization states s, Eq. (2.25). Then, the coefficients $a^B_{\ell m}(n, s)$, Eq. (5.30c), differ essentially only in sign for two different s, i.e. $a^B_{\ell 2}(n, L) = -a^B_{\ell,-2}(n, R)$. Therefore, their contributions will cancel out in expressions (5.40) for C^{TB}_{ℓ} and C^{EB}_{ℓ}. This statement is in agreement with Ref. [80].

Without having access to a 'theory of everything' which could predict one unique distribution of the CMB radiation field over the sky, we have to rely on the calculated statistical averages (5.40). We can also hope that our universe is a 'typical' one, so that the observed values of the correlation functions should not deviate too much from the statistical mean values.

5.4 Effects of Recombination Era

All our final graphs and physical conclusions in this work are based on exact formulas and numerical calculations, starting from numerical representation of the key functions

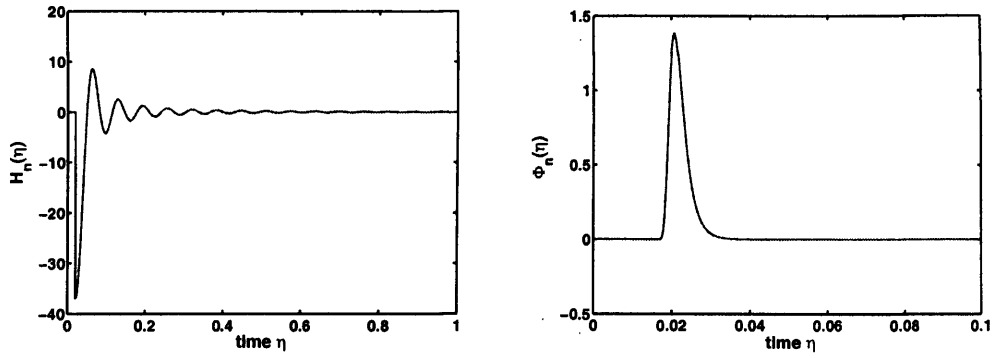

Figure 5.2: The 'source' functions $H_{n,s}(\eta)$ and $\Phi_{n,s}(\eta)$ ($n = 100$) of temperature and polarization anisotropies (the normalization is chosen such that $h_n(\eta_r) = 1$).

$H(\eta)$ and $\Phi(\eta)$, Eqs. (5.9), (5.15). However, we derive and explain all our results by developing manageable and accurate analytical approximations. At every level of calculations we compare exact numerical results with analytical ones.

5.4.1 Temperature anisotropy angular power spectrum

The temperature anisotropy power spectrum C_ℓ^{TT} is determined by the multipole coefficients $a_\ell^T(n,s)$, Eqs. (5.40), (5.30a), (5.31a). The typical graphs for the functions $H_{n,s}(\eta)$ and $\Phi_{n,s}(\eta)$ are shown in Fig. 5.2.

Since the visibility function $g(\eta)$ is a narrow function, a convenient analytical approximation is the limit of an instanteneous recombination. The function $e^{-\tau}$ is replaced by a step function changing from 0 to 1 at $\eta = \eta_{dec}$, $e^{-\tau} = h(\eta - \eta_{dec})$, and the function $g(\eta)$ is replaced by a delta-function, $g(\eta) = \delta(\eta - \eta_{dec})$. In this limit, the contribution to $a_\ell^T(n,s)$ from the scattering term $\Phi_{n,s}^{(0)}(\eta)$ is proportional to $\Delta\eta_{dec}$. It can be neglected in comparison with the contribution from the gravitational term $H_{n,s}(\eta)$. The ratio of these contributions is of the order of $n\Delta\eta_{rec}$, and it tends to zero in the limit of instanteneous recombination, $\Delta\eta_{dec} \to 0$.

Neglecting the scattering term, we write

$$a_\ell^T(n,s) = \gamma\sqrt{4\pi(2\ell+1)}\int_{\eta_{dec}}^{\eta_R} d\eta\, \frac{d\overset{s}{h}_n}{d\eta} T_\ell(\zeta). \tag{5.41}$$

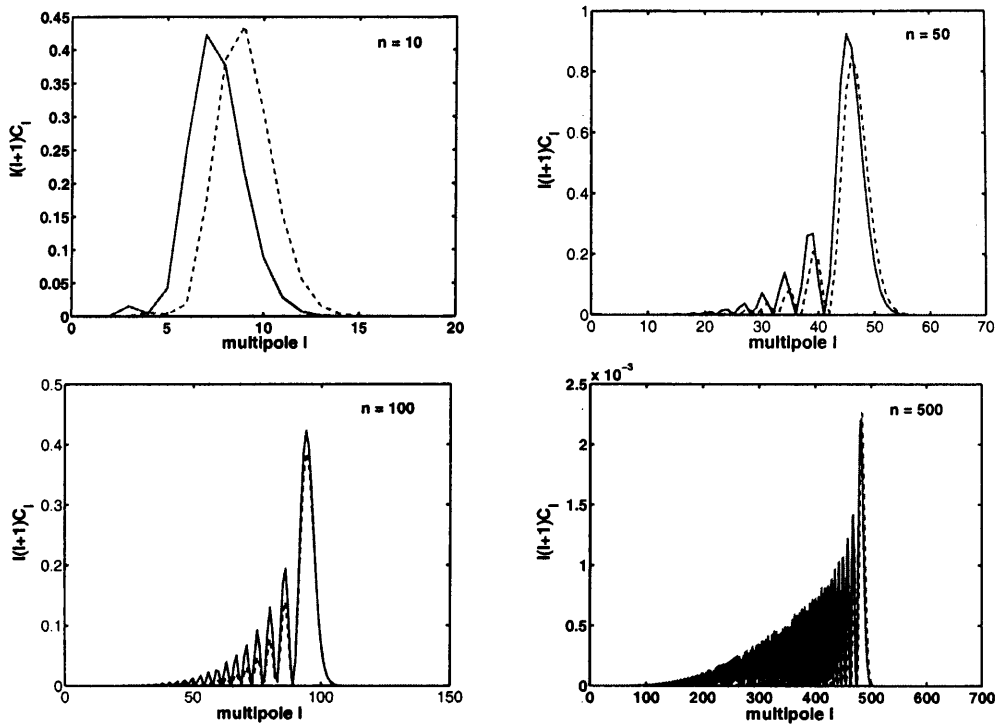

Figure 5.3: The contributions to the power spectrum $\ell(\ell+1)C_\ell^{TT}$ from an individual mode n. The solid line shows the exact result calculated according to (5.41), while the dashed line shows the approximation (5.42). The normalization has been chosen such that $h_n(\eta_r) = 1$.

This integral can be taken by parts,

$$a_\ell^T(n,s) = \gamma\sqrt{4\pi(2\ell+1)}\left[-\overset{s}{h}_n(\eta_{dec})T_\ell(\zeta_{dec}) + \int_{\eta_{dec}}^{\eta_R} d\eta\; n\,\overset{s}{h}_n(\eta)\frac{dT_\ell(\zeta)}{d\zeta}\right].$$

The remaining integral contains oscillating functions and its value is smaller, for sufficiently large n's, than the value of the integrated term. This is illustrated in Fig. 5.3. Therefore, we have

$$a_\ell^T(n,s) = -\gamma\sqrt{4\pi(2\ell+1)}\;\overset{s}{h}_n(\eta_{dec})T_\ell(\zeta_{dec}). \tag{5.42}$$

Finally, we put Eq. (5.42) into Eq. (5.40) and take into account the definition of the metric power spectrum (2.14). Then, we get

$$C_\ell^{TT} = 4\pi\gamma^2\int\frac{dn}{n}h^2(n,\eta_{dec})T_\ell^2(\zeta_{dec}). \tag{5.43}$$

The projection factor $T_\ell^2(\zeta_{dec})$ is given by Eq. (5.29a). Since the spherical Bessel functions reach maximum when the argument and the index are approximately equal,

$\zeta_{dec} \approx \ell$, a particular wavenumber n is predominantly projected onto the multipole $\ell \approx n$:

$$\ell \approx \zeta_{dec} = n(\eta_R - \eta_{dec}) \approx n. \tag{5.44}$$

This can also be seen in Fig. 5.3. Thus, the oscillatory features of the metric power spectrum $h^2(n, \eta_{dec})$ in the n-space are fully responsible for the oscillatory features of the angular power spectrum $\ell(\ell+1)C_\ell^{TT}$ in the ℓ-space [36]. (We use this opportunity to correct a misprint in Fig.2 of Ref. [36] : the plotted lines are functions C_l, not $l(l+1)C_l$.)

The g.w. metric power spectrum $h^2(n, \eta_{dec})$ for the case $\beta = -2$, and the function $\ell(\ell+1)C_\ell^{TT}$ caused by this spectrum, are shown in Fig. 5.5(a) and Fig. 5.5(b). The normalization of the metric power spectrum is such that the function $\ell(\ell+1)C_\ell^{TT}$ at $\ell = 2$ is equal to 1326 μK^2 [46]. The interval $\ell \lesssim 90$ is generated by waves with $n \lesssim 90$. These waves did not enter the Hubble radius by the time η_{dec}. Their amplitudes are approximately equal for all n's in this interval (compare with Fig. 2.1). The gradual decrease of the angular power spectrum at larger ℓ's is the reflection of the gradual decrease of power in shorter gravitational waves whose amplitudes have been adiabatically decreasing since the earlier times when the waves entered the Hubble radius.

5.4.2 Polarization anisotropy angular power spectrum

The decisive function for polarization calculations is $\Phi_{n,s}(\eta)$. We have approximated this function by $\Phi_{n,s}^{(0)}$, Eq. (5.27), and compared it with exact result in Fig. 5.1. For qualitative derivations it is useful to make further simplifications.

Since $g(\eta)$ is a narrow function, the integral in Eq. (5.27) is effective only within a narrow interval $\Delta\eta_{dec}$. Assuming that the function $d\overset{s}{h}_n(\eta)/d\eta$ does not vary signifi-

cantly within this interval, we can take this function from under the integral,

$$\Phi^{(0)}_{n,s}(\eta) \approx -\frac{1}{10}\frac{d\overset{s}{h}_n(\eta)}{d\eta}\left(g(\eta)\int_0^\eta d\eta'\, e^{-\frac{3}{10}\tau(\eta,\eta')}\right). \tag{5.45}$$

Clearly, the assumption that the function $d\overset{s}{h}_n(\eta)/d\eta$ is almost constant within the window $\Delta\eta_{dec}$ gets violated for sufficiently short waves. With (5.45), we expect degradation of accuracy for wavenumbers n approaching n_*. This is illustrated by a dotted line in Fig. 5.1. Nevertheless, the approximation (5.45) is robust for $n \lesssim n_*$, and it reveals the importance of first derivatives of metric perturbations for evaluation of the CMB polarization.

We now introduce the symbol P to denote either E or B components of polarization. In terms of multipoles $a^P_\ell(n,s)$, the angular power spectrum is given by Eq. (5.40). Putting (5.45) into Eqs. (5.31b), (5.31c) and denoting by $P_\ell(\zeta)$ the respective projection functions, we get

$$a^P_\ell(n,s) \approx \gamma\sqrt{4\pi(2\ell+1)}\int_0^{\eta_R} d\eta \left(-\frac{1}{10}\frac{d\overset{s}{h}_n(\eta)}{d\eta}P_\ell(\zeta)\right)\left[g(\eta)\int_0^\eta d\eta' e^{-\frac{3}{10}\tau(\eta,\eta')}\right]. \tag{5.46}$$

Again referring to the peaked character of $g(\eta)$ and assuming that the combination $(d\overset{s}{h}_n(\eta)/d\eta)P_\ell(\zeta)$ does not change significantly within the window $\Delta\eta_{dec}$, we take this combination from under the integral,

$$a^P_\ell(n,s) \approx \gamma\sqrt{4\pi(2\ell+1)}\; D(n)\left(-\frac{1}{10}\frac{d\overset{s}{h}_n(\eta)}{d\eta}P_\ell(\zeta)\right)\Bigg|_{\eta=\eta_{rec}} \Delta. \tag{5.47}$$

The two new factors in this expression, $D(n)$ and Δ, require clarification.

The factor $D(n)$ compensates for gradual worsening of our approximation when the wavenumber n approaches n_*. For large n's, the functions under the integrals change sign within the window $\Delta\eta_{dec}$, instead of being constant there. This leads to the decrease of the true value of the integral in comparison with the approximated one. The evaluation of this worsening suggests that it can be described by the damping

factor

$$D(n) \equiv \left[1 + \left(\frac{n\Delta\eta_{dec}}{2}\right)^2\right]^{-1}.$$

We inserted this factor 'by hand' in Eq. (5.47).

The factor Δ is the result of the remaining integration over η in Eq. (5.46) [69],

$$\Delta \equiv \int_0^{\eta_R} d\eta \;\; g(\eta) \left(\int_0^{\eta} d\eta' e^{-\frac{3}{10}\tau(\eta,\eta')} \right) = \frac{10}{7} \int_0^{\eta_R} d\eta \;\; \left[e^{-\frac{3}{10}\tau(\eta)} - e^{-\tau(\eta)} \right].$$

Since $e^{-\tau}$ rapidly changes from 0 to 1 around recombination, the integrand $\left(e^{-(3/10)\tau} - e^{-\tau}\right)$ is nonzero only there, and Δ is expected to be of the order of $\Delta\eta_{dec}$. To give a concrete example, we approximate $g(\eta)$ by a gaussian function

$$g(\eta) = \frac{1}{\sqrt{2\pi}(\Delta\eta_{dec}/2)} \exp\left(-\frac{(\eta - \eta_{dec})^2}{2(\Delta\eta_{dec}/2)^2} \right).$$

Then, the quantity Δ can be found exactly,

$$\Delta = \frac{5}{7}\Delta\eta_{dec} \int_{-\infty}^{+\infty} dx \left[\left(\frac{1}{2} + \frac{1}{2}\mathrm{erf}\left(\frac{x}{\sqrt{2}}\right) \right)^{\frac{3}{10}} - \left(\frac{1}{2} + \frac{1}{2}\mathrm{erf}\left(\frac{x}{\sqrt{2}}\right) \right) \right] \approx 0.96\Delta\eta_{dec}.$$

Clearly, factor Δ in Eq. (5.47) demonstrates the fact that the CMB polarization is generated only during a short interval of time around recombination.

Finally, substituting (5.47) into (5.40) and recalling (2.15), we obtain the polarization angular power spectrum:

$$C_\ell^{PP} \approx 2\pi\gamma^2 \frac{1}{100}\Delta^2 \int \frac{dn}{n} D^2(n) \sum_{s=1,2} \left| \frac{d \overset{s}{h}(n,\eta)}{d\eta} \right|_{\eta=\eta_{rec}}^2 P_\ell^2(\zeta_{rec}). \qquad (5.48)$$

Similarly to the case of temperature anisotropies, the projection factors $P_\ell(\zeta_{dec})$ predominantly translate n into ℓ according to Eq. (5.44). The oscillatory features of the power spectrum of the first time-derivative of metric perturbations get translated into the oscillatory features of the power spectra for E and B components of polarization. This is illustrated in Fig. 5.5(c) and Fig. 5.5(d). The waves with $n\eta_{dec} \ll \pi$ did not enter the Hubble radius by $\eta = \eta_{dec}$. They have no power in the spectrum of $dh(n,\eta)/d\eta$

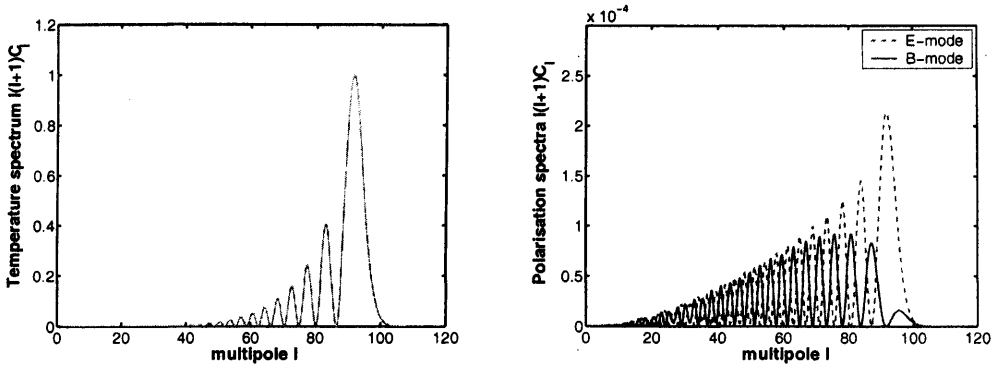

Figure 5.4: Relative contributions of an individual Fourier mode $n = 100$ to various multipoles ℓ in the power spectra $\ell(\ell+1)C_\ell$ for temperature and polarization. The normalization has been chosen arbitrarily but same in both the graphs.

at $n \ll 90$, and therefore there is no power in polarization at $\ell \ll 90$. On the other hand, the first gravitational peak at $n \approx 90$ gets reflected in the first polarization peak at $\ell \approx 90$.

There is certain difference, however, between the projection functions $E_\ell(\zeta_{dec})$ and $B_\ell(\zeta_{dec})$. This is shown in Fig. 5.4. The B-mode projections are more 'smeared' and their maxima are shifted to somewhat lower ℓ's. This explains the visible difference between C_ℓ^{EE} and C_ℓ^{BB} in Fig. 5.5. The polarization angular power spectra, plotted in Fig. 5.5, were found from exact numerical calculations.

5.4.3 Temperature-Polarization cross correlation

A very special role belongs to the TE cross-correlation spectrum. We will show below that the TE correlation at lower ℓ's must be negative for gravitational waves and positive for density perturbations. This distinctive signature can turn out to be more valuable for identification of relic gravitational waves than the presence of the B polarization in the case of gravitational waves and its absence in the case of density perturbations. The expected TE signal from gravitational waves is about two orders of magnitude stronger than the BB signal, and it is much easier to measure. At lower ℓ's, the contributions to TE from gravitational waves and density perturbations are comparable in absolute value, so the g.w. contribution is not a small effect. The total

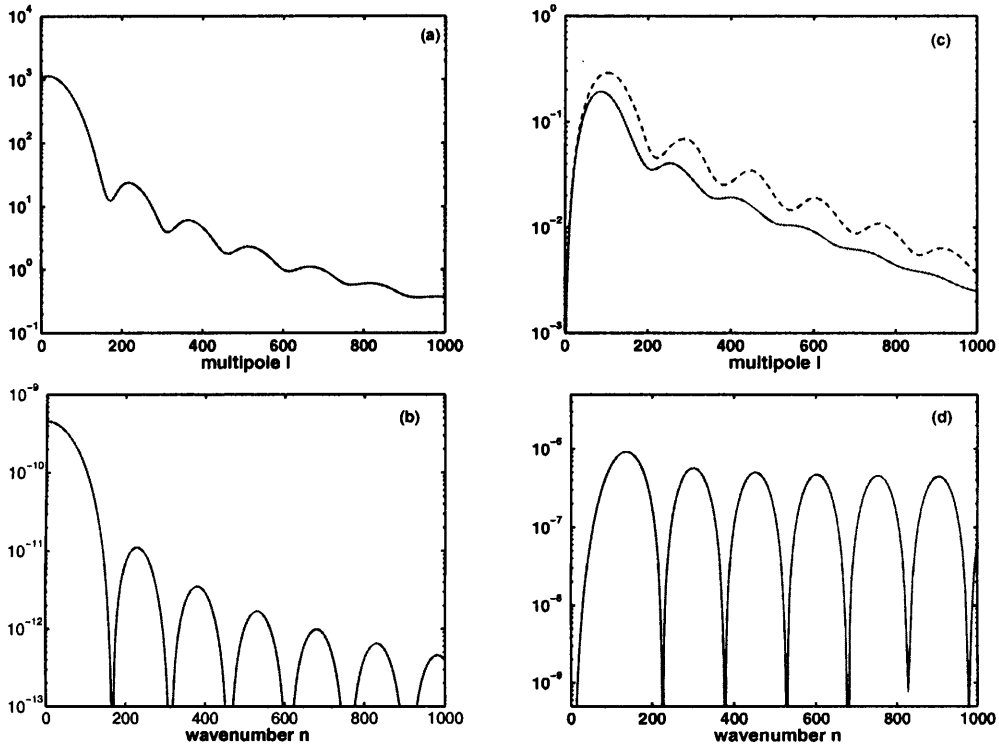

Figure 5.5: The left panel shows (a) the power spectrum of temperature anisotropies $\ell(\ell+1)C_\ell^{TT}$ (in $\mu\mathrm{K}^2$) generated by (b) the power spectrum of g.w. metric perturbations (2.14), $\beta = -2$. The right panel shows (c) the power spectra of polarization anisotropies $\ell(\ell+1)C_\ell^{BB}$ (solid line) and $\ell(\ell+1)C_\ell^{EE}$ (dashed line), panel (d) shows the power spectrum of the first time derivative of the same g.w. field, Eq. (2.16).

TE cross-correlation has already been measured at some level [81, 34].

To find the TE power spectrum we have to use the product of $a^T_{\ell m}(n,s)$ and $a^E_{\ell m}(n,s)$ in Eq. (5.40). For qualitative analysis we will operate with the approximate expressions (5.42) and (5.47). Then, the TE correlation reads

$$C_\ell^{TE} \approx \pi\gamma^2 \left(\frac{\Delta}{10}\right) \int \frac{dn}{n} D(n) \sum_{s=1,2} \left(\overset{s}{h^*}(n,\eta) \frac{d\,\overset{s}{h}(n,\eta)}{d\eta} + \overset{s}{h}(n,\eta) \frac{d\,\overset{s}{h^*}(n,\eta)}{d\eta} \right) \Bigg|_{\eta=\eta_{dec}} \Big(T_\ell(\zeta_{dec}) E_\ell(\zeta_{dec}) \Big) . \tag{5.49}$$

For a given ℓ, the projection factor $\big(T_\ell(\zeta_{dec})E_\ell(\zeta_{dec})\big)$ peaks at $n \approx \ell$ and is positive there. Therefore, the sign of C_ℓ^{TE} is determined by the sign of the term:

$$\frac{1}{2} \sum_{s=1,2} \left(\overset{s}{h^*}(n,\eta) \frac{d\,\overset{s}{h}(n,\eta)}{d\eta} + \overset{s}{h}(n,\eta) \frac{d\,\overset{s}{h^*}(n,\eta)}{d\eta} \right) \Bigg|_{\eta=\eta_{dec}} = \left(\frac{dh^2(n,\eta)}{d\eta} \right) \Bigg|_{\eta=\eta_{dec}} \tag{5.50}$$

The adiabatic decrease of the g.w. amplitude upon entering the Hubble radius is preceded by the monotonic decrease of the g.w. mode function $\overset{s}{h}_n(\eta)$ as a function of η. This behaviour is illustrated in Fig. 2.1. It is clear from the graph that for $n \lesssim 100$ the quantity (5.50) is negative, because the first derivative of $\overset{s}{h}_n(\eta)$ is negative. Therefore, for $\ell \lesssim 90$ the correlation C_ℓ^{TE} must be negative. For larger ℓ's the TE correlation goes through zero, changes sign and oscillates reflecting the oscillations of the function (5.50) in the n-space. An exact numerical graph for TE correlation caused by gravitational waves is depicted in Fig. 5.6. The graph clearly shows how the sign and features of the spectrum (5.50) get translated into the sign and features of the TE correlation.

It is shown in Appendix F that in the case of density perturbations the TE correlation must be positive at lower ℓ's. This is because the relevant metric perturbations associated with density perturbations are growing in time and therefore the first time-derivative of metric perturbations is positive. Because of other contributions, the TE correlation is expected to change sign at $\ell \approx 70$ [81], [45]. The region of intermediate multipoles $15 \leq \ell \leq 90$ should be of a particular interest. On one hand, the multipoles $\ell > 15$ are not affected by the reionization era and its uncertain details, except the

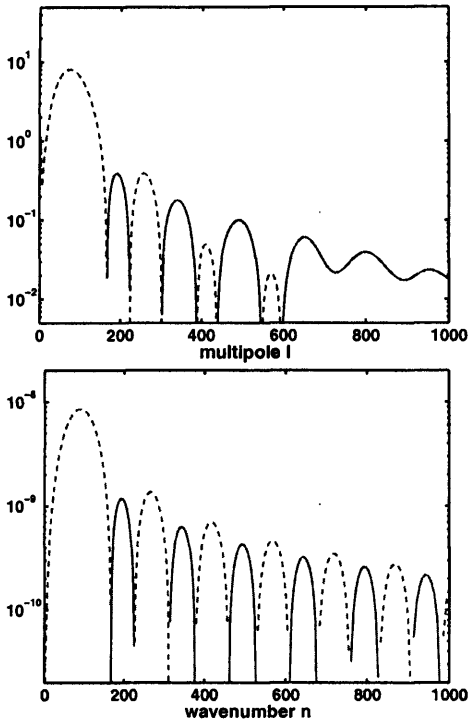

Figure 5.6: The bottom panel shows the spectrum (5.50) of gravitational waves, whereas the top panel shows the angular power spectrum $\ell(\ell+1)C_\ell^{TE}$ caused by these waves. The negative values of these functions are depicted by broken lines.

overall suppression by $e^{-2\tau_{reion}}$. On the other hand, at $\ell < 90$ the g.w. contribution to TE is not much smaller numerically than the contribution from density perturbations. The lower multipoles $\ell \lesssim 15$ are affected by reionization, and we shall study reionization in the next Section.

5.5 Effects of Reionization Era

The reionization of the intergalactic medium by first sources of light has occurred relatively late, at $z \sim 30 - 7$ (see, for example, [34, 82]). In contrast to the recombination part of the visibility function $g(\eta)$, which is narrow and high, the reionization part of $g(\eta)$ is broad and much lower (see Fig. D.1). For a crude qualitative analysis, one can still apply analytical formulas derived for recombination. One has to replace η_{dec} with η_{reion} and $\Delta\eta_{dec}$ with $\Delta\eta_{reion}$. The waves that start entering the Hubble radius at η_{reion}, i.e. waves with wavenumbers $n\eta_{reion} \sim \pi$, provide the most of power to

the spectrum of first time derivative of metric perturbations. Therefore, these waves, with $n \sim 12$, produce a 'bump' in polarization spectra at the projected $\ell \sim 6$. However, these wavenumbers are comparable with the wavenumber n_{**}, $n_{**}\Delta\eta_{reion} \sim 2\pi$, that characterizes the width of the visibility function at reionization. The assumption $n \ll n_{**}$ is not well satisfied, the analytical approximation becomes crude, and one has to rely mostly on numerics for more accurate answers.

The numerical solution to the integral equation (5.15) in the reionization era is shown in Fig. 5.7. One can see that the damping effect is expected to commence from $n \gtrsim 20$, as the polarization source function $\Phi_n(\eta)$ begins to show an oscillatory behaviour. The projection relationships are also far away from the almost one-to-one correspondence $\ell \approx n$ that was typical for recombination era. In Fig. 5.8 we show the contributions of a given n to various ℓ's in the polarization power spectra $\ell(\ell+1)C_\ell$. One can see that a considerable portion of power from a given n is distributed over many lower-order ℓ's.

The total effect of the reionization era is shown in Fig. 5.9. This numerical result was based on our simplified model of homogeneous reionization, as described in Appendix D. The reionization 'bumps' at lower multipoles for E and B components of polarization are similar in shape and numerical value.

5.6 Comparison with Available Observations; Signatures of Relic Gravitational Waves

The theory that we are using here is applicable to any primordial spectral index n. The initial conditions for gravitational waves, Eqs. (2.31), (2.32), as well as analogous initial conditions for density perturbations, hold β, and hence n, as a free constant parameter. The spectral index n can be larger, equal, or smaller than 1. However, from the theoretical point of view, the 'red' primordial spectra $n < 1$ ($\beta < -2$) seem to be unacceptable, or at least questionable. If $\beta < -2$, the mean square fluctuations

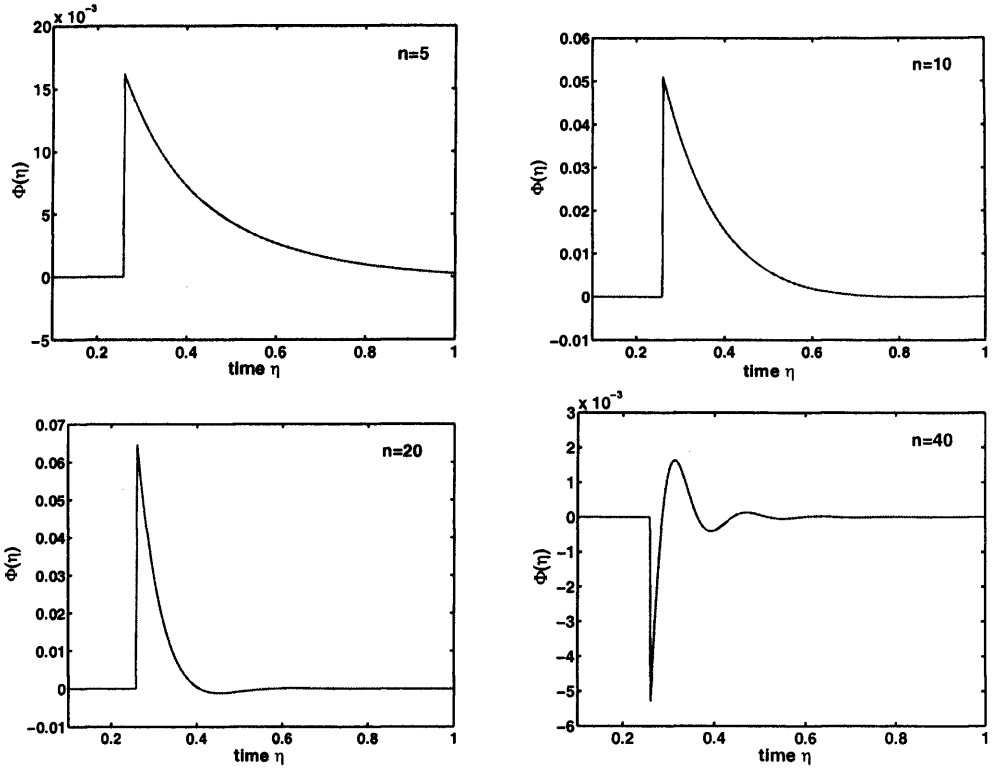

Figure 5.7: The source function $\Phi_n(\eta)$ in reionization era for different wavenumbers.

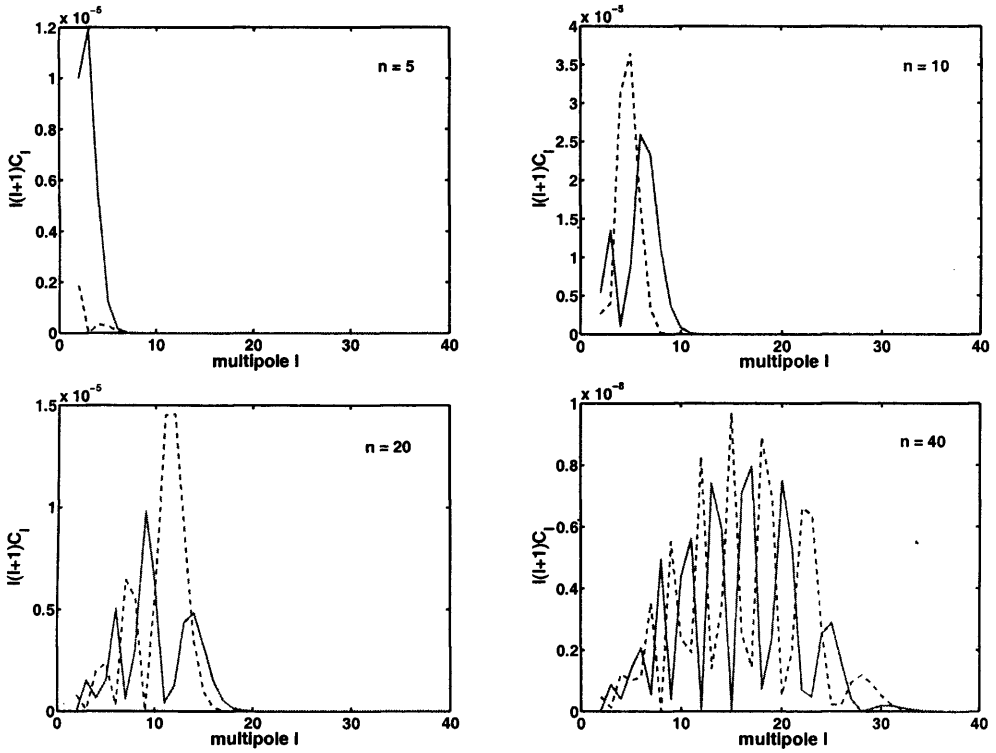

Figure 5.8: The contributions to the angular power spectra from an individual mode n. The dashed line is for $\ell(\ell+1)C_\ell^{EE}$ and the solid line is for $\ell(\ell+1)C_\ell^{BB}$.

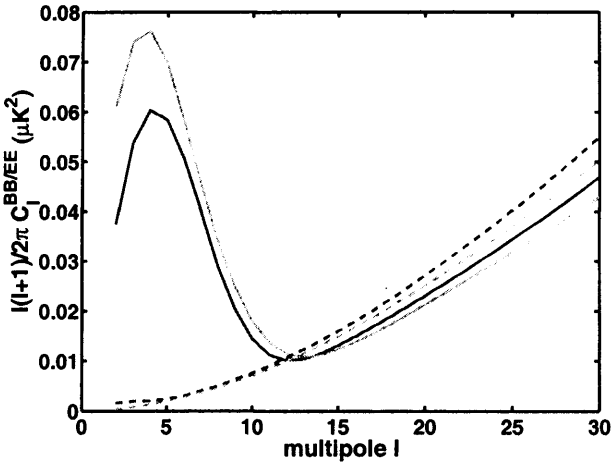

Figure 5.9: The reionization 'bump' in the polarization power spectra. The dashed lines show the spectra when the reionization era is ignored. The solid lines include both eras. The darker lines are for B-mode, and the lighter lines for E-mode.

of gravitational field, Eq. (2.13), are power-law divergent in the limit of very small wavenumbers n. One could argue that the extrapolation of the primordial spectrum to the 'infrared' region of very small n's is uncertain, and for some reason the shape of the spectrum bends in the 'infrared' region making the integral (2.13) convergent at the lower limit. We prefer not to hide behind this possibility. If the shape of the primordial spectrum is allowed to be varied, then practically anything in the CMB data can be explained by the properly adjusted primordial spectrum. Therefore, our theoretical preference (unless the data will enforce us to change this preference) is a constant primordial spectral index n > 1 ($\beta > -2$). Obviously, such primordial spectra entail no difficulty in the 'ultraviolet' region of very large n's, because such short-wavelength fluctuations (today's wavelength ~ 3 cm.) did not satisfy the requirements of superadiabatic amplification and simply have not been generated.

We now return to the TE correlation. In Fig. 5.10 we show the contributions to the TE correlation function from relic gravitational waves (gw) and primordial density perturbations (dp). (In order to enhance lowest ℓ's we use the combination $(\ell+1)C_\ell$ rather than $\ell(\ell+1)C_\ell$.) For this illustration, we choose a flat primordial spectrum n $= 1$ ($\beta = -2$) and assume equal contributions from (gw) and (dp) to the temperature

quadrupole: $R = 1$, where

$$R \equiv C_{\ell=2}^{TT}(gw)/C_{\ell=2}^{TT}(dp).$$

We include the effects of reionization according to the model with $\tau_{reion} = 0.09$. The (gw) contribution is numerically calculated from the solution to the integral equation (5.15), whereas the (dp) contribution is plotted according to the CMBfast code [65, 45]. One can see from the graph that the negative TE correlation function at lower ℓ's is only possible if there is a significant amount of primordial gravitational waves. One can also see from the graph that a mis-interpretation of the total TE effect as being caused by density perturbations alone, could lead to a serious mis-estimation of τ_{reion}.

The TE correlation at lower ℓ's measured by the WMAP mission [81, 34] shows clusters of data points, including the negative ones, that lie systematically below the theoretical curve based on density perturbations alone. It is true that the data points in the interval $10 \lesssim \ell \lesssim 70$ are concentrated near a zero level, the error bars are still large, and the measured TE correlation can be appreciably different from the theoretical statistically averaged TE correlation. However, the recent paper [34], page 26, explicitly emphasizes the detection of the TE anticorrelation by WMAP: "The detection of the TE anticorrelation near $\ell \approx 30$ is a fundamental measurement of the physics of the formation of cosmological perturbations...". As we have already stated several times, the TE anticorrelation at lower ℓ's, such as $\ell \approx 30$, can only take place (within the framework of all other common assumptions) when a significant amount of relic gravitational waves is present.

Our theoretical position,as also explained elsewhere in this thesis, is such that we are asking not 'if' relic gravitational waves exist, but 'where' they are hiding in the presently available data. We shall now discuss some models that fit the CMB data and contain significant amounts of relic gravitational waves. More accurate observations with WMAP, and especially Planck, should firmly settle on the issue of the sign and value of the TE correlation at lower multipoles. Hopefully, these observations will

establish the presence of relic gravitational waves beyond reasonable doubts.

To sharpen the discussion of allowed parameters, we take the model with n = 1.2, $\tau_{reion} = 0.09$ and $R = 1$. We take the values $\Omega_m h^2 = 0.03$, $\Omega_b h^2 = 0.12$, $h = 0.75$, and we normalize the g.w. contribution to $\frac{\ell(\ell+1)}{2\pi} C_\ell^{TT} = 440\ \mu\mathrm{K}^2$ at $\ell = 2$. In Fig. 5.11a we show our calculation of the TT correlation function in comparison with WMAP data and the best fit ΛCDM model [15], [45]. (If it comes to the necessity of explaining 'dark energy', natural modifications of general relativity will be superior to unnatural modifications of the matter sector [83].) One can see from the graph that even this model (which lies, arguably, on a somewhat extreme end) is consistent with the TT data at all ℓ's and significantly alleviates the much discussed tension between theory and experiment at $\ell = 2$. In Fig. 5.11b we show the TE correlation for exactly the same model. One can see that the inclusion of relic gravitational waves makes more plausible the negative data points at lower ℓ's. Since the relative contribution of gravitational waves becomes small at $\ell \gtrsim 90$, the higher ℓ portion of the graph is governed by density perturbations alone. Obviously, models with a little smaller n or R reach the same goals.

Finally, in Fig. 5.12 we combine together all correlation functions induced by relic gravitational waves. The graphs are based on the discussed model with n = 1.2, $R = 1$. The future detection of the BB correlation will probably be the cleanest proof of presence of relic gravitational waves. For the discussed model, the predicted level of the BB signal is $\frac{\ell(\ell+1)}{2\pi} C_\ell^{BB}\Big|_{\ell\approx 90} \sim 0.1\ \mu\mathrm{K}^2$ in the region near the first peak at $\ell \sim 90$. This level of B-mode polarization should be detectable by the experiments currently in preparation, such as CLOVER [84], BICEP [85] and others (see also [86]). Obviously, in this work, we ignore many complications, including astrophysical foregrounds. More information can be found in Ref. [87, 88, 89, 90].

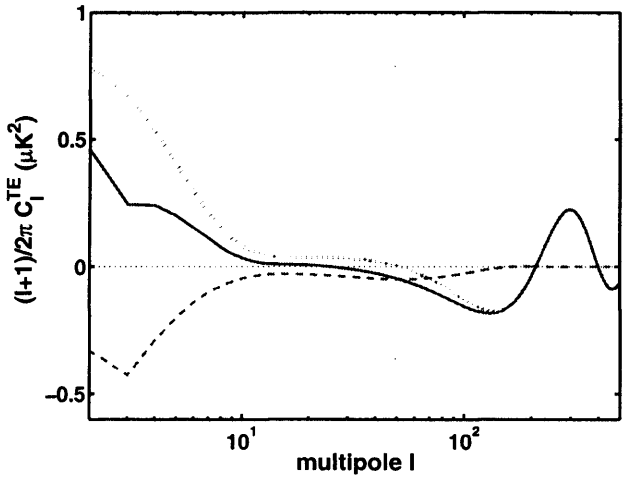

Figure 5.10: The dotted line shows the contribution of density perturbations alone, and the dashed line shows the contribution of gravitational waves alone. The solid line is the sum of these contributions. It is seen from the graph that the inclusion of g.w. makes the total curve to be always below the d.p. curve.

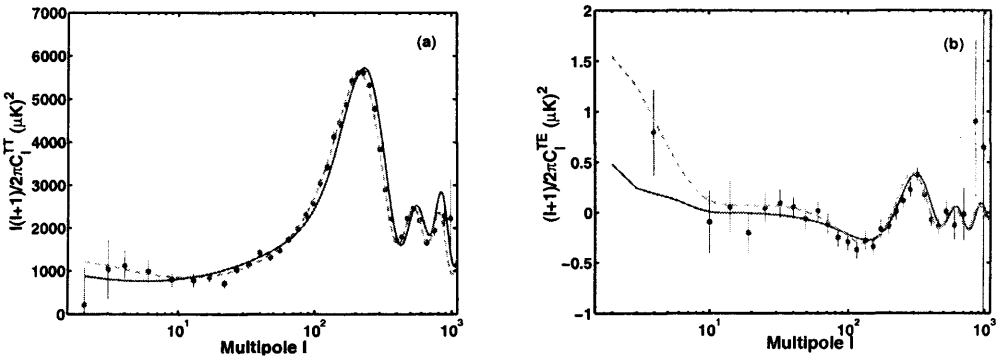

Figure 5.11: The dashed line shows the best fit ΛCDM model without gravitational waves. The solid line shows a model with spectral index $n = 1.2$ and gravitational waves $R = 1$.

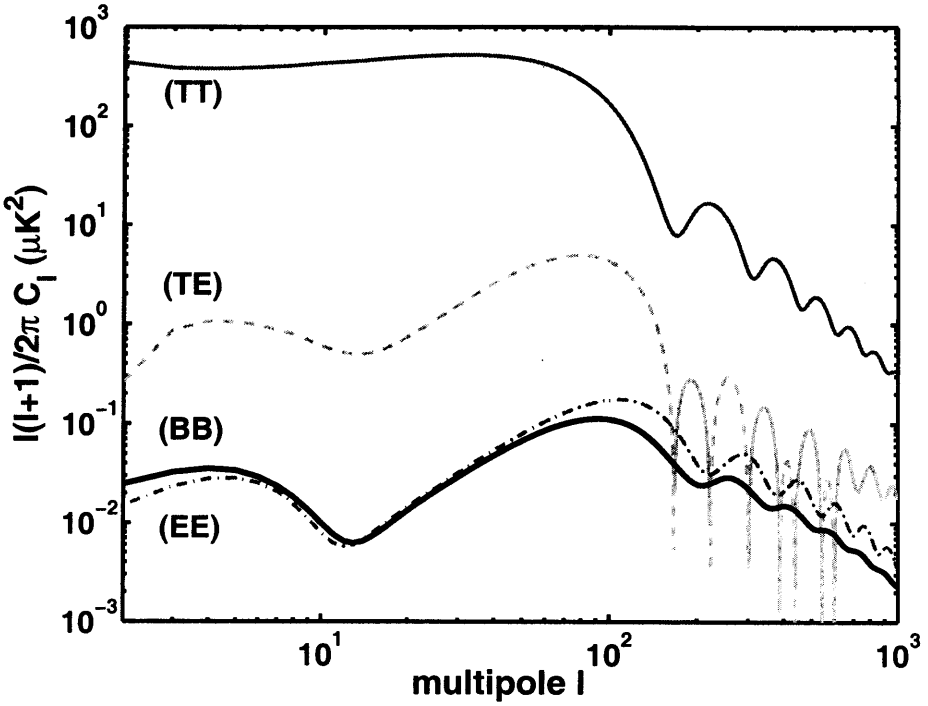

Figure 5.12: The summary of CMB temperature and polarization anisotropies due to relic gravitational waves with $n = 1.2$ and $R = 1$.

5.7 Conclusions

In this chapter, using the properties of relic gravitational waves relevant to CMB calculations, summarized in Chapter 2, and the framework of the general radiative transfer equations in a slightly perturbed FLRW Universe, developed in Chapter 4, we have worked out, essentially from first principles, a theory of CMB anisotropies induced by relic gravitational waves. Some parts of this theory are rederivations and confirmations of previous studies, some parts are new. The important advantage of our approach, as we see it, is a transparent physical picture. We believe we have demonstrated in the work that every detail of the derived correlation functions is under full analytical control. Clear understanding of the participating physical processes has led us to the conclusion that the TE correlation in CMB can be a valuable probe of relic gravitational waves. We compared our theoretical findings with the WMAP data. We believe that the TE anticorrelation detected by WMAP at $\ell \approx 30$ is certain evidence for relic

gravitational waves in the already available data. We propose more accurate observations of the TE correlation at lower ℓ's and believe that these observations have the potential of providing a firm positive result.

Chapter 6

Summary of the thesis

In this work we have touched upon two possible observational manifestations of gravitational waves. We have considered the effects of gravitational waves on ground based laser interferometric detectors, as well as their imprints on the CMB radiation. Although these two directions of enquiry are intended to probe two very different domains of gravitational wave astronomy, (one probing the gravitational wave background at $10 - 10^4 Hz$, and the other at $10^{-18} - 10^{-15} Hz$,) the main motivation to study them has been the fact that they currently represent the two most promising efforts at detecting gravitational waves.

In chapter 2, after a brief survey of gravitational waves, we proceed to the analysis of relic gravitational waves. Here we summarized the basic notations and the properties of gravitational wave field that would be required in the following chapters.

In chapter 3, analyzing the motion of free test particles in the field of a gravitational wave, using different methods, we have derived the presence and importance of the "magnetic" component of motion. We have shown how this "magnetic" component translates into a corresponding contribution to the variation of distance between the arms of an gravitational wave interferometer, and hence, to its response function. We have demonstrated that the correction in the response due to the "magnetic" component can reach up to 10% for the current ground based interferometers, and must be taken into account in advanced data analysis programs. We have also presented an invariant description of the interferometer response function in terms of spin-weighted

spherical harmonics.

In chapter 4 we began by giving a description of the radiation field in terms of the Stokes parameters, and constructing the polarization tensor. We then proceeded to construct the invariants of the polarization tensor which completely characterize the radiation field. After a brief introduction to the physics of Thomson scattering, we proceeded to develop a general formalism of radiative transfer in a slightly perturbed FLRW universe.

In chapter 5 we have studied the imprints of relic gravitational waves on the CMB radiation. We have shown that, for each individual Fourier mode, the equations of radiative transfer reduce to a single Voltairre type integral equation. The integral equation has been solved both numerically, and analytically in terms of an infinite series with a recursive relation for the consecutive terms in the expansion. We then shift our attention to the statistical properties of the CMB. We show how the statistical properties of the CMB radiation field follow directly from the statistical properties of the random gravitational wave field. Next, we proceed to show how the features in the power spectrum of temperature and polarization anisotropies of the CMB are related to the corresponding features in the spectrum of the metric of the underlying gravitational wave field and its derivative. One of our central points in the analysis of the CMB spectra, is the analysis of the TE correlation function. We show that at low multipoles, the TE correlation function must be negative, if it is induced by gravitational waves, and positive, if induced by density perturbations. We argue that the TE correlation can serve as a more valuable observational tool than the presence or absence of BB correlation. Comparing our results to WMAP, we conclude that there is evidence for relic gravitational waves in the already available CMB data, and the further study of the TE correlation at lower multipoles has the potential of a firm positive answer.

Finally, to summarize and recapitulate, the main results of the thesis are the following:

- Analyzing the motion of free test particles in the field of a gravitational wave, we have demonstrated the presence and importance of the "magnetic" component of motion. We have studied the consequences of the "magnetic" component of motion for the response of ground based interferometers. It has been shown that the "magnetic" component can lead to a correction of up to 10%. Ignoring this correction would cause inadmissible misestimation of parameters of the g.w. radiation source.

- A convenient description of the response function of the interferometer has been given in terms of spin-weighted spherical harmonics. It was shown that the technique of spin-weighted spherical harmonics bridges the diverse areas of astrophysical and cosmological gravitational waves.

- The equations of radiative transfer in a slightly perturbed FLRW universe have been reduced, for gravitational waves, to a single integral equation. This is a considerable improvement in comparison with the usual technique of infinite series of coupled ordinary differential equations.

- We show that the features in the CMB spectra are fully determined by the corresponding features in the spectra of gravitational waves. Specifically, the TT spectrum is determined by the spectrum of the metric, the EE and BB spectra are determined by the spectrum of the first time derivative of the metric, and the TE spectrum is determined by the spectrum of the product of the metric and its first time derivative.

- It was shown that the TE correlation function of the CMB, at low multipoles, must be negative if it is induced by gravitational waves, and positive if it is induced by density perturbations. It was proposed to use the TE correlation as a

valuable tool to detect gravitational waves in the CMB radiation. We compared our theoretical results with WMAP data and showed that there is evidence for the presence of relic gravitational waves in the already available data.

Appendix A

The principal axes for a monochromatic gravitational wave

In general, the metric components are given by Eq. (3.7), where ψ_+ and $\psi_\times$ are arbitrary independent constants. However, it is always possible to do a rotation in the (x^1, x^2) plane, such that in the new coordinate system $\tilde{x}^1, \tilde{x}^2$ the difference between $\psi_\times$ and ψ_+ is exactly $\frac{\pi}{2}$. The required transformation

$$\tilde{x}^1 = x^1 \cos\zeta + x^2 \sin\zeta, \qquad \tilde{x}^2 = -x^1 \sin\zeta + x^2 \cos\zeta, \tag{A.1}$$

has the angle ζ such that

$$\zeta = \frac{1}{2} \arctan \left[\left(\frac{h_\times^2 - h_+^2}{2h_+h_\times \cos(\psi_+ - \psi_\times)} \right) \pm \sqrt{\left(\frac{h_\times^2 - h_+^2}{2h_+h_\times \cos(\psi_+ - \psi_\times)} \right)^2 + 1} \right], \tag{A.2}$$

The rotation angle ζ is well defined, except for a circularly polarized wave, in which case the difference between $\psi_\times$ and ψ_+ is always $\frac{\pi}{2}$. In this new coordinate system $(\tilde{x}^1, \tilde{x}^2)$ the metric components take the form

$$\tilde{a} = \tilde{h}_+ \sin(k(x^0 + x^3) + \psi), \qquad \tilde{b} = -\tilde{h}_\times \cos(k(x^0 + x^3) + \psi), \tag{A.3}$$

where the amplitudes $\tilde{h}_+$ and $\tilde{h}_\times$ are given by

$$\begin{aligned} \tilde{h}_+ &= \left(h_+^2 \cos^2 2\zeta + 2h_+h_\times \sin 2\zeta \cos 2\zeta \cos(\psi_+ - \psi_\times) + h_\times^2 \sin^2 2\zeta\right)^{\frac{1}{2}}, \\ \tilde{h}_\times &= \left(h_\times^2 \cos^2 2\zeta - 2h_+h_\times \sin 2\zeta \cos 2\zeta \cos(\psi_+ - \psi_\times) + h_+^2 \sin^2 2\zeta\right)^{\frac{1}{2}}, \end{aligned} \tag{A.4}$$

and the phase ψ is given by

$$\psi = \arctan \left[\frac{h_+ \sin\psi_+ + h_\times \sin\psi_\times \tan 2\zeta}{h_+ \cos\psi_+ + h_\times \cos\psi_\times \tan 2\zeta} \right]. \tag{A.5}$$

We call the coordinates $\tilde{x}^1$ and $\tilde{x}^2$, in which the metric components take the form (A.3), the principal axes of the gravitational wave. In the text, we assume that the above transformation has already been performed. So, without loss of physical generality, we put $\psi_+ = \psi_\times - \frac{\pi}{2} = \psi$, and we do not use the tilde-symbol.

Appendix B

Coordinate transformation

A general gravitational wave (3.9), (3.8) is described in the coordinate system (x^1, x^2, x^3). For the observer, it is convenient to use the coordinate system (X^1, X^2, X^3) in which the arms of interferometer are located along the X^1 and X^2 axes. In this coordinate system, the incoming wave is characterized by the direction Θ, Φ and the angle Ψ between the observer's meridian and the wave's principal axis, as depicted in Fig. 3.7. The relationship between these two coordinate systems is given by the transformation

$$\begin{pmatrix} X^1 \\ X^2 \\ X^3 \end{pmatrix} = R \begin{pmatrix} x^1 \\ x^2 \\ x^3 \end{pmatrix}, \tag{B.1}$$

where the orthogonal rotation matrix R is

$$\begin{pmatrix} \cos\Phi\cos\Theta\cos\Psi - \sin\Phi\sin\Psi & -\sin\Phi\cos\Psi - \cos\Phi\cos\Theta\sin\Psi & \cos\Phi\sin\Theta \\ \sin\Phi\cos\Theta\cos\Psi + \cos\Phi\sin\Psi & \cos\Phi\cos\Psi - \sin\Phi\cos\Theta\sin\Psi & \sin\Phi\sin\Theta \\ -\sin\Theta\cos\Psi & \sin\Theta\sin\Psi & \cos\Theta \end{pmatrix}. \tag{B.2}$$

In the observer's frame, the end-mirrors have the coordinates $(X^1 = l, X^2 = 0, X^3 = 0)$ and $(X^1 = 0, X^2 = l, X^3 = 0)$. Therefore, in the g.w. frame, the coordinates of the end-mirrors are

$$l_i^{(1)} = R^{-1}\, l \begin{pmatrix} 1 \\ 0 \\ 0 \end{pmatrix} = l \begin{pmatrix} \cos\Phi\cos\Theta\cos\Psi - \sin\Phi\sin\Psi \\ -\sin\Phi\cos\Psi - \cos\Phi\cos\Theta\sin\Psi \\ \cos\Phi\sin\Theta \end{pmatrix}, \tag{B.3}$$

and

$$l_i^{(2)} = R^{-1}\, l \begin{pmatrix} 1 \\ 0 \\ 0 \end{pmatrix} = l \begin{pmatrix} \sin\Phi\cos\Theta\cos\Psi + \cos\Phi\sin\Psi \\ \cos\Phi\cos\Psi - \sin\Phi\cos\Theta\sin\Psi \\ \sin\Phi\sin\Theta \end{pmatrix}. \tag{B.4}$$

These formulae allow us to parameterize the positions of the end-mirrors in terms of l and the angles Θ, Φ, Ψ.

Appendix C

Polarization states and randomness of gravitational waves

As shown in Chapter 2, the quantities $|\overset{s}{h}_n(\eta)|^2$ describe the magnitude of the mean-square fluctuations of the g.w. field in the corresponding polarization states s. We consider a particular mode $\mathbf{n}$ of the field:

$$h_{ij}(\mathbf{n},\eta,\mathbf{x}) = \sum_{s=1,2} \overset{s}{p}_{ij}(\mathbf{n}) \left(\overset{s}{h}_n(\eta) e^{i\mathbf{n}\cdot\mathbf{x}} \overset{s}{c}_{\mathbf{n}} + \overset{s}{h}_n^{*}(\eta) e^{-i\mathbf{n}\cdot\mathbf{x}} \overset{s*}{c}_{\mathbf{n}} \right). \tag{C.1}$$

The lowest-order independent g.w. correlation functions amount to

$$\langle h_{ij}(\mathbf{n},\eta,\mathbf{x})\, \overset{s}{p}{}^{ij}(\mathbf{n})\, h_{kl}(\mathbf{n}',\eta,\mathbf{x}')\, \overset{s'}{p}{}^{kl}(\mathbf{n}') \rangle = 8 \left| \overset{s}{h}_n(\eta) \right|^2 \delta_{ss'} \delta^{(3)}(\mathbf{n}-\mathbf{n}'). \tag{C.2}$$

The action of the random g.w. field (C.1) on free particles leads to their relative oscillatory motion. We refer this motion to a local inertial frame. Let a ring of free particles lie in the $(\mathbf{l},\mathbf{m})$-plane; the ring encircles the axis $\mathbf{n}$. Then, the mean-square amplitude of oscillations in the '+' polarization state is determined by $|\overset{1}{h}_n|^2$, whereas the mean-square amplitude of oscillations in the '$\times$' polarization state is determined by $|\overset{2}{h}_n|^2$. In general, the random gravitational-wave field can be such that the oscillation amplitudes $|\overset{1}{h}_n|^2$ and $|\overset{2}{h}_n|^2$ are different. But if $|\overset{1}{h}_n|^2 \neq |\overset{2}{h}_n|^2$, then the (averaged) observed picture of oscillations is not symmetric with respect to rotations around $\mathbf{n}$.

Formally, the correlation functions of the field with $|\overset{1}{h}_n|^2 \neq |\overset{2}{h}_n|^2$ do not have symmetry with respect to the change of polarization basis. Indeed, the transition to the primed basis according to Eq. (2.8) brings the gravitational wave mode (C.1) to

the form

$$h_{ij}(\mathbf{n},\eta,\mathbf{x}) = \sum_{s=1,2} \overset{s}{p'}_{ij}(\mathbf{n}) \left(\overset{s}{b}_{\mathbf{n}}(\eta) e^{i\mathbf{n}\cdot\mathbf{x}} + \overset{s}{b}{}^{*}_{\mathbf{n}}(\eta) e^{-i\mathbf{n}\cdot\mathbf{x}} \right),$$

where

$$\begin{aligned} \overset{1}{b}_{\mathbf{n}}(\eta) &= \cos 2\psi \, \overset{1}{h}_n(\eta) \, \overset{1}{c}_{\mathbf{n}} + \sin 2\psi \, \overset{2}{h}_n(\eta) \, \overset{2}{c}_{\mathbf{n}}, \\ \overset{2}{b}_{\mathbf{n}}(\eta) &= -\sin 2\psi \, \overset{1}{h}_n(\eta) \, \overset{1}{c}_{\mathbf{n}} + \cos 2\psi \, \overset{2}{h}_n(\eta) \, \overset{2}{c}_{\mathbf{n}} . \end{aligned}$$

Taking into account the relationships (2.17), we can now derive the correlation functions for the new polarization components:

$$\begin{aligned} \langle \overset{1}{b}_{\mathbf{n}} \overset{1}{b}{}^{*}_{\mathbf{n}'} \rangle &= \left(|\, \overset{1}{h}_n \,|^2 \cos^2 2\psi + |\, \overset{2}{h}_n \,|^2 \sin^2 2\psi \right) \delta^{(3)}(\mathbf{n}-\mathbf{n}'), \\ \langle \overset{2}{b}_{\mathbf{n}} \overset{2}{b}{}^{*}_{\mathbf{n}'} \rangle &= \left(|\, \overset{1}{h}_n \,|^2 \sin^2 2\psi + |\, \overset{2}{h}_n \,|^2 \cos^2 2\psi \right) \delta^{(3)}(\mathbf{n}-\mathbf{n}'), \\ \langle \overset{1}{b}_{\mathbf{n}} \overset{2}{b}{}^{*}_{\mathbf{n}'} \rangle &= -\left(|\, \overset{1}{h}_n \,|^2 - |\, \overset{2}{h}_n \,|^2 \right) \sin 2\psi \cos 2\psi \; \delta^{(3)}(\mathbf{n}-\mathbf{n}'). \end{aligned} \tag{C.3}$$

It is seen from (C.3) that, in general, the ψ-dependence survives, and the assumption of statistical independence of polarization components in one basis is not equivalent to this assumption in another basis. However, one recovers the original correlation functions (C.2) from (C.3) if the conditions (2.19) are fulfilled.

Similar properties hold true for circular polarizations. A g.w. mode $h_{ij}(\mathbf{n},\eta,\mathbf{x})$ expanded over circular polarization states is given by

$$h_{ij}(\mathbf{n},\eta,\mathbf{x}) = \bar{h}_{ij}(\mathbf{n},\eta,\mathbf{x}) + \bar{h}^{*}_{ij}(\mathbf{n},\eta,\mathbf{x}),$$

where

$$\bar{h}_{ij}(\mathbf{n},\eta,\mathbf{x}) = \sum_{s=L,R} \overset{s}{p}_{ij}(\mathbf{n}) \, \overset{s}{h}_n(\eta) e^{i\mathbf{n}\cdot\mathbf{x}} \, \overset{s}{c}_{\mathbf{n}} . \tag{C.4}$$

We assume that the complex random coefficients $\overset{s}{c}_{\mathbf{n}}$ $(s = L, R)$, satisfy the statistical conditions (2.17).

The relevant independent correlation functions are calculated to be

$$\langle \bar{h}_{ij}(\mathbf{n},\eta,\mathbf{x}) \overset{s}{p}{}^{ij*}(\mathbf{n}) \, \bar{h}^{*}_{kl}(\mathbf{n}',\eta,\mathbf{x}') \, \overset{s'}{p}{}^{kl}(\mathbf{n}') \rangle = 4 \left| \overset{s}{h}_n(\eta) \right|^2 \delta_{ss'} \delta^{(3)}(\mathbf{n}-\mathbf{n}'), \quad (s = L, R). \tag{C.5}$$

If the observer views the motion of test particles from the $-\mathbf{n}$ direction, i.e. against the direction of the incoming gravitational wave, the function $\left|\overset{R}{h}_n(\eta)\right|^2$ is responsible for the mean-square amplitude of the right-handed (clockwise) rotations of individual particles. The function $\left|\overset{L}{h}_n(\eta)\right|^2$ is responsible for the left-handed (anti-clockwise) rotations. (For more details about the motion of free particles in the field of gravitational waves, see [77].)

Expansion (C.4) preserves its form under transformations (2.22), if one makes the replacements: $\overset{L}{h}{}'_n = \overset{L}{h}_n e^{i2\psi}$, $\overset{R}{h}{}'_n = \overset{R}{h}_n e^{-i2\psi}$. Therefore, the correlation functions (C.5) do not change, regardless the value of the amplitudes $\left|\overset{s}{h}_n(\eta)\right|^2$ $(s = L, R)$. On the other hand, discrete transformations (2.23) generate the replacements: $\overset{L}{h}{}'_n = \overset{R}{h}_n$, $\overset{R}{h}{}'_n = \overset{L}{h}_n$. Therefore, the sense of correlation functions (C.5) changes from L to R and viceversa. The symmetry between left and right is violated, unless the the conditions (2.24) are fulfilled.

Appendix D

Astrophysical prerequisites

(i) Ionization History

The ionization history of the Universe enters our equations through the density of free electrons $N_e(\eta)$, i.e. electrons available for Thompson scattering. Specifically, we operate with the quantity $q(\eta)$:

$$q(\eta) = \sigma_T a(\eta) N_e(\eta). \tag{D.1}$$

The optical depth τ between some instant of time η' and a later instant η is defined by the integral

$$\tau(\eta, \eta') = \int_{\eta'}^{\eta} d\eta'' q(\eta'').$$

The optical depth from some η to the present time η_R is denoted $\tau(\eta)$ and is given by

$$\tau(\eta) \equiv \tau(\eta_R, \eta) = \int_{\eta}^{\eta_R} d\eta' q(\eta').$$

It follows from the above definitions that $\tau(\eta, \eta') = \tau(\eta') - \tau(\eta)$.

A key role in our discussion is played by the quantity $g(\eta)$ called the visibility function:

$$g(\eta) = q(\eta) e^{-\tau(\eta)} = \frac{d}{d\eta} e^{-\tau(\eta)}, \qquad \int_0^{\eta_R} g(\eta) d\eta = 1$$

The state of ionization is determined by microphysical processes during all the evolution of the Universe [91, 92]. For our purposes it is sufficient to focus on two eras:

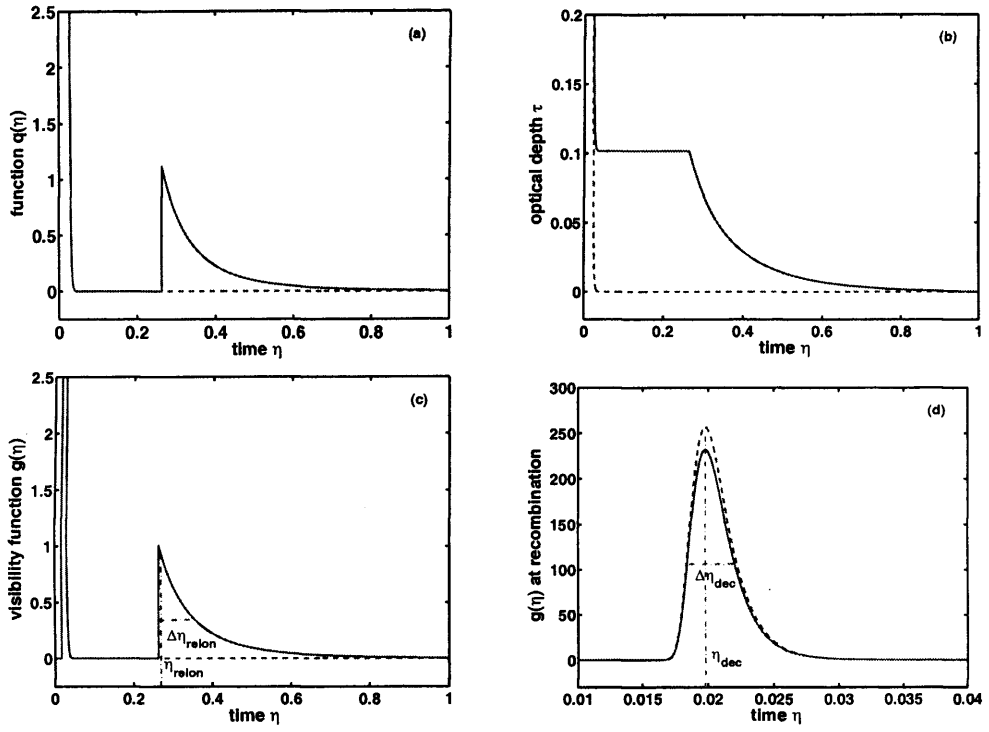

Figure D.1: The graphs (a), (b), (c) show the quantities $q(\eta)$, $\tau(\eta)$, $g(\eta)$. The graph (d) is a zoom of $g(\eta)$ in the region of recombination. The dashed line shows a model without reionization. The solid line takes reionization into account, with $\tau_{reion} = 0.1$.

early recombination and late reionization. The recombination of primordial plasma into atomic hydrogen and helium is accompanied by decoupling of CMB radiation from the rest of matter. (For simplicity, we do not distinguish here the notions of recombination and decoupling.) This relatively quick process has happened at redshifts around $z_{dec} \approx 1100$. Much later, at redshifts around $z_{reion} \sim 10$ [34] the intergalactic medium has become ionized again, presumably, by ionizing radiation of first condensed objects.

The density of free electrons is modelled [93] by the expression

$$N_e(\eta) = \left(1 - \frac{Y_p}{2}\right) \frac{X_e(\eta)\Omega_b \rho_c}{m_p} \left(\frac{a(\eta_R)}{a(\eta)}\right)^3,$$

where $Y_p \approx 0.23$ is the primordial helium mass fraction, $X_e(\eta)$ is the fraction of ionized electrons, Ω_b is the baryon content, and m_p is the mass of a proton. In the framework of linear perturbation theory it is sufficient to regard the electron density as homogeneous, i.e. depending only on η. For $X_e(\eta)$ we use the fitting formula [94]:

$$X_e(\eta) = \left(1 - \frac{Y_p}{2}\right)^{-1} \left(\frac{c_2}{1000}\right) \left(\frac{m_p}{2\sigma_T l_H \rho_c}\right) \Omega_b^{c_1 - 1} \left(\frac{z}{1000}\right)^{c_2 - 1} \left(\frac{a'}{a}\right) (1+z)^{-1}, \quad \text{(D.2)}$$

where $c_1 = 0.43$, $c_2 = 16 + 1.8 \ln \Omega_B$, and z is a redshift.

As for the reionization, we assume that it was practically instantaneous and happened at a redshift $z_{reion} \approx 16$. The function X_e is determined by Eq. (D.2) for $z > z_{reion}$ and $X_e = 1$ for $z \leq z_{reion}$.

To plot the graphs for $q(\eta)$, $\tau(\eta)$ and $g(\eta)$ in Fig. D.1, we use the above-mentioned parameters and $\Omega_b = 0.046$ [15, 45]. It is seen from Fig. D.1 that the visibility function $g(\eta)$ is sharply peaked at the era of recombination. The peak can be characterized by the position of its maximum η_{dec}, and the characteristic width $\Delta\eta_{dec}$. A similar, but less pronounced, peak is present also at the era of reionization.

(ii) Frequency dependence of the Stokes parameters

As is seen from Eq. (4.14), the frequency dependence of both, temperature and polarization, anisotropies is governed by the function $f(\tilde{\nu})$ [69]. We assume that the

unperturbed radiation field has a black-body spectrum,

$$n_0(\tilde{\nu}) = \frac{1}{exp\left(h\tilde{\nu}/k\tilde{T}\right) - 1},$$

where $\tilde{T} = Ta(\eta)$ and the present-day value of T is $T(\eta_R) \approx 2.73K$.

It follows from these formulae that $f(\tilde{\nu})$ is approximately 1 in the Rayleigh-Jeans part of the spectrum, and $f(\tilde{\nu})$ varies as $h\tilde{\nu}/k\tilde{T}$ in the Wein part. In practice, we are usually interested in the total intensity, i.e. Stokes parameters integrated over all photon frequencies. This integration produces the factor γ:

$$\gamma \equiv \int d\tilde{\nu}\ \frac{h\tilde{\nu}^3}{c^2} n_0(\tilde{\nu}) f(\tilde{\nu}) = -4I_0, \tag{D.3}$$

where $I_0 = \int d\tilde{\nu}\ \frac{h\tilde{\nu}^3}{c^2} n_0(\tilde{\nu})$ is the total intensity of the unperturbed radiation field. The factor γ often appears in the main text.

Appendix E

Two essential variables for temperature and polarization

It is seen from Eq. (5.2) that the frequency dependence of $\hat{\mathbf{n}}^{(1)}$ is determined by the factor $f(\tilde{\nu})n_0(\tilde{\nu})$. Therefore, we can single out this factor and write

$$\hat{\mathbf{n}}^{(1)}(\eta, \tilde{\nu}, \mu, \phi) = \frac{1}{2} f(\tilde{\nu}) n_0(\tilde{\nu}) \hat{\mathbf{n}}^{(1)}(\eta, \mu, \phi).$$

The equation that follows from (5.2) and (5.3) reads

$$\left[\frac{\partial}{\partial \eta} + q(\eta) + in\mu\right] \hat{\mathbf{n}}^{(1)}(\eta, \mu, \phi) =$$

$$= (1-\mu^2) e^{\pm 2i\phi} \frac{dh_n}{d\eta} \hat{\mathbf{u}} + \frac{q(\eta)}{4\pi} \int_{-1}^{+1} \int_{0}^{2\pi} d\mu' d\phi' \, \hat{\mathbf{P}}(\mu, \phi; \mu', \phi') \hat{\mathbf{n}}^{(1)}(\eta, \mu', \phi'). \quad \text{(E.1)}$$

The quantity $\hat{\mathbf{n}}^{(1)}(\eta, \mu, \phi)$ as a function of ϕ can be expanded in a series

$$\hat{\mathbf{n}}^{(1)}(\eta, \mu, \phi) = \sum_{m=-\infty}^{+\infty} \hat{\mathbf{n}}_m^{(1)}(\eta, \mu) e^{im\phi}. \quad \text{(E.2)}$$

The explicit structure of the Chandrasekhar matrix $\hat{\mathbf{P}}(\mu, \phi; \mu', \phi')$ is given by the expression [66] (equation(220) on p.42):

$$\hat{\mathbf{P}}(\mu, \phi; \mu', \phi') = \mathbf{Q} \left[\mathbf{P}^{(0)} + (1-\mu^2)^{\frac{1}{2}} (1-\mu'^2)^{\frac{1}{2}} \mathbf{P}^{(1)} + \mathbf{P}^{(2)}\right],$$

where matrices $\mathbf{Q}$, $\mathbf{P}^{(0)}(\mu; \mu')$, $\mathbf{P}^{(1)}(\mu, \phi; \mu', \phi')$, $\mathbf{P}^{(2)}(\mu, \phi; \mu', \phi')$ read

$$\mathbf{Q} = \begin{pmatrix} 1 & 0 & 0 \\ 0 & 1 & 0 \\ 0 & 0 & 2 \end{pmatrix},$$

$$\mathbf{P}^{(0)} = \frac{3}{4}\begin{pmatrix} 2\left(1-\mu^2\right)\left(1-\mu'^2\right)+\mu^2\mu'^2 & \mu^2 & 0 \\ \mu'^2 & 1 & 0 \\ 0 & 0 & 0 \end{pmatrix},$$

$$\mathbf{P}^{(1)} = \frac{3}{4}\begin{pmatrix} 4\mu\mu'\cos\left(\phi'-\phi\right) & 0 & -2\mu\sin\left(\phi'-\phi\right) \\ 0 & 0 & 0 \\ 2\mu'\sin\left(\phi'-\phi\right) & 0 & \cos\left(\phi'-\phi\right) \end{pmatrix},$$

$$\mathbf{P}^{(2)} = \frac{3}{4}\begin{pmatrix} \mu^2\mu'^2\cos 2\left(\phi'-\phi\right) & -\mu^2\cos 2\left(\phi'-\phi\right) & -\mu^2\mu'\sin 2\left(\phi'-\phi\right) \\ -\mu'^2\cos 2\left(\phi'-\phi\right) & \cos 2\left(\phi'-\phi\right) & \mu'\sin 2\left(\phi'-\phi\right) \\ \mu\mu'^2\sin 2\left(\phi'-\phi\right) & -\mu\sin 2\left(\phi'-\phi\right) & \mu\mu'\cos 2\left(\phi'-\phi\right) \end{pmatrix}.$$

The structure of the Chandrasekhar matrix $\hat{\mathbf{P}}(\mu,\phi;\mu',\phi')$ is such that it does not mix the $m\phi$-dependence, that is,

$$\frac{1}{4\pi}\int_{-1}^{+1}\int_{0}^{2\pi} d\mu' d\phi'\ \hat{\mathbf{P}}(\mu,\phi;\mu',\phi')\hat{\mathbf{n}}_m^{(1)}(\eta,\mu')e^{im\phi'} \sim e^{im\phi}.$$

Moreover, this integral vanishes for all $|m| > 2$. This means that Eq. (E.1) is a homogeneous differential equation for all $\hat{\mathbf{n}}_m^{(1)}$ with $m \neq \pm 2$. Assuming zero initial conditions at some initial η, we obtain $\hat{\mathbf{n}}_m^{(1)} = 0$ for all $m \neq \pm 2$. Hence, we are left with three functions of (η,μ):

$$\hat{\mathbf{n}}^{(1)}(\eta,\mu,\phi) = \hat{\mathbf{n}}^{(1)}(\eta,\mu)e^{\pm 2i\phi}. \tag{E.3}$$

We are now able to show that only two out of the three functions $\hat{\mathbf{n}}^{(1)}(\eta,\mu)$ are independent. Indeed, using (E.3) in Eq. (E.1) we arrive at a system of three linear equations for the components of $\hat{\mathbf{n}}^{(1)}(\eta,\mu)$:

$$\left(\frac{\partial}{\partial\eta}+q(\eta)+in\mu\right)\begin{pmatrix}\hat{n}_1(\eta,\mu)\\ \hat{n}_2(\eta,\mu)\\ \hat{n}_3(\eta,\mu)\end{pmatrix} = (1-\mu^2)\frac{dh_n}{d\eta}\begin{pmatrix}1\\1\\0\end{pmatrix}+\frac{3}{8}q(\eta)\begin{pmatrix}\mu^2\\-1\\\pm 2i\mu\end{pmatrix}\mathcal{I}(\eta), \tag{E.4}$$

where $\mathcal{I}(\eta)$ is the remaining integral that was left over from the last term in Eq. (E.1):

$$\mathcal{I}(\eta) = \frac{1}{2}\int_{-1}^{+1} d\mu'\left[\mu'^2\hat{n}_1(\eta,\mu') - \hat{n}_2(\eta,\mu') \pm i\mu'\hat{n}_3(\eta,\mu')\right]. \tag{E.5}$$

Despite the complicated appearance, only two of the three equations (E.4) are really coupled. Indeed, making linear combinations of equations (E.4) it is easy to show that the combination $2i\mu(\hat{n}_1 - \hat{n}_2) \mp (1+\mu^2)\hat{n}_3$ satisfies a homogeneous differential equation. Assuming zero initial conditions, we derive

$$2i\mu(\hat{n}_1 - \hat{n}_2) \mp (1 + \mu^2)\hat{n}_3 = 0.$$

As two independent and essential variables we choose

$$\alpha(\eta, \mu) = \frac{\hat{n}_1(\eta, \mu) + \hat{n}_2(\eta, \mu)}{(1 - \mu^2)}, \qquad \beta(\eta, \mu) = \frac{\hat{n}_1(\eta, \mu) - \hat{n}_2(\eta, \mu)}{(1 + \mu^2)} = \pm\frac{\hat{n}_3(\eta, \mu)}{2i\mu}.$$

In terms of α and β equations of radiative transfer reduce to Eq. (5.5) and Eq. (5.6), and the definition (E.5) for $\mathcal{I}(\eta)$ takes the form of Eq. (5.7).

Although we have considered a gravitational wave perturbation, the existence of only two essential variables is a general statement and it applies to density and rotational perturbations as well. In general, the perturbed radiative transfer equation contains an arbitrary function $f(\eta, \mu, \phi)$ in front of $\hat{\mathbf{u}}$, rather than a specific combination $(1 - \mu^2)e^{\pm 2i\phi}dh_n/d\eta$ quoted in Eq. (E.1). Function $f(\eta, \mu, \phi)$ can be expanded in a series similar to Eq. (E.2):

$$f(\eta, \mu, \phi) = \sum_{m=-\infty}^{+\infty} f_m(\eta, \mu)e^{im\phi}.$$

Since the scattering integral (second term in the r.h.s of Eq. (E.1)) vanishes for all $|m| > 2$, the functions $\hat{\mathbf{n}}_m^{(1)}(\eta, \mu)$ are fully determined by $f_m(\eta, \mu)$ ($|m| > 2$) and describe the temperature variations only. To discuss polarization, we have to consider three remaining cases $m = 0, \pm 1, \pm 2$.

The explicit identification of the two essential variables $\alpha(\eta, \mu)$ and $\beta(\eta, \mu)$ for the case $m = \pm 2$ has been given above. Specifically for gravitational waves, $f_2 = (1 - \mu^2)d\overset{L}{h}_n(\eta)/d\eta$, $f_{-2} = (1 - \mu^2)d\overset{R}{h}_n(\eta)/d\eta$.

The identification of the two essential variables for the case $m = 0$ proceeds in a similar manner. Having calculated the scattering integral for $m = 0$ one can show that

the equation, analogous to Eq. (E.4), will now read

$$\left(\frac{\partial}{\partial\eta}+q(\eta)+in\mu\right)\begin{pmatrix}\hat{n}_1(\eta,\mu)\\ \hat{n}_2(\eta,\mu)\\ \hat{n}_3(\eta,\mu)\end{pmatrix}=$$

$$=\left(f_0(\eta,\mu)+q(\eta)I_0^{(1)}(\eta)\right)\begin{pmatrix}1\\1\\0\end{pmatrix}+\frac{3}{8}q(\eta)\begin{pmatrix}3\mu^2-2\\1\\0\end{pmatrix}\mathcal{J}(\eta),$$

where

$$I_0^{(1)}(\eta)=\frac{1}{4}\int_{-1}^{+1}d\mu'\left[\hat{n}_1(\eta,\mu')+\hat{n}_2(\eta,\mu')\right],$$

$$\mathcal{J}(\eta)=\frac{1}{3}\int_{-1}^{+1}d\mu'\left[(3\mu'^2-2)\hat{n}_1(\eta,\mu')+\hat{n}_2(\eta,\mu')\right].$$

Obviously, $\hat{n}_3$ satisfies a homogeneous equation and can be put to zero. Specifically for density perturbations (see Appendix F), function $f_0(\eta,\mu)$ consists of terms representing gravitational field perturbations and the Doppler term arising due to the baryon velocity:

$$f_0(\eta,\mu)=\frac{1}{2}\left(\frac{dh}{d\eta}-\mu^2\frac{dh_l}{d\eta}+iq(\eta)\mu v_b(\eta)\right).$$

We have checked that in the case $m=\pm1$ the problem also reduces to only two essential variables. The combination $\hat{n}_1-\hat{n}_2\mp i\mu\hat{n}_3$ vanishes at the zero initial data.

Appendix F

Temperature and polarization anisotropies caused by density perturbations

To discover relic gravitational waves in the CMB data we have to distinguish their effects from the effects of density perturbations. We shall work in a synchronous coordinate system. In this coordinate 'gauge', the theory of temperature and polarization anisotropies caused by primordial density perturbations is very much similar to the theory of relic gravitational waves. We start from the metric Fourier expansion (2.11) with the polarization tensors (2.10). Having derived and solved integral equations of radiative transfer in the presence of density perturbations, we arrive at our final goal of distinguishing the TE cross-correlations.

(i) Radiative transfer equations

The equations of radiative transfer in the presence of a single mode n of density perturbations are similar to Eq. (5.2) and read

$$\left[\frac{\partial}{\partial\eta} + q(\eta) + ie^i n_i\right] \hat{\mathbf{n}}_{\mathbf{n}}^{(1)}(\eta, \tilde{\nu}, e^i) =$$
$$= \frac{f(\tilde{\nu}) n_0(\tilde{\nu})}{2} \left[e^i e^j \overset{s}{p}_{ij}(\mathbf{n}) \frac{d\,\overset{s}{h}_n(\eta)}{d\eta} - q(\eta) e^i v_i\right] \hat{\mathbf{u}} + \frac{q(\eta)}{4\pi} \int d\Omega'\, \hat{\mathbf{P}}(e^i; e'^j) \hat{\mathbf{n}}_{\mathbf{n}}^{(1)}(\eta, \tilde{\nu}, e'^j), \tag{F.1}$$

where the extra term $e^i v_i$ takes care of the movement of scattering electrons with respect to the chosen synchronous coordinate system [95, 96, 97].

For technical reasons, it is convenient to work with the 'scalar' $h(\eta)$ and 'longitudinal' $h_l(\eta)$ polarization mode functions, instead of the original $\overset{s}{h}_n\ (\eta)$ [37]. The relationship between them is

$$\overset{1}{h}_n\ (\eta) = \sqrt{\frac{3}{2}}\left(h(\eta) - \frac{1}{3}h_l(\eta)\right), \quad \overset{2}{h}_n\ (\eta) = \sqrt{\frac{1}{3}}h_l(\eta),$$

where the wavenumber index n on $h(\eta)$ and $h_l(\eta)$ is implicit. Both polarization components of metric perturbations participate in Eq. (F.1). In the frame associated with the density wave, i.e. for $\mathbf{n}/n = (0,0,1)$, the structures $e^i e^j\ \overset{s}{p}_{ij}$ (see Eq. 2.10) and $e^i v_i = -i\mu v_b$ depend on $\mu = \cos\theta$, but not on the azimuthal angle ϕ.

By arguments similar to those in Appendix E, one can show that a solution (not vanishing on zero initial data) to Eq. (F.1) must have the form

$$\hat{\mathbf{n}}_n^{(1)}(\eta,\tilde{\nu},\mu) = \frac{f(\tilde{\nu})n_0(\tilde{\nu})}{2}\left[\alpha_n(\eta,\mu)\begin{pmatrix}1\\1\\0\end{pmatrix} + \beta_n(\eta,\mu)\begin{pmatrix}1\\-1\\0\end{pmatrix}\right]. \tag{F.2}$$

Substituting Eq. (F.2) into Eq. (F.1) we arrive at a system of coupled equations for α and β

$$\left[\frac{\partial}{\partial\eta} + q(\eta) + in\mu\right]\alpha_n(\eta,\mu) = \frac{1}{2}\left(\frac{dh}{d\eta} - \mu^2\frac{dh_l}{d\eta}\right) + q(\eta)\left(\mathcal{I}_1 + i\mu v_b - \frac{1}{2}P_2(\mu)\mathcal{I}_2\right), \tag{F.3a}$$

$$\left[\frac{\partial}{\partial\eta} + q(\eta) + in\mu\right]\beta_n(\eta,\mu) = \frac{1}{2}q(\eta)\left(1 - P_2(\mu)\right)\mathcal{I}_2, \tag{F.3b}$$

where

$$\mathcal{I}_1(\eta) = \frac{1}{2}\int_{-1}^{+1} d\mu\ \alpha_n(\eta,\mu), \tag{F.4a}$$

$$\mathcal{I}_2(\eta) = \frac{1}{2}\int_{-1}^{+1} d\mu\ \left[(1 - P_2(\mu))\,\beta_n(\eta,\mu) - P_2(\mu)\alpha_n(\eta,\mu)\right] \tag{F.4b}$$

The quantity $\mathcal{I}_1$ is the monopole component of the perturbed radiation field, whereas $\mathcal{I}_2$ is the quadrupole ($\ell = 2$) component, responsible for the generation of polarization.

To make contact with previous work we note that the variables α and β are closely related to the variables Δ_T and Δ_P from Ref. [65]. Assuming a black body unperturbed

radiation field, we have $\Delta_T = -\alpha$, $\Delta_P = -\beta$. We also note that the mode functions h and h_l are related to the mode functions h and η used in [97, 65] by $h = -2\eta$, $h_l = -(\mathrm{h} + 6\eta)$. Keeping in mind the difference in notations, one can verify that equations (F.3a) and (F.3b) are equivalent to equations (11) in Ref. [65].

(ii) Integral equations and their solutions

A formal solution to equations (F.3a) and (F.3b) can be written as

$$\alpha_n(\eta,\mu) = \int_0^\eta d\eta' e^{-\tau(\eta,\eta')-in\mu(\eta-\eta')}\left[\frac{1}{2}\left(\frac{dh}{d\eta}-\mu^2\frac{dh_l}{d\eta}\right)+q\left(\mathcal{I}_1+i\mu v_b-\frac{1}{2}P_2(\mu)\mathcal{I}_2\right)\right], \tag{F.5a}$$

$$\beta_n(\eta,\mu) = \frac{1}{2}\Big(1-P_2(\mu)\Big)\int_0^\eta d\eta' e^{-\tau(\eta,\eta')-in\mu(\eta-\eta')}\mathcal{I}_2. \tag{F.5b}$$

Proceeding in a manner similar to that in Sec. 5.2, we substitute (F.5a) and (F.5b) into (F.4a) and (F.4b). After certain rearrangements we arrive at two coupled integral equations for $\mathcal{I}_1$ and $\mathcal{I}_2$:

$$\begin{aligned}\mathcal{I}_1(\eta) = &\int_0^\eta d\eta' q(\eta') e^{-\tau(\eta,\eta')}\left[\mathcal{I}_1(\eta')j_0(x)+\frac{1}{2}\mathcal{I}_2(\eta')j_2(x)\right]\\ &+\int_0^\eta d\eta' e^{-\tau(\eta,\eta')}\left[\frac{1}{2}\left(\frac{dh}{d\eta'}j_0(x)+\frac{dh_l}{d\eta'}\frac{d^2j_0}{dx^2}\right)+q(\eta')v_b(\eta')j_1(x)\right],\end{aligned} \tag{F.6a}$$

$$\begin{aligned}\mathcal{I}_2(\eta) = &\int_0^\eta d\eta' q(\eta') e^{-\tau(\eta,\eta')}\left[\mathcal{I}_1(\eta')j_2(x)+\mathcal{I}_2(\eta')\left(\left(\frac{18}{x^2}-\frac{1}{2}\right)j_2(x)-\frac{3}{2x}j_1(x)\right)\right]\\ &+\int_0^\eta d\eta' e^{-\tau(\eta,\eta')}\left[\frac{1}{2}\left(\frac{dh}{d\eta'}j_2(x)+\frac{dh_l}{d\eta'}\left(j_2(x)+3\frac{d^2j_0}{dx^2}\right)\right)+q(\eta')v_b(\eta')\frac{dj_2}{dx}\right],\end{aligned} \tag{F.6b}$$

where the argument of spherical Bessel functions $j_\ell(x)$ is $x = n(\eta - \eta')$.

Equations (F.6a) and (F.6b) together with the continuity equations for matter perturbations and Einstein equations for metric perturbations (see for example [97, 37]), form a closed system of coupled integro-differential equations. In previous treatments

[96, 97, 65], the radiative transfer equations were presented as an infinite series of coupled ordinary differential equations.

Similarly to what was done in Sec. 5.2.2, we can analyze Eqs. (F.6a), (F.6b) in terms of expansions in powers of n,

$$\mathcal{I}_1 = \sum_{k=0}^{\infty} \mathcal{I}_1^{(k)} n^{2k}, \qquad \mathcal{I}_2 = \sum_{k=0}^{\infty} \mathcal{I}_2^{(k)} n^{2k}.$$

The kernels of Eqs. (F.6a), (F.6b) are expanded in powers of x. In the long-wavelength approximation, i.e. for $x \ll 1$, we can limit ourselves by first non-vanishing terms. The zero order approximation brings us to the equations

$$\mathcal{I}_1^{(0)}(\eta) = \int_0^\eta d\eta' q(\eta') e^{-\tau(\eta,\eta')} \mathcal{I}_1^{(0)}(\eta') + \int_0^\eta d\eta' e^{-\tau(\eta,\eta')} \left[\frac{1}{2} \left(\frac{dh}{d\eta'} - \frac{1}{3} \frac{dh_l}{d\eta'} \right) + \frac{1}{3} q(\eta') v_b(\eta') x \right],$$

$$\mathcal{I}_2^{(0)}(\eta) = \frac{7}{10} \int_0^\eta d\eta' q(\eta') e^{-\tau(\eta,\eta')} \mathcal{I}_2^{(0)}(\eta') + \frac{1}{15} \int_0^\eta d\eta' e^{-\tau(\eta,\eta')} \left[-\frac{dh_l}{d\eta'} + 2q(\eta') v_b(\eta') x \right].$$

The solution to these equations is given by

$$\mathcal{I}_1^{(0)}(\eta) = \int_0^\eta d\eta' \left[\frac{1}{2} \left(\frac{dh}{d\eta'} - \frac{1}{3} \frac{dh_l}{d\eta'} \right) + \frac{1}{3} n \int_0^{\eta'} d\eta'' q(\eta'') e^{-\tau(\eta',\eta'')} v_b(\eta'') \right], \tag{F.8a}$$

$$\mathcal{I}_2^{(0)}(\eta) = \frac{1}{15} \int_0^\eta d\eta' e^{-\frac{3}{10}\tau(\eta,\eta')} \left[-\frac{dh_l}{d\eta'} + 2n \int_0^{\eta'} d\eta'' q(\eta'') e^{-\tau(\eta',\eta'')} v_b(\eta'') \right]. \tag{F.8b}$$

(iii) Multipole coefficients

We are mostly interested in the present-day values of α and β and, hence, we put $\eta = \eta_R$ in (F.5a) and (F.5b). Irrespective of approximation in which the functions $\mathcal{I}_1(\eta)$, $\mathcal{I}_2(\eta)$ are known, the multipole coefficients for the radiation field can be found in a way similar to that in Sec. 5.3:

$$\begin{gathered} a_{\ell m}^T(n) = (-i)^\ell \gamma \sqrt{4\pi(2\ell+1)} \delta_{m0} a_\ell^T(n), \\ a_{\ell m}^E(n) = (-i)^\ell \gamma \sqrt{4\pi(2\ell+1)} \delta_{m0} a_\ell^E(n), \\ a_{\ell m}^B(n) = 0, \end{gathered}$$

where $a_\ell^T(n)$, $a_\ell^E(n)$ are given by

$$a_\ell^T(n) = \int_0^{\eta_R} d\eta \left[e^{-\tau} \left(\frac{1}{2}\frac{dh}{d\eta} + \frac{1}{2}\frac{dh_l}{d\eta}\frac{d^2}{d\zeta^2} \right) + g(\eta) \left(\mathcal{I}_1 + v_b \frac{d}{d\zeta} - \frac{3}{4}\mathcal{I}_2 \left(1 + \frac{d^2}{d\zeta^2} \right) \right) \right] j_\ell(\zeta), \tag{F.9a}$$

$$a_\ell^E(n) = \frac{3}{4} \left(\frac{(\ell+2)!}{(\ell-2)!} \right)^{\frac{1}{2}} \int_0^{\eta_R} d\eta \; g(\eta) \mathcal{I}_2 \frac{j_\ell(\zeta)}{\zeta^2}, \tag{F.9b}$$

and $\zeta = n(\eta_R - \eta)$. As expected, in the case of density perturbations all $a_{\ell m} = 0$ for $m \neq 0$ and $a_{\ell m}^B(n) = 0$ [98], [65, 68, 99]. The formal reason for this is that all quantities in (F.2) do not depend on ϕ (A more detailed exposition can be found in [65, 68]).

Let us start from the temperature multipoles. For illustration, we consider an instanteneous recombination. We replace $e^{-\tau}$ with the step function, $g(\eta)$ with the δ-function, and we neglect the $\mathcal{I}_2$ term. Then, we get

$$a_\ell^T(n) = \left[\left(\mathcal{I}_1 + v_b \frac{d}{d\zeta} \right) j_\ell(\zeta) \right] \Big|_{\eta=\eta_{dec}} + \frac{1}{2} \int_{\eta_{dec}}^{\eta_R} d\eta \left(\frac{dh}{d\eta} + \frac{dh_l}{d\eta}\frac{d^2}{d\zeta^2} \right) j_\ell(\zeta).$$

This expression can be further simplified by taking the remaining integral by parts. After some rearrangements we arrive at the final expression

$$\begin{aligned} a_\ell^T(n) = & \left(\frac{1}{2n^2}\frac{d^2 h_l}{d\eta^2}\delta_{\ell 0} + \frac{1}{6n}\frac{dh_l}{d\eta}\delta_{\ell 1} \right) \Big|_{\eta=\eta_R} \\ & + \left[\left(-\frac{1}{2n^2}\frac{d^2 h_l}{d\eta^2} + \mathcal{I}_1 + \left(-\frac{1}{2n}\frac{dh_l}{d\eta} + v_b \right) \frac{d}{d\zeta} \right) j_\ell(\zeta) \right] \Big|_{\eta=\eta_{dec}} \\ & + \frac{1}{2} \int_{\eta_{dec}}^{\eta_R} d\eta \left(\frac{dh}{d\eta} + \frac{1}{n^2}\frac{d^3 h_l}{d\eta^3} \right) j_\ell(\zeta). \end{aligned} \tag{F.10}$$

For the growing mode of density perturbations in the matter-dominated era, the integrand of the remaining integral vanishes. If, in addition, the intrinsic temperature perturbation $\mathcal{I}_1$ and the plasma velocity v_b are zero at $\eta = \eta_{dec}$, we recover from Eq. (F.10) the four terms of the full Sachs-Wolfe formula (43) in Ref. [100]. We would like to note in passing that the origin of the often used, including this work, combination $\ell(\ell+1)C_\ell$ is in fact a historical accident, when a wrong motivation leads to a convenient notation. This combination arises in the essentially incorrect formula $\ell(\ell+1)C_\ell = \text{const}$

that can be derived after the unjustified neglect of three out of four terms in the original Sachs-Wolfe formula (43) in Ref. [100]. This clarification is important not only by itself, but also for correct physical interpretation of reasons for the rise toward the 'first peak' at $\ell \approx 220$ of the actually observed function $\ell(\ell+1)C_\ell$. For more details, see [101].

We now turn to polarization anisotropies. We use the zero order approximation (F.8b) in (F.9b),

$$a_\ell^E = \frac{1}{20}\left(\frac{(\ell+2)!}{(\ell-2)!}\right)^{\frac{1}{2}} \times \\ \times \int_0^{\eta_R} d\eta\, q e^{-\frac{7}{10}\tau} \frac{j_\ell(\zeta)}{\zeta^2} \int_0^{\eta} d\eta' e^{-\frac{3}{10}\tau(\eta')} \left(-\frac{dh_l}{d\eta'} + 2n \int_0^{\eta'} d\eta'' q(\eta'') e^{-\tau(\eta',\eta'')} v_b(\eta'')\right).$$

As $g(\eta)$ is a narrow function, the integrand is localized near $\eta = \eta_{dec}$. By the same arguments that were used in Sec. 5.4.2, the above expression can be reduced to quantities evaluated at $\eta = \eta_{dec}$,

$$a_\ell^E(n) \approx \frac{1}{20}\left(\frac{(\ell+2)!}{(\ell-2)!}\right)^{\frac{1}{2}} \left[\frac{j_\ell(\zeta)}{\zeta 2}\left(-\frac{dh_l}{d\eta}\Delta + 2nv_b\tilde{\Delta}\right)\right]\Big|_{\eta=\eta_{dec}}, \qquad \text{(F.11)}$$

where the factors Δ and $\tilde{\Delta}$ are of the order of the width of $g(\eta)$ in the recombination era. Explicitly, they are given by

$$\Delta = \int_0^{\eta_R} d\eta\, g(\eta) \int_0^{\eta} d\eta' e^{-\frac{3}{10}\tau(\eta,\eta')}, \quad \tilde{\Delta} = \int_0^{\eta_R} d\eta\, g(\eta) \int_0^{\eta} d\eta' e^{-\frac{3}{10}\tau(\eta,\eta')} \int_0^{\eta'} d\eta'' q(\eta'') e^{-\tau(\eta',\eta'')}.$$

The angular power spectra in the case of density perturbations are described by formulas analogous to (5.40). By the steps similar to those in Section 5.3.3 it can be shown that the power spectra are given by

$$C_\ell^{XX'} = \frac{\mathcal{C}^2}{\pi} \int n dn a_\ell^X(n) a_\ell^{X'}(n). \qquad \text{(F.12)}$$

(iiii) Temperature-polarization correlations

We focus on the TE correlation at the relatively small multipoles, $\ell \lesssim 70$. The dominant contribution to these multipoles comes from density perturbations that did not enter the Hubble radius at recombination, $n \lesssim 70$. It is sufficient to consider the early time evolution of these perturbations in the matter-dominated era.

Restricting our analysis to the growing mode, we write for the metric and matter perturbations (see, for example, [37]):

$$h(\eta) = B_n = \text{const}, \quad h_l(\eta) = B_n(n\eta)^2, \quad \mathcal{I}_1^{(0)} = -\frac{2}{3}B_n(n\eta)^2, \quad v_b = -\frac{2}{9}B_n(n\eta)^3.$$

Substituting this solution into (F.10), (F.11) and taking into account only the lowest-order terms in n (the long-wavelength approximation) we arrive at

$$a_\ell^T \approx -B_n \, j_\ell(\zeta)\Big|_{\eta=\eta_{dec}}, \tag{F.13a}$$

$$a_\ell^E \approx -\frac{1}{10}n^2 B_n \eta_{dec}\Delta \left(\frac{(\ell+2)!}{(\ell-2)!}\right)^{\frac{1}{2}} \left(\frac{j_\ell(\zeta)}{\zeta^2}\right)\Big|_{\eta=\eta_{rec}}. \tag{F.13b}$$

Finally, from Eq. (F.12) we obtain for the TE correlation:

$$C_\ell^{TE} \approx \frac{C^2}{\pi}\frac{\eta_{dec}\Delta}{10}\left(\frac{(\ell+2)!}{(\ell-2)!}\right)^{\frac{1}{2}} \int dn \; n^3 B_n^2 \left(\frac{j_\ell(\zeta)}{\zeta}\right)^2\Big|_{\eta=\eta_{dec}}. \tag{F.14}$$

All terms in the above expression are strictly positive. Therefore, the TE correlation caused by density perturbations, in contrast to the case of gravitational waves, must be positive at lower multipoles $\ell \lesssim 50$ where our approximations are still valid. As mentioned before, this difference between gravitational waves and density perturbations boils down to the difference in the sign of first time-derivative of the associated metric perturbations.

Bibliography

[1] L. D. Landau and E. M. Lifshitz. *The classical theory of fields.* Oxford, Pergamon Press, 4th rev. engl. ed., 1975.

[2] C. Misner, K. S. Thorne and J. A. Wheeler, *Gravitation*, (San Fransisco: Freeman, 1973).

[3] R. M. Wald, *General Relativity*, (Chicago and London: The University of Chicago Press, 1984).

[4] S. Weinberg, *Gravitation and Cosmology*, (New York: J. Wiley and Sons, 1972).

[5] B. S. Sathyaprakash, *Current Science*, **89**, 2129 (2005).

[6] J. H. Taylor, *Rev. Mod. Phys.*, **66**, 711 (1994).

[7] L. P. Grishchuk, *Update on gravitational-wave research*, in *Astrophysics Update*, (Heidelberg: Springer-Verlag, 2003, p.281). (gr-qc/0305051)

[8] K. S. Thorne, in *300 years of gravitation*, (Ed. S.W. Hawking and W. Israel), (Cambridge: Cambridge University Press, 1987), p.330.

[9] K. S. Thorne, *Proceedings of the Snowmass'94 Summer Study on Particle and Nuclear Astrophysics and Cosmology*, (Ed. E. W. Kolb and R. Peccei), (World Scientific, Singapore, 1995), p.398.

[10] B. F. Schutz, *Class. Quant. Grav.*, **16**, A131 (1999).

[11] L. P. Grishchuk , V. M. Lipunov, K. A. Postnov, M. E. Prokhorov and B. S. Sathyaprakash, *Usp. Fiz. Nauk* **171**, 3, (2001) [*Physics-Uspekhi* **44**, 1, (2001)]. (astro-ph/0008481)

[12] C. Cutler and K. S. Thorne, in *Proceedings of GR16*, (Durban, South Africa, 2001).

[13] S. A. Hughes, *Annals Phys.* **303**, 142-178, (2003).

[14] G. F. Smoot et. al., *Astrophys. J. Lett.*,**396**, L1 (1992).

[15] D. N. Spergel et. al., *arXiv:astro-ph/0603449.*

[16] L. P. Grishchuk, *Physics-Uspekhi,* **48***(12) 1235-1247* (2005) *[Russian version: Uspekhi Fiz. Nauk,* **175(12)** *1289-1303 (2005)], arXiv:gr-qc/0504018.*

[17] L. P. Grishchuk. *Zh. Eksp. Teor. Fiz.* **67**, *825* (1974)*[Sov. Phys. JETP* **40**, *409 (1975)]; Ann. NY Acad. Sci.* **302**, *439 (1977); Pisma Zh. Eksp. Teor. Fiz.* **23**, *326 (1976) [JETP Lett.* **23**, *293 (1976)].*

[18] W. Hu, in *LNP Vol. 470: The Universe at High-z, Large-Scale Structure and the Cosmic Microwave Background, eds. E. Martinez-Gonzalez, J.L. Sanz, Springer-Verlag, 1996, p. 207. arXiv:astro-ph/9511130.*

[19] W. Hu and M. White, *New Astron.* **2**, *323* (1997). *arXiv:astro-ph/9706147.*

[20] A. Kosowsky, *New Astron. Rev.,* **43**, *157*(1999). *arXiv:astro-ph/9904102.*

[21] A. Kosowsky, in *Modern cosmology, eds. S. Bonometto, V. Gorini and U. Moschella, Series in high energy physics, cosmology and gravitation, Bristol: Institute of Physics Publishing, 2002, p.219. arXiv:astro-ph/0102402.*

[22] A. Challinor, in *The Physics of the Early Universe, ed. E. Papantonopoulos, Lecture Notes in Physics, vol. 653, Berlin: Springer, 2004, p.71. arXiv:astro-ph/0403344.*

[23] A. Challinor, *arXiv:astro-ph/0502093.*

[24] P. R. Saulson, *Interferometrical gravitational wave detectors,* (Singapore: World Scientific publication Co., 1994).

[25] R. B. Partridge, *3K: The Cosmic Microwave Background Radiation,* (Cambridge University Press, 1995).

[26] C. L. Bennett et. al., *Astrophys. J.,***148**, 1 (2003).

[27] J. Bock et. al., *arXiv:astro-ph/0604101.*

[28] LIGO website *http://www.ligo.caltech.edu.*

[29] L. P. Grishchuk, *Usp. Fiz. Nauk* **121**, 629 (1977), [*Sov. Phys. Usp.* **20**, 319, (1977)].

[30] Ya. B. Zel'dovich and A. A. Starobinsky, *Zh. Eksp. Teor. Fiz.* **61**, *2161* (1971)*[Sov. Phys-JETP 34, 1159 (1972)].*

[31] L. P. Grishchuk and A. G. Polnarev, *in: General Relativity and Gravitation, 100 Years After the Birth of A. Einstein, ed. A. Held, vol. 2 (Plenum Press, NY, p.393, 1980).*

[32] V. N. Lukash, *Physics-Uspekhi* **49**, *1* (2006) *[Russian version: Uspekhi Fiz. Nauk,* **176** *113-116 (2006)].*

[33] H. V. Peiris et. al., *Astrophys. J. Suppl.* **148**, *213* (2003).

[34] L. Page et. al., *arXiv:astro-ph/0603450.*

[35] The Planck Collaboration, *arXiv:astro-ph/0604069.*

[36] S. Bose and L. P. Grishchuk. *Phys. Rev. D* **66**, *043529* (2002).

[37] L. P. Grishchuk, *Phys. Rev. D* **50**, *7154* (1994).

[38] E. Newman and R. Penrose, *J. Math. Phys.* **7**, *863* (1966).

[39] J. N. Goldberg et al., *J. Math. Phys.* **8**, *2155* (1967).

[40] K. S. Thorne, *Rev. Mod. Phys.* **52**, *299* (1980).

[41] E. M. Lifshitz, *Zh. Eksp. Teor. Phys.* **16**, *587* (1946).

[42] Y. Watanabe and E. Komatsu, *arXiv:astro-ph/0604176.*

[43] L. P. Grishchuk and M. Solokhin, *Phys. Rev. D* **43**, *2566* (1991).

[44] L. P. Grishchuk, *LNP vol. 562: Gyros, Clocks, Interferometers ...: Testing Relativistic Gravity in Space, 167* (2001).

[45] Legacy Archive for Microwave Background Data Analysis (LAMBDA), *http://lambda.gsfc.nasa.gov.*

[46] G. Hinshaw et. al., *arXiv:astro-ph/0603451.*

[47] L. P. Grishchuk, *Usp. Fiz. Nauk* **156**, *297* (1988)*[Sov. Phys. Usp.* **31**, *940-954 (1988)].*

[48] B. Allen and J. D. Romano, *Phys. Rev. D* **59**, *102001* (1999).

[49] V. Corbin and N. J. Cornish, *Class. Quant. Grav.* **23**, *2435* (2006).

[50] L. A. Boyle and P. J. Steinhardt, *arXiv:astro-ph/0512014.*

[51] T. L. Smith, M. Kamionkowski, and A. Cooray, *Phys. Rev. D* **73**, *023504* (2006).

[52] S. Chongchitnan and G. Efstathiou, *arXiv:astro-ph/0603118.*

[53] V. Mandic and A. Buonanno, *Phys. Rev. D* **73**, *063008* (2006).

[54] S. L. Bazanski, *Ann. Inst. H.Poincare* **A27**, 115, (1977).

[55] R. Kerner , J. W. van Holten and R. Colistete Jr., *Class. Quant. Grav.* **18**, 4725, (2001).

[56] C. Chicone and B. Mashhoon, *Class. Quant. Grav.***19**, (2002), 4231-4248.

[57] L. P. Grishchuk, *Zh. Eksp. Teor. Fiz.* **66**, 833, (1974), [*Sov. Phys. JETP* **39**, 402, (1974)].

[58] F. B. Estabrook and H. D. Wahlquist, *GRG vol. 6*, No. 5, 439, (1975).

[59] M. Tinto, F. B. Estabrook and J. W. Armstrong, *Phys. Rev. D* **65**, 082003, (2002).

[60] N. J. Cornish and L. J. Rubbo, *Phys.Rev. D* **67**, 022001, (2003).

[61] LISA website, *http://lisa.jpl.nasa.gov.*

[62] S. L. Larson, W. A. Hiscock and R. W. Hellings, *Phys. Rev. D* **62**, 062001, (2000).

[63] B. F. Schutz , and M. Tinto, *Mon. Not. R. astr. Soc.* **224**, 131, (1987).

[64] R. Penrose and W. Rindler, *Spinors and space-time, volume 1: two spinor calculus and relativistic fields*, Cambridge: Cambridge University Press, 1984.

[65] M. Zaldarriaga and U. Seljak, *Phys. Rev. D* **55**, *1830* (1997).

[66] S. Chandrasekhar, *Radiative Transfer*, New York, Dover Publications Inc., 1960.

[67] W. Hu, U. Seljak, M. White and M. Zaldarriaga, *Phys. Rev. D* **57**, *3290* (1998).

[68] M. Kamionkowski, A. Kosowsky, and A. Stebbins, *Phys. Rev. D* **55**, *7368* (1997).

[69] M. M. Basko and A. G. Polnarev, *Sov. Astron.* **24**, *268* (1980).

[70] A. G. Polnarev, *Sov. Astron.* **29**, *607* (1985).

[71] R. W. Lindquist, *Ann. Phys.* **37**, *487* (1966).

[72] N. Caderni et. al., *Phys. Rev. D* **17**, *1901* (1978).

[73] P. Naselsky, D. Novikov, and I. Novikov, *Adv. Space Research* **31***(2), 417* (2003).

[74] R. Crittenden et. al., *Phys. Rev. Lett.* **71**, *324* (1993).

[75] U. Seljak and M. Zaldarriaga, *Phys. Rev. Lett.* **78**, *2054* (1997).

[76] R. A. Frewin, A. G. Polnarev, and P. Coles, *Mon. Not. R. Astron. Soc.* **266**, *L21* (1994).

[77] D. Baskaran and L. P. Grishchuk, *Class. Quant. Grav.* **21**, *4041* (2004).

[78] A. N. Varshalovich, D. A. Moskalev and V. K. Khersonskii, *Quantum theory of angular momentum.* World Scientific, 1988.

[79] L. P. Grishchuk and J. Martin, *Phys. Rev. D* **56**, *1924* (1997).

[80] A. Lue, L. Wang, and M. Kamionkowski, *Phys. Rev. Lett.* **83**, *1506* (1999).

[81] A. Kogut et. al., *Astrophys. J. Suppl.* **148**, *161* (2003).

[82] B. Keating and N. Miller, *New Astron. Review* **50**, *184* (2006).

[83] S. V. Babak and L. P. Grishchuk, *Int. J. Mod. Phys. D* **12**, *1905* (2003).

[84] B. Maffei et. al., *arXiv:astro-ph/0407148.*

[85] B. G.Keating et. al., *in: Polarimetry in Astronomy, ed. S. Fineschi, Proceedings of the SPIE, vol. 4843, 284* (2003).

[86] B. Keating, A. G. Polnarev, N. Miller, and D. Baskaran, *Int. J. Mod. Phys. A* **21**, *2459* (2006).

[87] B. Keating et. al., *Astrophys. J.* **495**, *580* (1998).

[88] M. V. Sazhin, G. Sironi, and O. S. Khovanskaya, *New Astron.* **9***(2), 83* (2004).

[89] P. D. Naselsky, I. D. Novikov, and L.-Y. Chiang, *Astrophys. J.* **642***(2), 617* (2006).

[90] A. Lewis and A. Challinor, *Phys. Rep.* **429**, *1 (2006).*

[91] P. D. Naselskii and A. G. Polnarev, *Astrofizika* **26**, *543* (1987)*[Astrophysics* **26***(3), 327 (1987)].*

[92] A. G. Doroshkevich, I. P. Naselsky, P. D. Naselsky, and I. D. Novikov, *Astrophys. J.* **586**, *709* (2003).

[93] P. J. E. Peebles, *Principles of physical cosmology*, Princeton, Princeton University Press, 1993.

[94] W. Hu and N. Sugiyama, *Astrophys. J.* **444**, *498* (1994).

[95] N. Kaiser, *Mon. Not. R. Astron. Soc.* **202**, *1169* (1983).

[96] J. R. Bond and G. Efstathiou, *Astrophys. J. Lett.* **L45**, *285* (1984).

[97] C.-P. Ma and E. Bertschinger, *Astrophys. J.* **455**, *7* (1995).

[98] U. Seljak, *Astrophys. J.* **482**,*6* (1997).

[99] W. Hu and M. White, *New Astron.* **2**, *323* (1997).

[100] R. K. Sachs and A. M. Wolfe, *Astrophys. J.* **147**, *73* (1967).

[101] A. Dimitropoulos and L. P. Grishchuk, *Int. J. Mod. Phys. D* **11**, *259* (2002).